

INFLAMMATION, NLRP3 INFLAMMASOMES, MACROPHAGES AND BREAST  
CANCER PROGRESSION

by

Katherine Holtzman

A dissertation submitted to the faculty of  
The University of North Carolina at Charlotte  
in partial fulfillment of the requirements  
for the degree of Doctor of Philosophy in  
Biological Sciences

Charlotte

2021

Approved by:

---

Dr. Didier Dréau

---

Dr. Andrew Truman

---

Dr. Richard Chi

---

Dr. Ian Marriott

---

Dr. Martha Cary Eppes

©2021  
Katherine Holtzman  
ALL RIGHTS RESERVED



## ABSTRACT

KATHERINE HOLTZMAN. Inflammation, NLRP3 Inflammasome, macrophages and Breast Cancer Progression. (Under the direction of DR. DIDIER DRÉAU)

One in 8 women will be diagnosed with breast cancer in their lifetime and while breast cancer mortality has declined since the 1980s, it remains the 2<sup>nd</sup> leading cause of cancer-related deaths among women. Standard of care is determined by anatomical staging and molecular biomarkers, but generally includes surgery, systemic or targeted chemotherapy or immunotherapy. Therapy resistance remains challenging and is exacerbated by the presence of cancer-stem cells and inflammation. Tumor microenvironment heterogeneity – especially high macrophage infiltration - in breast cancer is associated with larger tumor size, increased vascularization, lower hormone and growth factor expression and lower overall survival. Macrophage phenotype is highly plastic and on a continuum between M1 and M2 macrophages. M1 or classically-activated macrophages are phagocytic, pro-inflammatory and express high levels of inducible nitric oxide synthase (iNOS). In contrast, M2 or alternatively activated macrophages are endocytic and only partially phagocytic, immunosuppressive, and associated with poor prognostic outcomes. Additionally, M2 macrophages express arginase 1 and surface marker CD206 and secrete VEGF and matrix metalloproteinases that promote angiogenesis and matrix remodeling, respectively. Macrophage activation occurs, in part, through cell membrane bound pattern recognition receptors (PRRs) interacting with external pathogen-associated molecular patterns (PAMPs) and damage-associated molecular patterns (DAMPs) including inflammasomes. In particular, the NLRP3 inflammasome is a multiprotein complex which consists of the intracellular receptor, NLRP3, the adaptor,

ASC1, and effector caspase, caspase 1. Upon activation, these proteins oligomerize and, through caspase activity, cleave pro-inflammatory IL-1 $\beta$  and IL-18 cytokines into their mature active forms. Furthermore, pyroptosis, i.e., an inflammatory form of cell death, that can supersede inflammasome activation is mediated by cleavage of gasdermin D and membrane pore formation.

First, our results demonstrate through *in vitro* treatment of macrophages with known inflammasome activators and secretions from tumor cells that macrophages differentially express NLRP3 inflammasomes and NLRP3 inflammasome activation was associated with the development of a pro-tumorigenic macrophage phenotype. Second, our *in vivo* data in immunocompetent, orthotopic, pre-clinical, murine model injected with 4T1 tumors alone or combined with J774 macrophages demonstrate that NLRP3 inflammasome activation in macrophages support tumor proliferation by increased cancer-stem cells and metastasis. Our findings also determined the efficacy of NLRP3 inflammasome inhibition and chemotherapy in *in vitro* co-cultures and *in vivo* immunocompetent, orthotopic, preclinical, murine models demonstrating that the MCC950+5-FU treatment combination decreased inflammasome complex expression and tumor proliferation *in vitro* and reduced *in vivo* tumor growth and leukocyte infiltration in mice co-implanted with 4T1 tumor cells and J774 macrophages. Lastly, our mechanism investigations assessed whether NLRP3 inflammasome activation or pore-mediated cytokine secretion and subsequent autocrine signaling were involved in the generation of the pro-tumorigenic shift in macrophage phenotype associated with NLRP3 inflammasome activation. While following incubation with specific P2RX7 antagonist and gasdermin D inhibitor, inflammasome protein expression remained unchanged, the gasdermin D inhibition using disulfiram effectively

limited pro-inflammatory IL-1 $\beta$  cytokine secretion. Moreover, blocking either P2RX7 signaling or gasdermin D pore formation reversed macrophage polarization toward an M2-like pro-tumorigenic phenotype.

Taken together, our work highlights the role of the NLRP3 inflammasome activation in the pro-tumorigenic and immunosuppressive phenotype shift in macrophages. Ongoing and future studies will further explore the potential of targeting the NLRP3 inflammasome pathway to alter to modulate pro-tumorigenic and immunosuppressive macrophage within the tumor microenvironment to more effectively prevent breast cancer progression.

## ACKNOWLEDGEMENTS

Many people have contributed to the completion of this work, and I would like to express my gratitude. First and foremost, I would like to extend my deepest thanks to my advisor and mentor, Dr. Didier Dréau, for his invaluable supervision, support, and tutelage during my PhD degree. Without your extensive knowledge, advice, and unwavering encouragement this dissertation would not have happened. I would like to extend my deepest appreciation to my committee - Dr. Andrew Truman, Dr. Richard Chi, Dr. Ian Marriott, and Dr. Martha Eppes – for their insightful suggestions and guidance throughout this project. I gratefully acknowledge the many undergraduate and graduate researchers in the Dréau Lab, present and past, who have contributed to this work. Especially, Deepika Suryaprakash, Melissa Aiello, Madison Snyder, Priscille Kabongo, and Layla Abu-al-halaweh who assisted with the animal study and imaging presented in this dissertation. Thanks should also go to the UNCC Graduate School, UNCC Department of Biology and my fellow graduate students who have supported through this dissertation process. Finally, I wish to thank my family and friends who supported me through this process. Many thanks to my mom, April Holtzman; my partner, James Dominic; my sister, Sarah Veulens; my brother-in-law, Eric Veulens, and my cousin, Tommy Holtzman, for their encouragement and support.

## TABLE OF CONTENTS

LIST OF TABLES	vii
LIST OF FIGURES	viii
LIST OF ABBREVIATIONS	ix
CHAPTER 1: INTRODUCTION	1
1.1. Breast Cancer and Treatment	1
1.1.a. Breast Tissue Development, Organization and Function	1
1.1.b. Breast Cancer Staging	2
1.1.c. Breast Cancer Treatments	5
1.2. Tumor Microenvironment and Breast Cancer Progression	7
1.2.a. Tumor Heterogeneity	7
1.2.b. Tumor Microenvironment	9
1.2.c. Macrophages	11
1.3. Inflammasomes and Cancer	14
1.3.a. Cell Types Expressing Inflammasomes	14
1.3.b. Additional Inflammasome Subtypes	14
1.3.c. Relevance to Breast Cancer	15
1.3.d. Inflammasome Formation	17
1.3.e. Mechanisms of Activation	20
1.3.f. Pro-Inflammatory Cytokines	25
1.4. Rationale	32
1.5. Objectives	33
1.6. Figures	34

1.7. Tables	39
CHAPTER 2. NLRP3 INFLAMMASOME ACTIVATION IN MACROPHAGES PROMOTES BREAST CANCER PROGRESSION.	43
2.1. Introduction	43
2.2. Methodology	46
2.3. Results	53
2.4. Discussion	59
2.5. Figures	63
2.6. Table	70
2.7. Supplemental Figures	72
CHAPTER 3. COMBINING 5-FU AND THE NLRP3 INFLAMMASOME INHIBITOR, MCC950, TO PREVENT BREAST TUMOR PROGRESSION.	74
3.1. Introduction	74
3.2. Methodology	78
3.3. Results	83
3.4. Discussion	88
3.5. Figures	91
3.6. Supplement Figures	99
CHAPTER 4. BLOCKING P2RX7 ATP RECEPTOR SIGNALING AND GASDERMIN D PORE FORMATION LIMITS NLRP3 INFLAMMASOME- INDUCED PRO-TUMORIGENIC MACROPHAGE POLARIZATION.	101
4.1. Introduction	101
4.2. Methodology	104

4.3. Results	107
4.4. Discussion	111
4.5. Figures	115
4.6. Supplemental Figures	124
CHAPTER 5: CONCLUSION AND FUTURE DIRECTIONS	125
5.1. Conclusions	125
5.2. Future Directions	130
5.3. Figures	132
REFERENCES	135
APPENDIX A: LAY ABSTRACT	169

## LIST OF TABLES

TABLE 1.1.	Commonly Prescribed Chemotherapies for the Treatment of Breast Cancer.	39
TABLE 1.2.	Targeted Therapies for Breast Cancer.	40
TABLE 1.3.	Known Activators of the NLRP Family.	41
TABLE 2.1.	Genetic Alterations of Macrophage Polarization Markers and Cytokines Impact Overall Survival in Human Breast Cancer.	71



## LIST OF FIGURES

FIGURE 1.1. Structure of Normal Mammary Gland Tissue.	34
FIGURE 1.2. Domains of the NLRP Family.	35
FIGURE 1.3. Amplifications and Deletions of Phylogenetically Related NLRPs in Human Breast Cancer Impacts Patient Overall Survival (OS).	36
FIGURE 1.4. NLRP3 Inflammasome Activation Occurs by Two Signals.	37
FIGURE 1.5. IL-1 $\beta$ and IL-18 Signaling Pathway.	38
FIGURE 2.1. NLRP3 Inflammasome Expression is Elevated in J774 Macrophages.	63
FIGURE 2.2. Pro-Inflammatory Cytokine Secretion by Macrophages.	64
FIGURE 2.3. NLRP3 Inflammasome Activation in Macrophages Results in Pro-Tumorigenic Macrophages.	65
FIGURE 2.4. NLRP3 Inflammasome Competent Macrophages Promote Tumor Growth.	66
FIGURE 2.5. Macrophage Infiltration is Associated with a Pro-Inflammatory Microenvironment <i>In Vivo</i> .	67
FIGURE 2.6. Pro-Tumorigenic Macrophages Promote Tumor Growth and Stemness <i>In Vivo</i> .	68
FIGURE 2.7. Co-Implantation with J774 Macrophages Promotes Metastasis.	69
FIGURE 2.8. Schema of the Proposed Effects of NLRP3 Inflammasome Activation on Breast Cancer Cells.	70
SUPPLEMENTAL FIGURE 2.1. NLRP3 Inflammasome Expression is	72

Elevated in J774 Macrophages.	
SUPPLEMENTAL FIGURE 2.2. Pro-Inflammatory Cytokine Secretion is Positively Associated with Tumor Growth and Pro-Tumorigenic Macrophages.	73
FIGURE 3.1. 4T1 Tumor Cells are Less Sensitized to MCC950 when Co-Cultured with J774 Macrophages.	91
FIGURE 3.2. Co-Cultures of 4T1 Tumor Cells and J774 Macrophages Expressed Less NLRP3 Receptor When Treated with MCC950 and the Addition of 5-Fluorouracil is Inflammasome Activating.	92
FIGURE 3.3. Co-Cultures of 4T1 Tumor Cells and J774 Macrophages Secreted Less IL-18 When Treated with MCC950 and the Addition of 5-Fluorouracil is Inflammasome Activating.	93
FIGURE 3.4. In an Immunocompetent Mouse Model, the Combination of MCC950 and 5-Fluorouracil Decreased 4T1 Tumor Growth.	94
FIGURE 3.5. Cell Death is Elevated When Mice Implanted with 4T1 Tumor Cells Alone are Treated with MCC950 and 5-FU, an Effect Opposite of That Demonstrated in 4T1 and J774 Co-Implanted Mice.	95
FIGURE 3.6. Immune Cell Infiltration of Tumors in Altered by Macrophage Co-Implantation and MCC950 and 5-FU Treatment.	96
FIGURE 3.7. The MCC950 and 5-Fluorouracil Combination Reduced the Pro-Tumorigenic Phenotype of Tumor Infiltrating	97

Macrophages.	
FIGURE 3.8. The MCC950 and 5-Fluorouracil Combination Reduced the Pro-Inflammatory Cytokine Secretion.	98
SUPPLEMENTAL FIGURE 3.1. J774 Macrophage Proliferation was Reduced by the Combination of MCC950 and 5-Fluorouracil.	99
SUPPLEMENTAL FIGURE 3.2. 4T1 Tumor Cell Growth is Accelerated by the Co-Implantation of J774 Macrophages.	100
FIGURE 4.1. NLRP3 Inflammasomes are Activated by LPS and ATP and Tumor Conditioned Media Treatment in J774 Macrophages.	115
FIGURE 4.2. NLRP3 Inflammasome Activating Treatments are Associated with a Pro-Tumorigenic Macrophage Phenotype.	116
FIGURE 4.3. NLRP3 Inflammasome Activation is not Inhibited by the P2RX7 Antagonist, A438079, in J774 Macrophages.	117
FIGURE 4.4. Pro-Inflammatory IL-1 $\beta$ Secretion is Altered by A438079 Treatment in J774 Macrophages.	118
FIGURE 4.5. Pro-Tumorigenic Phenotype is Reduced Following Treatment with P2RX7 Antagonist, A438079.	119
FIGURE 4.6. NLRP3 Inflammasome Activation is not Inhibited by Gasdermin D Inhibitor, Disulfiram, Treatment in J774 Macrophages.	120
FIGURE 4.7. Pro-Inflammatory IL-1 $\beta$ Secretion is Inhibited by Disulfiram Treatment in J774 Macrophages.	121
FIGURE 4.8. Pro-Tumorigenic Phenotype is Reduced Following Treatment	122

with Gasdermin D Inhibitor, Disulfiram.

FIGURE 4.9. Graphical Representation of the Pro-Tumorigenic Effect of the NLRP3 Inflammasome.	123
SUPPLEMENTAL FIGURE 4.1. NLRP3-Specific Inflammasome Inhibitor, MCC950, and NF- $\kappa$ B Inhibitor, MG-132, Reduced the Ratio of Arginase to iNOS, But Did Not Reverse the Reduced Phagocytic Activity Associated with NLRP3 Inflammasome Activation.	124
FIGURE 5.1. NLRP3 Inflammasome Pharmacological Inhibitors Target Both Priming and Activation Steps.	132
FIGURE 5.2. Pro-Inflammatory Cytokines Production Within Tumors is Associated with Pro-Tumorigenic Immune Response.	133
FIGURE 5.3. NLRP3 Inflammasome Activation in Macrophages Results in a Pro-Tumorigenic Microenvironment.	134

## LIST OF ABBREVIATIONS

M1	Classically-Activated Macrophage Polarization Subgroup 1
M2	Alternatively-Activated Macrophage Polarization Subgroup 2
iNOS	Inducible Nitrous Oxide Synthase
CD206	Macrophage Mannose Receptor
VEGF	Vascular Endothelial Growth Factor
PRRs	Pattern Recognition Receptors
PAMPs	Pathogen Associated Molecular Patterns
DAMPs	Damage Associated Molecular Patterns
NLRP3	NOD-Like Receptor Protein 3
ASC1	Apoptosis-Associated Speck-Like Protein Containing CARD 1
IL-1 $\beta$	Interleukin-1 Beta
IL-18	Interleukin-18
5-FU	5-Fluorouracil
P2RX7	Purinergic Receptor P2X7
IGF-1	Insulin-Like Growth Factor
ER	Estrogen Receptor
PR	Progesterone Receptor
HER2	Human Epidermal Growth Factor Receptor 2
TNBC	Triple Negative Breast Cancer
PD-L1	Programmed Death-Ligand 1
PD-1	Programmed Cell Death Protein 1
MIB-1	Tumor Proliferation Marker Ki67

CSCs	Cancer Stem Cells
EMT	Epithelial-Mesenchymal Transition
ZEB1	Zinc Finger E-Box Binding Homeobox 1
MAPK	Mitogen-Activated Protein Kinase
JAK1	Janus Kinase 1
JNK1	c-Jun N-Terminal Kinase 1
STAT3	Signal Transducer and Activator of Transcription 3
CD133	Prominin 1
ALDH1	Aldehyde Dehydrogenase 1
TNF- $\alpha$	Tumor Necrosis Factor Alpha
NF- $\kappa$ B	Nuclear Factor Kappa B
Bcl-XL	B-Cell Lymphoma Extra Large
ICAM-1	Intracellular Adhesion Molecule 1
VCAM-17	Vascular Cell Adhesion Molecule 17
ELAM-1	Endothelial Leukocyte Adhesion Molecule 1
MMP	Matrix Metalloprotease
CXCR4	CXC Motif Chemokine Receptor 4
TIMP-1	TIMP Metalloproteinase Inhibitor 1
ERK1/2	Extracellular Signal-Regulated Kinase 1/2
TGF- $\beta$	Transforming Growth Factor Beta
IFN- $\gamma$	Interferon Gamma
CXCL12	CXC Motif Chemokine Ligand 12
$\alpha$ SMA	Smooth Muscle Actin

IL-2	Interleukin 2
CXCL7	CXC Motif Chemokine Ligand 7
MVD	Micro Vessel Density
TAMs	Tumor Associated Macrophages
pCR	Pathological Complete Response
COX2	Cyclooxygenase 2
CD68	Macrosialin
CSF-1	Colony Stimulating Factor 1
EGF	Epidermal Growth Factor
TLR4	Toll-Like Receptor 4
LPS	Lipopolysaccharide
MyD88	Myeloid Differentiaton Factor 88
DAG	Diacylglycerol
TRIF	TIR Domain Containing Adapter Inducing Interferon Beta
CMPK2	Cytidine/Uridine Monophosphate Kinase
MAVS	Mitochondrial Antiviral-Signaling Protein
PLC	Phospholipase C
PTMs	Post Translational Modifications
MARCO	Macrophage receptor with collagenous structure
SR-A	Scavenger Receptor A
ATP	Adenosine Triphosphate
NOD	Nucleotide Binding and Oligomerization Domain
ECM	Extracellular Matrix

ROS	Reactive Oxygen Species
ARG1	Arginase 1
PYD	Pyrin Domain
CARD	Caspase Associated Recruitment Domain
NACHT	Nucleotide Binding Domain
LRR	Leucine Rich Repeats
MATER	Maternal Antigen That Embryos Require
SCMC	Subcortical Maternal Complex
AIM2	Absent in Melanoma 2
PYCARD	PYD and CARD Domain Containing
NEK7	NIMA Related Kinase 7
RACK1	Receptor of Protein Kinase C (PKC) Isoform $\beta$ II
MDSCs	Myeloid-Derived Suppressor Cells
KO	Knock Out
CM	Conditioned Media
BMDM	Bone Marrow Derived Macrophages
GSDMD	Gasdermin D
CK2	Casein Kinase 2
IRF-4	Interferon Regulatory Factor 4
HIF1 $\alpha$	Hypoxia Inducible Factor 1 Subunit Alpha
PBMCs	Peripheral Blood Mononuclear Cells
GSDMD	Gasdermin D
HMGB1	High Mobility Group Box 1



Cyt C	Cytochrome C
ESCRT	Endosomal Sorting Complexes Required for Transport
VSP4A	Vacuolar Protein Sorting 4 Homolog A
CHMP3	Charged Multivesicular Body Protein 3
Casp11	Caspase 11
IRAK-1	Interleukin 1 Receptor Associated Kinase 1
TRAF6	TNF Receptor Associated Factor 6
TAB2	TGF Beta Activated Kinase 1
TAK1	Transforming Growth Factor Beta Activated Kinase 1
IKK $\beta$	Inhibitor of Nuclear Factor Kappa B Kinase Beta
IL-1RA	Interleukin 1 Receptor Antagonist
IL-18BP	Interleukin 18 Binding Protein
TSLP	Thymic Stromal Lymphopoietin
Treg	Regulatory T-cells
NK cells	Natural Killer Cells
IL-1R	Interleukin 1 Receptor
IL-1RAP	Interleukin 1 Receptor Accessory Protein
dsDNA	Double-stranded Deoxyribonucleic Acid

## CHAPTER 1. INTRODUCTION.

### 1.1. Breast Cancer and Treatment

#### 1.1.a. Human Breast Tissue Development, Organization and Function

Normal breast tissue consists primarily of glandular and adipose tissue held together by fibrous connective tissue (29). The glandular tissue is comprised of a tree-like series of lobes formed by a cluster of lobules which connect to draining ducts converging to the lactiferous sinus before narrowing and terminating at the surface of the nipple (29).

Mammary development *in utero* begins around week 6, when the primary mammary bud extends into the mesenchyme and expands to form secondary buds and, eventually, ducts (34). A basic framework of a branching nest of mammary ducts is reached at the gestational age of 6 months and differentiation of the bilayer epithelium has been established (34). This mammary, bilayer epithelium consists of an apical, epithelial layer lining lumen of the lobules and ducts and a basal, myoepithelial layer connecting to the basement membrane (Fig. 1.1.) (38). By the start of third trimester, a dense fibroconnective tissue has formed around the glandular tissue in a process aided by fetal liver or yolk-sack derived macrophages (34, 40). This stromal development continues into the third trimester as loose connective tissue is added to the stroma and the mammary pit develops into a nipple (34). Following birth and in response to falling maternal estrogen, the breast tissue of infants transiently enlarges with tissue of females remaining slightly larger due to the higher estradiol levels (34). The breast tissue remains quiescent until puberty (34).

For females, the surge of estrogen during puberty, in combination with insulin-like growth factor-1 (IGF-I), leads to enlargement of the breasts and areola as well as an increase in connective and adipose tissue and increased ductal formation and dichotomous

branching (34). During each menstrual cycle more alveoli are formed though the degree to which these alveoli are formed is insignificant until pregnancy (34). Macrophages play a critical role in the clearing of apoptotic debris and extracellular matrix remodeling during the lateral branching extension at puberty, the alveoli expansion during pregnancy and lactation and the involution post-lactation (40). Alterations associated with the normal epithelial-to-mesenchymal transition during embryogenesis and tissue remodeling during breast development are also involved during breast cancer progression.

### **1.1.b. Breast Cancer Staging**

Breast cancer originates through the loosening of tight control of epithelial cell division of cells through combinations of DNA mutations and of microenvironment signaling resulting in poorly controlled cell growth of ductal epithelial cells (more on the mechanism of cancer progression in Section 1.2.) (52). Early versions of clinical staging of breast cancer mainly relied on tumor size and location (54). Currently, cell infiltration and molecular expression of specific tumor cell markers are also parameters included in breast cancer staging (27, 54).

#### **American Joint Committee on Breast Cancer Staging**

The TNM diagnostic staging is based on three criteria: primary tumor size (T), lymph node involvement (N), and metastasis (M). Currently, in the US, the majority of breast cancer patients are diagnosed with localized (64%) or regional (27%) breast cancer while metastatic disease is diagnosed in 6% of breast cancer patients (55).

Stage I is defined as a primary tumor less than 20 mm in size with or without micro-metastases in lymph nodes (54). Stage II consists of a primary tumor greater than 50 mm

without nodal involvement or metastasis or a primary tumor less than 50 mm with metastases to lymph nodes, but no metastases to distant organs (54). Stage III breast cancer is the broadest category incorporating primary tumor directly extending into the chest wall, resulting in macroscopic skin changes or edema without nodal involvement or tumors ranging from less than 1 mm to greater than 50 mm with significant nodal involvement but no distant metastasis (54). Any clinical or histological indications of distant organ metastasis is indicative of stage IV breast cancer regardless of the size of the primary tumor or lymph node dissemination (54).

### **Molecular Staging**

Prognostic staging, as opposed to anatomical staging, considers factors like grade and molecular biomarkers. Tumor grade is an indication of histological cell differentiation: the lower the differentiation, the more aggressive the cancer, and the worse the prognosis (54).

In particular, the expression of hormone receptors for estrogen (ER), progesterone (PR), and human epidermal growth factor (HER2) are also considered for prognostic staging. Approximately 73% of mammary carcinomas express hormone receptors (ER and/or PR), but not HER2 and 11% of breast cancer cases both express hormone receptors (ER and/or PR) and HER2 (55). These marker patterns define luminal A and luminal B sub-types, respectively, with luminal A having the more favorable outcome (55). Indeed, luminal B subtype is generally associated with more proliferative or higher grade tumors and have poorer prognostic outcomes (55). Notably, the majority of breast cancers (~90%) are associated with the luminal layer of epithelium (38).

Tumor staging incorporates molecular biomarkers for anatomical stage migration. For example, a carcinoma between 20 and 50 mm with no nodal involvement and no metastases would be classified as stage IIA by TNM anatomical staging. However, if this carcinoma is ER+ and/or PR+ and HER2-, then the prognostic stage would be downgraded to stage IA (54). The least common subtype with regard to hormone expression is the HER2-enriched (ER-, PR-, HER2+) subtype comprising of 4% of breast cancers (55).

Patients with triple negative breast cancer (TNBC) i.e., ER-, PR- and HER2- breast cancer cells have a 5-year survival rate of 77% (55). Triple negative or basal-like breast cancers account for 12% of breast carcinomas and are typically upstaged (54, 55), that is a triple-negative tumor greater than 50 mm without node or distant metastases is defined as stage of IIB anatomically but staged at IIIB when accounting for molecular markers (54).

#### **Other Tumor Features Associated with Increased Breast Cancer Progression**

*Extracellular matrix accumulation* or fibrosis has been associated with breast cancer progression. Indeed, women with patterns of nodular density, an indication of fibrotic changes, are 37 times more likely to develop breast cancer (59).

*Immune infiltration* defines inflammatory breast cancer, is a rare breast cancer subtype affecting 1-5% of breast cancer patients, and rapidly progressing breast cancer (60). Inflammatory breast cancers are staged as stage IIIB or greater (59). IBC does not result in the formation of a solid tumor and is, therefore, generally missed by self-exams (60). Moreover, the symptoms of redness, swelling and warmth are often initially misdiagnosed as infection or mastitis further delaying treatment (60).

### 1.1.c. Breast Cancer Treatments

Anatomical staging and molecular biomarkers are central factors for determining appropriate breast cancer treatment. Patients with stage 0, or ductal carcinoma *in situ*, are often treated with breast conserving surgery or mastectomy and tamoxifen or aromatase inhibitor treatment for the five subsequent years if the tumor is estrogen or progesterone positive (61). For stages I-III, breast conserving surgery or mastectomy followed by radiation therapy and combined with systemic therapy is the standard (62). For patients with stage I or II breast cancer, adjuvant chemotherapy, HER2/neu receptor inhibitors or hormone therapy may be recommended following surgery (62). For stage III patients, neoadjuvant therapy is usually recommended and, for HER2-positive tumors, HER2/neu receptor inhibitors are again prescribed for one year following surgery and radiation therapy (62). Stage IV breast cancer treatment consists of a combination of systemic therapies including immunotherapy – surgery and radiation therapy generally are not prescribed (63).

*Systemic chemotherapy* can be used as a neoadjuvant therapy to reduce tumor size to prior to breast conserving surgery or as an adjuvant to treat residual cancer post-surgery (64). Commonly used neoadjuvant and adjuvant chemotherapies are often given in combinations of 2 or 3 for localized disease (64) (see table 1.1.). Prior to surgery, neoadjuvant treatment with carboplatin led to an ~15% increase in pathological complete responses from 37% to 52.1% (65). For residual, post-surgery disease, adjuvant treatment with a combination anthracyclines and taxanes is standard (65). Conversely, anthracycline and taxane combination therapy are not recommended for patients with non-metastatic disease prior to surgery (66). For advanced disease, chemotherapy remains the main

treatment (64). Single agent chemotherapies are often administered to treat advanced disease (64) (see table 1.1.).

*Targeted chemotherapies* are therapeutic regimens that focus on specific features of the tumor cells and have led to some clinical success. Targets include hormones especially estrogen, growth factors (e.g., epidermal growth factor receptor) (See Table 1.2.).

*Immunotherapies* support specific immune response promoting tumor cell killing (67). Recent success in preventing inhibition of immune response by tumor cells through inhibition of the PD-L1/PD1 signaling in non-small cell lung cancer (68, 69), colorectal cancer (70), cervical cancer (71), renal carcinoma (69), melanoma (69), and has been tested in breast cancer patients (22). Pembrolizumab (Keytruda®) can be used as a neoadjuvant with chemotherapy or alone as an adjuvant treatment for early-stage, triple-negative breast cancer that expresses PD-L1 (18). Atezolizumab (Tecentriq®) is indicated for use in advanced, triple-negative breast cancer expressing PD-L1 and is often combined with the chemotherapy Abraxane (18).

Cancer immunotherapy, especially the promotion of adaptive immune responses and anti-PD-1 treatments have demonstrated some effectiveness in TNBC patients (17, 19). Patients with metastatic TNBC treated with anti-PD-L1 Atezolizumab in combination with NAB-paclitaxel had significantly improved both progression-free survival (7.2 vs 5.5 months) and overall survival (21.4 vs 17.6 months) compared to patients treated with NAB-paclitaxel alone (13). Of note, among those patients, the subset of patients with PD-L1 positive tumors displayed similar improvement in progression-free survival (7.5 vs 5.0 months) but markedly higher overall survival (25.0 vs. 15.5 months) (13).

## **1.2. Tumor Microenvironment and Breast Cancer Progression**

### **1.2.a. Tumor Heterogeneity**

Tumors are now widely accepted to be heterogeneous in nearly all phenotypic characteristics (19, 72-78). Clinically, intra-tumoral heterogeneity in the expression of ER, PR, HER2, p53 and MIB-1 has been demonstrated by punch biopsies (73). Tumor heterogeneity originates by either clonal expansion of the tumor cells each acquiring distinct mutations and/or through inherited cellular hierarchy with cancer stem cells differentiating into cancer cells with distinct phenotypes and levels of plasticity (76). This heterogeneity, specifically, the presence of cancer stem cells remains a major therapeutic challenge (78).

Tumor progression and relapse decades after remission is, in part, associated with quiescent cancer stem cell (CSC) chemoresistance (79, 80). The quiescent stem cells are located within hypoxic, acidic and necrotic tumor regions, which also promote a migratory phenotype (79). Interestingly, increased expression of intracellular proteins related epithelial-mesenchymal transition (such as ZEB1) has been reported in breast cancer stem cells (79). Indeed, EMT and the activation of the Ras-MAPK and IL-6/JAK1/STAT3 induced signaling cancer stem cell features in human mammary epithelial cells (81, 82). Many CSC markers have been identified including CD133 and increased aldehyde dehydrogenase 1 (ALDH1) expression (79, 80). The presence of ALDH1<sup>high</sup> TNBC cells is a prognostic factor associated with poor chemotherapy response and recurrence (80). Additionally, a recent analysis of 466 invasive breast carcinomas and 8 breast cancer cell lines indicated that basal-like breast cancers including TNBCs, contained a higher



proportion of CSCs (83, 84). Moreover, the increased proportion of CSCs was associated with poor chemotherapy response, metastasis and poor overall survival (83, 84).

The diverse signaling pathways through which CSCs promote self-renewal explain their reduced susceptibility to chemotherapy and hormone therapy and thus the associated lower therapeutic efficacy in breast cancer. Specifically, STAT3 signaling in CD44<sup>+</sup>/CD24<sup>-/low</sup> breast CSCs led to tamoxifen resistance (85). In ER<sup>+</sup> breast cancer post-hormone therapy, the self-renewal of 133<sup>+</sup> CSCs is primary driven by IL-6/Notch3 signaling rather than estrogen signaling (86). Moreover, remaining residual cells following endocrine therapy combined with letrozole or docetaxel chemotherapy were associated with CSC markers including low CD44<sup>+</sup>/CD24<sup>-/low</sup>, and claudin, and high metalloproteinase 2, and vimentin protein expression (87).

Inflammation plays a major role in the transition from the differentiated to the dedifferentiated state of CSCs as demonstrated in breast cancer mouse models (88). Interestingly, although not as a direct result of, TNF- $\alpha$  and IL-6 cytokine concentrations often elevated in association with inflammasome activation also alter tumor stemness by promoting a mesenchymal phenotype (75). Activation of NF- $\kappa$ B, a critical step in inflammasome priming, in tumor cells leads to upregulation of specific genes that promote growth (i.e., cyclin D1 and c-Myc), resistance to apoptosis (i.e., survivin and Bcl-XL), and invasion (i.e., ICAM-1, VCAM-17, ELAM-1 and MMP) (89). Tumors with high IL-1 $\beta$  intra-tumoral concentrations have worse prognosis, likely because IL-1 $\beta$  promotes growth and metastasis in an autocrine/paracrine manner (89). Indeed, activation of IL-1 $\beta$  signaling in MCF-7 cells led to an aggressive tumor phenotype mediated by  $\beta$ -catenin nuclear

translocation and resulting in reduced E-cadherin junctions and increases in CXCR4, cyclin D, MMP2 and c-Myc expression (90).

### **1.2.b. Tumor Microenvironment**

The tumor stroma or the tumor microenvironment is comprised of non-malignant cells and an extracellular matrix associated with the tumor mass. A high degree of tumor microenvironment heterogeneity in invasive breast cancer is associated with poor prognosis (72). Interactions between tumor and its stroma promote tumor progression by promoting angiogenesis, growth, and migration, inducing tumor cell stemness, and aiding in immune evasion (91-94).

*The extracellular matrix* functions as scaffold for tissues and organs providing biochemical and biophysical support. In normal mammary gland tissue, the basement membrane consists of collagen type IV, laminin-111, laminin-332, epiligrin, entactin and proteoglycans (95). The fibrotic stromal matrix of breast cancer consists of collagen type I, III and V, elastin, vitronectin and oncofetal fibronectin (95). In the tumor microenvironment, concentrations of hyaluronan, collagen I and chondroitin sulfate are high, while collagen IV and laminin-111 concentrations are low (95). Hyaluronan regulates migration and invasion of cancer cells by acting as a ligand for receptors including CD44 (95). Hyaluronan synthase is overexpressed in invasive breast cancer (96). *In vitro*, hyaluronan synthase promotes breast cancer cell invasion by inhibiting TIMP-1 (97). MMP-2 and MMP-9 degrade basement membrane collagen IV (95). Collagen I supports breast cancer migration and proliferation through signaling leading to increase in intracellular  $\text{Ca}^{2+}$  and activation ERK1/2; and is associated with an increase in circulating

tumor cells and lung metastases (98, 99). Interestingly, collagen type I alpha I (COL1A1) is associated with poor survival in breast cancer and a knockdown of COL1A1 reduced breast cancer metastasis (100). Fibronectin is mainly secreted by cancer-associated fibroblasts (CAFs) in response to TGF- $\beta$ 1 and IFN- $\gamma$  signaling; and upregulation of fibronectin and the ligand, integrin  $\beta$ 1, is associated with decreased patient survival (101-103). Fibronectin induces EMT in breast cancer by STAT3 signaling and upregulation of N-cadherin and vimentin (104, 105).

*Cancer-associated fibroblasts*, in large part, mediate extracellular matrix remodeling. Mesenchymal-derived cancer-associated fibroblasts are generated in response to upregulation of TGF- $\beta$ 1 caused tumor-derived osteopontin (106). Moreover, CXCL12 (i.e., stromal cell-derived factor 1, SDF1) is upregulated by TGF- $\beta$  leading to differentiation of fibroblasts to CAFs (107). Furthermore, TGF- $\beta$  upregulates  $\alpha$ SMA, fibronectin, and laminin in CAFs; while TGF- $\beta$ 1, IL-4, IL-13 and MMP2 upregulates the expression of collagen I and IV and fibronectin (108, 109). Aside from extracellular matrix remodeling, tumor-associated fibroblasts, as well as macrophages secrete IL-6, IL-8 and CXCL7, which activate STAT3 signaling promoting self-renewal of CSCs (110).

*Endothelial cells* and angiogenesis provide oxygen and nutrients to tumor cells and are critical supports for breast cancer progression. Tumor endothelial markers (TEMs) are elevated in breast cancer compared to normal mammary tissue and are positively correlated with recurrent disease and death (111). Expression of the angiogenic factor, VEGF, and micro-vessel density (MVD) are strongly correlated with tumor grade, lymph node status and tumor-associated macrophage (TAM) infiltration (112). Moreover, vascular remodeling provides a route for immune cell infiltration and tumor cell migration.

*Immune cell* infiltration, specifically, lymphocyte infiltration following neoadjuvant chemotherapy is indicative of increased pathologic complete response rates (pCR) in both TNBC and HER2<sup>+</sup> breast cancers (113). In contrast, infiltration of immune cells including lymphocytes and macrophages as active participants lead to breast cancer progression (114). Indeed, inflammatory breast cancers i.e., breast cancer with high infiltration of immune cells have a poor prognosis (115, 116). Infiltration of CD4<sup>+</sup> T cells (Th1, Treg and Th17 cells) are also associated with negative clinical outcomes; while increased CD8<sup>+</sup> T cells is a positive prognostic indicator (116, 117). Similarly, high neutrophil-to-lymphocyte ratio is significantly associated with mortality in breast cancer (118). Such imbalance in regulatory to effector cells is generally immunosuppressive (119, 120). Mice pre-treated with radiation prior to tumor implantation developed more rapidly growing tumors with immunosuppressive characteristics mimicking observations made in patients treated with radiation therapy such as higher macrophage and lower cytotoxic T cell and NK cell contents, while COX2, TGF- $\beta$  and PD-L1 expression were increased (121).

### **1.2.c. Macrophages**

In some breast cancer subtypes, TAMs comprise up to 50% of the cells within the tumor and such infiltration is associated with reduced overall survival (75, 122). The presence of CD68<sup>+</sup> cells – likely macrophages - correlates to larger tumor size, increased vascularization, lower hormone and growth factor expression and lower overall survival (123). Moreover, TAMs are known to suppress the response to chemotherapy and radiation (124). High macrophage infiltration in invasive breast cancer is predictive of reduced

relapse-free survival and reduced overall survival; and has been associated with increased IL-1 $\beta$  secretions, a marker of aggressive breast cancer (122). Indeed, in the breast cancer microenvironment, tumor cells secrete CSF-1, which stimulates macrophages, and macrophages in turn secrete epidermal growth factor (EGF) which stimulates tumor cell proliferation; this crosstalk leads to tumor cell intravasation and metastasis (125). Breast tumors secreting high CSF-1 concentrations were associated with higher metastatic burden and lower survival (126). Tumors in a transgenic CSF-1 overexpressing model compared to wild-type displayed increased angiogenesis and early macrophage infiltration (122, 127). Moreover, blocking the CSF-1 receptor through administration of PLX-3397 or antibodies to CSF-1, along with paclitaxel treatment, slowed tumor growth and reduced lung metastasis and improved the survival of mammary tumor bearing mice (122, 128). *In vitro* experiments suggest that IFN- $\gamma$  secretion by M2 macrophages polarized by increased TGF- $\beta$  following radiation, is responsible for the morphogenic changes to breast epithelium (121).

Macrophages are a heterogeneous and plastic population influenced by microenvironment signaling and function in innate immunity by engulfing pathogens, regulating inflammation, and initiating acquired immunity (129, 130). Macrophage activation occurs, in part, through cell membrane bound pattern recognition receptors (PRRs) interacting with external pathogen-associated molecular patterns (PAMPs) and damage-associated molecular patterns (DAMPs) (131, 132). Toll-like receptors (TLRs) bind a variety of PAMPs and DAMPs. TLR4/MD2 heterodimer recognizes the bacterial lipopeptide LPS and TLRs: 3, 7, 8 and 9 recognize extracellular DNA and RNA and stimulate phagosome formation (133). These TLR interactions lead to downstream

signaling through MyD88 to activate the transcription factor NF- $\kappa$ B (133). Other PRRs that induce phagosome development include the mannose receptor (MRC1, CD206), Dectin-1, the scavenger receptor A (SR-A) and the macrophage receptor with collagenous structure (MARCO) which bind fungi and gram-negative and gram-positive bacteria (133). After engulfing the target, NADPH-oxidase produces reactive oxygen species, phospholipase A2 produces free fatty acids, and ATPase creates an acidic environment within the phagosome (133). Following target degradation, macrophages can present peptide antigens on their MHC class II to activate helper T cells or release degraded ligands to activate cytosolic PRRs such as NOD-like receptors (NLRs) (133).

Macrophages promote growth and dissemination of tumors by a variety of processes including secretions promoting tumor growth, angiogenesis, and extracellular matrix (ECM) remodeling (112, 130, 134). Macrophage phenotype is highly plastic and on a continuum between M1 and M2. M1 or classically-activated macrophages are phagocytic, pro-inflammatory and express high levels of IL-2, IL-12, IFN- $\gamma$ , TNF- $\alpha$ , ROS, inducible nitric oxide synthase (iNOS) and surface markers: CD80 and CD86 (122-124, 135). In contrast, M2 or alternatively activated macrophages are endocytic and only partially phagocytic (135). M2 macrophages are immunosuppressive and associated with poor prognostic outcomes (116). Additionally, M2 macrophages express IL-4, IL-10, IL-13, TGF- $\beta$ , arginase 1 (ARG1) and surface markers CD163, CD204, CD206, CD200R and CD209; and secrete VEGF and matrix metalloproteinases that promote angiogenesis and matrix remodeling, respectively (122-124, 135). Tumor-associated macrophages (TAMs) are generally closely related to M2 or alternatively-activated macrophages.

### **1.3. Inflammasomes and Cancer**

#### **1.3.a. Cell Types Expressing Inflammasomes**

Most of the research related to inflammasome activation *in vitro* has been conducted on macrophages. However, inflammasome processing of IL-1 $\beta$  has been demonstrated in multiple cell types including human keratinocytes, hepatocytes, goblet cells, endothelial cells, fibroblasts, myoblasts, hepatic stellate cells, astrocytes, and microglia (136-138). Moreover, innate and adaptive immune cells such as neutrophils, CD4 and CD8 T cells, macrophages, B cells, eosinophils have been demonstrated to express inflammasomes and secrete pro-inflammatory cytokines (139-144).

#### **1.3.b. Additional Inflammasome Subtypes**

The NLRP3 inflammasome is the most extensively studied. However, additional inflammasomes of the NLRP family have been identified, along with the AIM 2 inflammasome and non-canonical inflammasomes (described in section 1.3.d.).

Of the NOD-like receptor proteins (NLRPs) family, 14 members are identified. The NLRP family of inflammasomes share a similar structure (Fig. 1.2.) consisting of an N-terminal pyrin domain (PYD), a central nucleotide binding domain (NACHT) and – except for NLRP10 – a series of C-terminal leucine-rich repeats (LRR). A BLAST alignment of NLRP family members revealed 3 distinct phylogenetic branches (Fig. 1.3.).

The first branch, a cluster of similarly related NLRPs, specifically, *Nlrp4*, 5, 8, 9, 11, 13, and 14, is essential for mammalian reproduction and these NLRPs are highly expressed in human oocytes (145, 146). *Nlrp4*, specifically, has been identified as a possible cancer-testis gene (145, 146). Moreover, NLRP5, also known as MATER

(Maternal Antigen That Embryos Require), is a member of the subcortical maternal complex (SCMC) that plays a role in preimplantation embryogenesis and the c.1061C>T variant is associated infertility resulting in embryonic arrest between the 8 and 16-cell stages (147-150). Genetic amplifications of this related, reproductively significant cluster are associated with significant reductions in overall survival of breast cancer patients (Fig. 1.3.).

In the two other phylogenic branches – except for *NLRP3* and *10* - homologous deletions are associated with reduced overall survival (Fig. 1.3.). The following related NLRPs - 1, 2, 3, 6, 7, 9, 10 and 12 - interact with the adaptor protein, ASC1 or PYCARD, suggesting that they may oligomerize into complexes leading to the cleavage and activation of caspase 1 and/or caspase 11 and secretion of pro-inflammatory cytokines (9, 12, 23, 25, 28, 151) (Table 1.3.). The function of NLRP family members and the mechanism behind their significance in breast cancer has yet to be determined. To date the best known of the NLRPs is the NLRP3 inflammasome.

Another inflammasome forming PRR is Absent in Melanoma 2 (AIM 2). AIM 2, in particular, has been shown to suppress proliferation in breast cancer (152), gastric cancer (153) and colorectal cancer (154). Mechanistically, both AIM 2 and NLRP3 require ASC1 for caspase 1 activation and AIM 2 may antagonize NLRPs activities in dendritic cells (155-158).

### **1.3.c. Relevance to Breast Cancer**

Inflammasome activation in breast cancer progression has been partially investigated. Indeed, NLRP3 KO of MDA-MB-231 and MCF-7 cells had reduced



migration and invasion (159). Additionally, NLRP3 inhibition by MCC950 (50 - 100 $\mu$ M) treatment of MDA-MB-231 also reduced migration and invasion (159). Furthermore, the use of Sh-NLRP3 inhibited migration, proliferation, and VEGF expression in MCF-7 cells (160). And *in vivo*, mice inoculated with sh-NLRP3 - MDA-MB-231 cells had reduced tumor size and reduced metastases (159). Endogenous miR-233 and NLRP3 expression are inversely correlated; with miR-233 mimics reducing migration, proliferation and VEGF, IL-1 $\beta$  and IL-18 expression in MCF-7 cells and reducing tumor volume and increasing overall survival in *in vivo* preclinical models (160). Moreover, in human breast cancer, miR-233 expression was inversely correlated tumor growth and migration (160). Interestingly, caspase-1 and NLRP3 knockout mice implanted with EO771 and PyT8 tumors also had smaller tumors and reduced lung metastatic burden (161, 162).

Tumor growth is, in part, driven by the effect of stroma cells' NLRP3 inflammasome activation. Transcription of NLRP3 inflammasome signaling genes (*NLRP3*, *PYCARD*, *CASP1*, *IL-1 $\beta$* , *P2RX7*) is upregulated in cancer-associated fibroblasts in both MMTV-PyMT mice and human infiltrating ductal carcinoma samples, but not in normal breast stroma (163). Indeed, inflammasome activation in mammary cancer-associated fibroblasts led to increased expression of *P2RX7*, *NLRP3*, *CASP1*, *IL-1 $\alpha$*  and *IL1 $\beta$* ; the presence of which was associated with increased breast cancer growth and lung metastasis (164). Tumors in *Nlrp3*<sup>-/-</sup> mice injected with sh-NLRP3 transfected PyMT mammary cells and wild-type normal mammary fibroblasts were significantly larger than mice co-injected with *Nlrp3*<sup>-/-</sup> normal mammary fibroblasts (163). Additionally, more CD11b<sup>+</sup>Gr1<sup>+</sup> cells (MDSCs) were recruited to tumors co-implanted with wild-type fibroblasts (163). Furthermore, mice with *Il1b*<sup>-/-</sup> fibroblasts had significantly fewer lung

metastases and reduced CD11b<sup>+</sup>Gr1<sup>+</sup> cell infiltration than mice with wild-type fibroblasts (163). Moreover, endothelial cells incubated with conditioned media from wild-type fibroblasts demonstrated upregulated expression of adhesion molecules which facilitate tumor intravasation and extravasation (Selectin P and VCAM-1) than endothelial cells incubated with *Il1b*<sup>-/-</sup> fibroblast CM (163). Caspase-1 KO reduced infiltration of MDSCs (CD11b<sup>+</sup>Gr1<sup>+</sup>) and cells of myeloid-lineage than wild-type mice (162). This reduction is likely associated with increased NK cell function and decreased IL-1 $\beta$  production, as treatment with IL-1 receptor antibody and the use of IL-1 $\beta$  deficient mice yielded similar observations (161, 165, 166).

#### **1.3.d. Inflammasome Formation**

##### **NLRP3 Structure and Binding Partners**

The intracellular receptor, NLRP3, has 3 major domains: pyrin, NOD or nucleotide-binding domain (NACHT), and leucine-rich repeat domain (LRR). The N-terminal pyrin domain interacts with the pyrin domain of the ASC1 adaptor. The caspase recruitment domain (CARD) of ASC1 interacts with the CARD of caspase-1 leading to dimerization and autoproteolysis. NLRP3 inflammasome forms filamentous chains by ASC1 pyrin and caspase recruitment domains (CARD) (167). Given the diversity of NLRP3 inflammasome activators (Table 1.3.), rather than direct interactions, activators likely regulate mediators upstream of inflammasome assembly.

RACK1 (receptor of protein kinase C (PKC) isoform  $\beta$ II) is one of the mediators upstream of inflammasome assembly. In BMDMs following LPS and ATP treatment, RACK1 interacts with NEK7 and NLRP3, but not directly with ASC1 (168). Interestingly,

RACK1 knockdown inhibits caspase-1 activation, IL-1 $\beta$  maturation and GSDMD cleavage associated with LPS and ATP treatment, but did not affect caspase-1 activation, IL-1 $\beta$  maturation, nor GSDMD cleavage when treated with poly(dA:dT) or *Salmonella*, which are specific activators of AIM2 and NLRC4, respectively (169-171). These data support RACK1 as a specific mediator of NLRP3 inflammasome activation (168). Following nigericin treatment, RACK1 knockdown cells exhibit partially activated NLRP3 suggesting that RACK1 is key to full NLRP3 inflammasome activation (168).

Besides RACK1, NEK7 critically participates in NLRP3 inflammasome activation by interacting through its C-terminal lobe with a region between LRR and NACHT domains of NLRP3 and perhaps joining adjacent NLRP3 (172). Moreover, phosphorylation of NLRP3 at Y859 inhibits NLRP3 activation by steric hindrance of NEK7 (172). Limiting ATP-triggered, potassium efflux through KCl excess prevented NEK7 and NLRP3 binding and associated caspase-1 activation (173). Chloride efflux promoted NEK7-NLRP3 interaction and ASC1 speck formation (174-176). In NEK7 knockdown BMDMs, LPS and nigericin treatment only achieved minimal inflammasome activation as measured by IL-1 $\beta$  secretion and ASC speck formation (173). Interestingly, NLRP3 inflammasome activation is likely restricted to cell interphase as NEK7 along with NEK6 and NEK9 are highly expressed and support mitotic spindle and centrosome assembly (177).

### **The Adaptor Protein, ASC1**

Apoptosis-associated speck-like protein containing a CARD (ASC1) is a member of Death Domain superfamily and is encoded by the gene *PYCARD* (178). Clinically,

elevated expression of *PYCARD* is associated with more proliferative tumors and lymph node positivity (179).

ASC1 contains two domains: PYD and CARD connected by a 23 residue, dynamic linker (178). Transfected PYD- or CARD- only ASC1 fragments form filamentous structures suggesting endogenous ASC1 forms dense, crosslinking aggregates i.e., speck-like aggregates (167, 178). The consensus model of inflammasome oligomerization suggests homotypic, parallel PYD-PYD and CARD-CARD interactions (178). NLRP3 nucleates ASC1 via the PYD domain interactions resulting in a helical speck with CARD domains proximal for caspase 1 CARD polymerization (167). ASC1<sup>PYD</sup> R41A and D48A mutants do not nucleate suggesting these residues are critical for ASC1 polymerization (180).

### **Effector Caspases and Canonical Versus Non-Canonical Inflammasomes**

*Canonical* inflammasome activation involves an internal sensor protein, e.g., NLRP3 which mediates signaling and is often bridged by the adaptor protein, ASC1 (181). ASC1 stabilizes pro-caspase-1 interactions by bringing monomers in proximity leading to their dimerization and auto-cleavage (181). CARD17 (aka INCA) caps caspase-1 filaments inhibiting polymerization; and, in monocytes, INCA inhibits NLRP3 inflammasome activation (182).

*Non-canonical* inflammasome activation is the result of direct activation of the effector caspase by the stimuli. Caspase-1 and caspase-11 (in mice; or caspase-4 and caspase-5 in humans) can be activated by direct recognition of intracellular LPS via the CARD domain resulting in dimerization and activation (181). Additionally, *Leishmania* lipophosphoglycan, *Fasciola hepatica* cathepsin L3 and the oxidized phospholipid

(oxPAPC) have been shown to promote non-canonical inflammasome activation (181). Moreover, non-canonical activation of caspase-11 can cross-recruit caspase-1 by activating the NLRP3 inflammasome (181).

### **1.3.e. Mechanisms of Activation**

Inflammasomes are intracellular, pattern recognition receptors which respond to a variety of DAMPs and PAMPs (Table 1.3.). The NLRP3 inflammasome is a multiprotein complexes which consists of the intracellular receptor, NLRP3, the adaptor, ASC, and effector caspase, caspase-1 (183). Upon activation, these proteins oligomerize and, through caspase activity, cleave pro-inflammatory IL-1 $\beta$  and IL-18 cytokines into their active forms (184). An inflammatory form of cell death called pyroptosis can supersede inflammasome activation and is mediated by cleavage of gasdermin D and membrane pore formation (185).

Within normal cells, activation of the NLRP3 inflammasome (Figure 1.4.) occurs through a two-step mechanism: 1. Priming and 2. Oligomerization (184). First, signaling through PAMPs or DAMPs (step 1) results in the autophosphorylation of a toll-like receptor (TLR), which in turn (step 2) stimulates expression of pro-IL-1 $\beta$  and NLRP3 by nuclear translocation of NF- $\kappa$ B (184). The diversity of stimuli leading to NLRP3 inflammasome oligomerization suggests that the NLRP3 sensor protein does not directly interact with the stimuli (185). To date, three mechanisms i.e., ionic flux, reactive oxygen species (ROS) or mitochondrial dysfunction, and lysosomal degradation leading to NLRP3 inflammasome oligomerization have been described.

### **Toll-Like Receptors and Priming**

Cell priming mainly through NF- $\kappa$ B activation leading to pro-IL-1 $\beta$  and NLRP3 expression is a necessary and rate limiting step (186). Although this step is critical for NLRP3 and pro-IL-1 $\beta$  expression, it has no impact of the expression of other proteins (i.e., ASC1, pro-caspase1, and pro-IL-18) associated in the NLRP3 multiprotein complex (18). Inflammasome activation is generally mediated through Toll-like Receptor (TLR) signaling and TLR2 (Pam3CysK4), TLR3 (Poly(I:C)), TLR4 (LPS) and TLR7 (R848) signaling specifically activate NLRP3 inflammasomes (186). Priming with LPS via TLR4 prior to treatment with particulate matter (e.g., SiO<sub>2</sub>, Al(OH)<sub>3</sub>, CPPD crystals) enhanced IL-1 $\beta$  release (187).

Recent results indicate that in BMDMs, incubation with LPS prior to ATP treatment activates the NLRP3 inflammasome without an upregulation in NLRP3 expression suggesting that priming is controlled by regulatory PTMs (188). Additionally, increased NLRP3 expression following LPS priming resulted from a decrease in proteasomal degradation of NLRP3 through regulation of ubiquitin ligase FBXL2 degradation and not through an increase in NLRP3 mRNA production (189). Indeed, at rest, NLRP3 is highly ubiquitinated and its protein expression is tightly regulated by proteasomal degradation with 2 E3 ligases (Pellino2 and TRAF6) positively regulating NLRP3 expression (190). Furthermore, BRCC3 (via BCC3-containing BRISC complex or BRCC36 in humans) controls NLRP3 activation by de-ubiquitination of the NLRP3 LRR domain (191). Additionally, priming signals lead to critical S194 phosphorylation of NLRP3 mediated by JNK1 that precedes NLRP3 self-assembly (192). PTMs are also suggested to regulate NLRP3 oligomerization.

### **Purinergic Receptors and Ion Flux**

Potassium efflux is required for NLRP3 inflammasome activation (187). Potassium efflux occurs in response to ATP stimulus and in tandem with sodium influx (185). Purigenic P2RX7-ATP interaction drives the recruitment of pannexin-1 and hemi-channel formation responsible for potassium efflux (184). Furthermore, NEK7 (NIMA-related kinase 7) binds directly to NLRP3, facilitating oligomerization following potassium efflux, an action limited by the use of culture media with high potassium concentrations (173, 185). Moreover, LPS-induced caspase11 activation leads to pannexin-1 channel activation and subsequent potassium efflux that activates NLRP3 inflammasomes (193). Additionally, pannexin-1 formation releases ATP which induces pore formation and cell death via P2RX7 (193).

P2RX7-mediated endoplasmic reticulum calcium release and extracellular calcium influx also participates to ATP-induced inflammasome activation through Phospholipase C (PLC) signaling (194). Upon ATP treatment, PLC translocates from the cell membrane to the cytosol and endoplasmic reticulum calcium is released in response to an increase in second messenger IP<sub>3</sub> binding to the IP<sub>3</sub> receptor (194). Potassium efflux also occurs following particulate / crystal (SiO<sub>2</sub>, Al(OH)<sub>3</sub>, CPPD) phagocytosis (187). Moreover, leak or rupture of phagolysosomes induces calcium mobilization, which, in turn, leads to mitochondrial damage and ROS generation involved in other inflammasome activation pathways (194).

### **Reactive-Oxygen Species and Mitochondrial Dysfunction**

Resting NLRP3 co-localized to the endoplasmic reticulum while active inflammasomes (NLRP3 and ASC1) colocalize with both the endoplasmic reticulum and

mitochondria (195). Following treatment with ATP or silica, mitochondrial cardiolipin physically interacts with the LRR domain of NLRP3 inflammasome and dose-dependently activate NLRP3 inflammasomes (196). NLRP3 and caspase1 independently associate with externalized cardiolipin following priming by LPS or TLR1/2, TLR3, and TLR4 stimulation (197). Additionally, nigericin treatment leading to elevated cytosolic calcium results in ASC1 localizing to the mitochondria (197). Pharmacological inhibition of ROS prior to LPS priming resulted in reduced active caspase1 and reduced colocalization of NLRP3 and caspase1 at the mitochondrial membrane (197). Furthermore, the mitochondria-associated adaptor molecule (MAVS) is required for optimal inflammasome activation as it promotes ASC1 speck formation via the recruitment of TNFR-associated factor 3 (TRAF3) for E3 ligase-mediated ubiquitination of ASC1 at Lys174 (56, 198, 199). Also, mitochondrial ROS potentiated by ATP are key to the de-ubiquitination of NLRP3 (188).

NLRP3 associates with mitochondrial membrane adjacent to the trans-Golgi Network via ionic interactions between the four lysine residues between Pyrin and NACHT domains and phospholipids PtdIns(3,4,5)P<sub>3</sub> and PtdIns(4,5)P<sub>2</sub> (200, 201). Following mitochondrial damage, increased DAG production leads to increased protein kinase D (PKD) activity at the Golgi (200). Activated PKD releases NLRP3 from the mitochondrial membrane by phosphorylating Ser293 allowing for inflammasome oligomerization in the cytosol (200).

NEK7 has also been implicated in ROS-dependent NLRP3 activation. Indeed, NEK7-deficient cells failed to produce IL-1 $\beta$  following treatment with the TLR7 agonist and ROS producer, Imiquimod (185). Furthermore, LPS-stimulation and nigericin



treatment increased NEK7-NLRP3 interaction (177). In contrast, treatment with the ROS scavenger, N-acetylcysteine, reduced both NEK7 phosphorylation and NEK7-NLRP3 interactions in J774A.1 macrophages (177).

Inhibiting mt-ROS via the mitochondrial ROS scavenger, Mito-TEMPO, prevented macrophage LPS and ATP induced IL-1 $\beta$  secretions. However, Mito-TEMPO had negligible effect on macrophage LPS- and monosodium urate-induced or LPS- and poly(dA:dT)-induced IL-1 $\beta$  secretions. These results suggest that ROS-mediated inflammasome activation is stimulus dependent (202). Furthermore, the mitochondrial dysfunction responsible for mt-ROS release also results in mtDNA release into the cytosol leading to further activation of the NLRP3 inflammasome (202) with apoptosis oxidized mtDNA binding to NLRP3 inflammasomes resulting in further IL-1 $\beta$  secretion (203). Likewise, mtDNA synthesized following TLR activation through MyD88 and TRIF to promote IRF1-dependent transcription of CMPK2 also promotes NLRP3 inflammasome activation (204).

### **Lysosomal Damage**

Lysosomal damage and rupture including following phagocytosis of silica and aluminum crystals leads to NLRP3 inflammasome activation (33, 205). Lysosome acidification following monosodium urate crystal phagocytosis leads to a release of sodium and passive water influx that lowers potassium concentration to activate NLRP3 inflammasome (206). IL-1 $\beta$  secretion decreases following treatment with inhibitors of lysosomal acidification (ammonium chloride, chloroquine) and aquaporins (mercury chloride, phloretin) (206).

Lysosomal dysfunction activates NLRP3 activation, in part, through the lysosomal protease, cathepsin B (184). Particulates such as silica, alum, cholesterol, and monosodium urate crystals lead to lysosome destabilization and the release of cathepsin B which in turn activate NLRP3 inflammasomes (184, 185, 205, 207, 208). Indeed, treatment with the cathepsin B inhibitor, Ca074Me, reduced macrophage IL-1 $\beta$  release following palmitate-LPS treatment (209). Additionally, in response to particulate matter or crystals, cathepsins B, L, C, S and X redundantly activate NLRP3 inflammasome and subsequent IL-1 $\beta$  secretion can be inhibited by treatments with pan-cathepsin inhibitors e.g., Ca074Me and cystatin B and C (210).

### **1.3.f. Pro-Inflammatory Cytokines**

Pro-inflammatory cytokines, IL-1 $\beta$  and IL-18, are cleaved and secreted following caspase-1 and murine caspase-11 (and human homolog caspase 4/5) activation. Although the cleavage of both cytokines occurs via the same enzymes, the expression and subsequent signaling of each are distinct.

#### **IL-1 $\beta$ Expression**

IL-1 $\beta$  mRNA expression is induced by LPS treatment *in vitro* and *in vivo* (211, 212). In monocytes, PU.1 and C/EBP $\beta$  transcription factors are bound to the IL-1 $\beta$  promoter in both stimulated and non-stimulated conditions (212). The constitutively active Ser/Thr protein kinase CK2 is a critical mediator of IL-1 $\beta$  expression. Indeed, CK2 phosphorylates PU.1 before associating with the IL-1 $\beta$  promoter. Inhibition of CK2 activity with apigenin and emodin decreased IL-1 $\beta$  transcription by 97% and 68%, respectively (212). Moreover, in LPS stimulated monocytes, IRF-4 is recruited to the IL-

1 $\beta$  enhancer, but not in unstimulated monocytes (212). LPS stimulation switches cell metabolism from mitochondrial oxidative phosphorylation to aerobic glycolysis increasing succinate concentrations, which in turn stabilizes HIF1 $\alpha$  bound to hypoxia responsive elements (HRE) upstream of the *Il1b* transcription start site (213). Additionally, through the transcription factor, PU.1, IL-1 $\beta$  induces further autocrine IL-1 $\beta$  expression (214).

### **IL-18 Expression**

IL-18 is constitutively produced in peripheral blood mononuclear cells (PBMCs) and its mRNA expression is only modestly increased in the presence of IL-1 $\beta$  inducers such as LPS as shown in C57BL6 mice spleens (211). In epithelial cells during *T. gondii* infection, IL-22 promotes IL-18 production (213). While the IL-18 promotor has no TATA box, it contains a PU-box (a purine-rich sequence binding PU.1), a NF- $\kappa$ B-recognition sequence, an ISRE site and GAS elements (211, 213).

### **IL-1 $\beta$ and IL-18 Secretion & Gasdermin D**

Gasdermin D (GSDMD) is necessary for LPS-induced pyroptosis and the release - but not the maturation of IL-1 $\beta$  (215-217). Following LPS and nigericin or poly(dA:dT) treatment, GSDMD knockout iBMDM failed to undergo pyroptosis and activate NLRP3 and AIM2 inflammasomes (217). GSDMD cleavage and N-terminal relocation to the plasma membrane has been demonstrated in HEK293T cells transfected with wild type caspase-11 (216). GSDMD is cleaved at Asp276 (in mice) and Asp275 (in humans) by caspase-1 and -11 (4/5 in humans) and the N-terminal fragment (GSDMD-NT) oligomerizes at the membrane to form transient pores (216, 217). GSDMD-NT strongly binds to mitochondrial lipids, phosphatidylinositol phosphates (PIPs), and cardiolipin (216). Additionally, GSDMD-NT binds with less strength to phosphatidylserine and

phosphatidic acid but not to phosphatidylethanolamine (PE) or phosphatidylcholine (PC) (216). Thus, GSDMD-NT selectively interacts with lipids on the inner leaflet of the plasma membrane (216). The structural conformation of 33 human GSDMD subunits forms a membrane pre-pore that becomes a full pore through the insertion of  $\beta$ -barrel and conformational changes (218).

Electrochemical interactions within the GSDMD pore favors the secretion of mature IL-1 $\beta$  and IL-18, preventing pro-IL-1 $\beta$  and pro-IL18 secretions (218). The GSDMD pore is predominately acidic due to glutamic acid and aspartic acid residues in the  $\beta$ -barrel favoring the secretion of neutral or basic charged proteins via GSDMD pores. Both pro-IL-1 $\beta$  and pro-IL-18 are acid and, following cleavage, become basic. Besides IL-1 $\beta$  and IL-18, Rac-1, HMGB1 and Cyt C are also rapidly secreted via GSDMD pores (218).

Gasdermins (A, B, C, D, E) are partially redundant. Like GSDMD, GSDME is cleaved by caspase-1 or caspase-8 following inflammasome activation leading to IL-1 $\beta$  release and cell death (219). Gasdermin E (i.e., DFNA5, deafness, autosomal dominant 5) is cleaved by caspase-3 following treatment with chemotherapeutics (Mitoxantrone, Doxorubicin, Actinomycin-D) leading to pyroptosis (220). Moreover, in the absence of GSDMD, low GSDME expression is sufficient for cytokine release, but not pyroptosis, supporting inflammasome activation independent of cell lysis (219).

While inflammasome activation and subsequent GSDMD pore formation has been associated with cell death, recent data suggests that in some cases GSDMD formed pores are transient. Indeed, following calcium influx through the GSDMD pores, membrane repair can be completed by the endosomal sorting complexes required for transport (ESCRT) machinery (221). Interestingly, in BMDM transient expression of VSP4A mutant

or truncated CHMP3 augmented IL-1 $\beta$  and cell death following of LPS treatment (221). In contrast, Casp11<sup>-/-</sup> or GSDMD<sup>-/-</sup> cells, depletion of ESCRT had no effect on cytokine secretions (221). Notably, ESCRT-III membrane repair has been identified as a pharmacological target for chemotherapy resistance (222).

### **IL-1 $\beta$ and IL-18 Signaling**

IL-1 $\beta$  signaling occurs through binding to Toll/interleukin-1 receptor (TIR) family receptors: IL-1R1 or IL-1R2 combined with IL-1RAcP to form heterodimers (Fig. 1.5.). Similarly, IL-18 binds to a heterodimer comprised of IL-18R $\alpha$  (i.e., IL-1R5) and IL-18R $\beta$  (i.e., IL-1R7) (223, 224). The C-terminal TIR domains of the heterodimer receptor interacts with the myeloid differentiation primary-response protein 88 (MyD88) (223). The IRAK-1/Toll complex moves to the active IL-1 receptor; and IRAK-1, a serine/threonine kinase, associates with the receptor complex at the N-terminal death domain of MyD88 (223). IRAK-1 becomes phosphorylated, either by auto- or cross-phosphorylation or phosphorylation by IRAK-4 (223). Following phosphorylation, IRAK-1 interacts with TRAF6; and, in parallel, TRAF6 interacts with TAB2, an adaptor of MAPKKK TGF $\beta$ -activated kinase 1 (TAK1) and its activator TAB1 (223). TAK1 is activated by TRAF6 then phosphorylates I $\kappa$ B-kinase  $\beta$  (IKK $\beta$ ) and MKK leading to the activation of NF- $\kappa$ B, p38 and c-Jun N-terminal kinase (JNK) (223). Specifically, the rapid degradation of I $\kappa$ B, the inhibitor of NF- $\kappa$ B, allows for NF- $\kappa$ B activity (225). This MyD88 signaling pathway is discontinued by IRAK-1 and/or TRAF6 degradation (223).

### **Pro-Inflammatory Cytokine Regulation via IL1RA & IL18BP**

Pro-inflammatory effects of IL-1 $\beta$  and IL-18 secretions are regulated by endogenous antagonists that block cytokine and respective receptor interactions.

The IL-1R1 receptor antagonist (IL-1RA), the endogenous antagonist to the IL-1 $\beta$  pro-inflammatory cytokine (224) is constitutively expressed in carcinoma (226). IL-1RA expression is promoted by LPS, IL-10 and type 1 IFNs but also by IL-1 $\alpha/\beta$  (213). For example, IL-10 through STAT3 induces IL-1RA expression (213). In addition, in monocytes, ERK1/2- or p38-activated MSK1 and 2 (mitogen stress-activated protein kinase 1 and 2) stimulate IL-1RA expression (227). IL1RA expression is induced by AP-1 dependent of C/EBP $\alpha/\beta$ , PU.1 and NF- $\kappa$ B IL-1RA gene (*IL1RN*) promoter modulation (213, 226).

Endogenous IL-18BP abrogates the activity of pro-inflammatory, IL-18, by directly binding IL-18 and thereby preventing its interactions with the IL-18R $\alpha$  and IL-18R $\beta$  receptors (224). Human spleen cells constitutively secrete the IL-18BP isoform A which is also induced by IFN- $\gamma$  signaling (213, 228). IL-18BP gene promoter region contains binding sites to GAS, ISRE, C/EBP $\beta$  and, in response, to IFN- $\gamma$  signaling IRF-1 and C/EBP $\beta$  form a complex and interact at the GAS site (213). Notably, IL-37 also inhibits IL-18 activity by binding to IL-18R $\alpha$  and IL-1R8 receptors and blocking the IL18- IL-18R $\alpha$  and IL-18R $\beta$  interactions preventing IL-18 signaling (229).

### **The IL-1 $\beta$ and IL-18 Pro-Inflammatory Environment**

Pro-inflammatory cytokine, IL-1 $\beta$  and IL-18, secretions support breast cancer progression through promotion of angiogenesis, tumor invasiveness and metastasis (184, 230, 231).

In a breast cancer pre-clinical murine models, IL-1 $\beta$  overexpression led to increased hindlimb metastasis compared to IL-1 $\beta^{-/-}$  mice (232). Moreover, *in vivo* administration of IL-1RA (Anakinra<sup>®</sup>) reduced tumor size and bone metastasis and increased overall survival

(162, 232, 233). Furthermore, the combination IL-1RA (Anakinra<sup>®</sup>) and TGF- $\beta$ -neutralizing antibodies in the Hs578T - NOD/SCID $\beta_2^{-/-}$  mouse model led to reduced tumor size (234). Additionally, Anakinra<sup>®</sup> treatment in breast cancer preclinical models led to reduced microvessel formation and lower endothelin-1, IL-1 $\beta$  and TNF- $\alpha$  expression in hindlimb bones (233).

In contrast, the combination EGF (epidermal growth factor) and IL-1 $\beta$  *in vitro*, through increased phospho-ERK1/2 and MMP-9 expression, promoted growth and tissue modeling and migration of BT474 invasive ductal carcinoma cells (235). Furthermore, tumor cell transmigration across blood and lymphatic endothelial monolayers was increased following treatment with activated or IL-1 $\beta$ -producing macrophage conditioned media (236). Moreover, tumor-derived IL-1 $\beta$  promoted epithelial-to-mesenchymal transition marked by N-cadherin upregulation and E-cadherin downregulation (237). Likewise, IL-18 participates in breast cancer cell migration by down-regulating claudin-12 expression and stimulating the activation of the p38 MAPK pathway (238).

Clinically, IL-1 $\beta$  secretion and tumor stage are positively correlated (234). Specifically, stage II, III, and IV patient tumors expressed significantly more IL-1 $\beta$  compared to earlier stages (234). Intra-tumoral expression of IL-1 $\beta$  and TNF- $\alpha$  was highest in relapsing invasive ductal carcinoma (239). Additionally, elevated serum IL-18 was associated with metastatic disease and decreased relapse-free survival in breast cancer (240, 241).

Human breast tumor IL-1 $\beta$  secretions were also correlated with myeloid CD11c<sup>+</sup> cell infiltration, and with IL-13, IFN- $\gamma$  and TSLP (thymic stromal lymphopoietin) secretions (234). Elevated IL-13 and IFN- $\gamma$  support a shift towards a Th2 immune response

(234). IL-1RA treatment blocked IL-1 $\beta$ -induced transcription of TSLP by MB-MDA-231 cells *in vitro*. *In vivo*, blocking the IL-1 $\beta$  signaling reduced tumor size, lung metastases and CD11b<sup>+</sup> infiltrates (162, 234). Moreover, tumor-derived IL-18 contributes to immune suppression in breast cancer through differentiation of CD11b<sup>+</sup> cells to monocytic myeloid-derived suppresser cells that suppress T-cell proliferation (242), and through increased immune checkpoint (PD-1) expression by NK cells (243).

IL-1 $\beta$  signaling promotes tumor progression by increasing tumor growth, angiogenesis, and metastasis in part through tumor cell mesenchymal phenotype shift and heightened recruitment of immunosuppressive myeloid lineage cells (184, 230, 231). However, whether NLRP3 inflammasome activation skews macrophages toward a tumor-promoting phenotype in breast cancer remains unclear.



#### **1.4. Rationale**

As highlighted in the background section above, inflammasomes especially NLRP3 have been most extensively studied for their role in promoting inflammation during infections (13, 16, 170, 195). More recently, the role of inflammasome activation in cancer has garnered more attention. In light of the development of targeted immunotherapies that likely may have reduced efficacy against pro-inflammatory tumors (244, 245), a better understanding of inflammasome activation within the tumor microenvironment is needed.

## 1.5. Objectives

Here, we hypothesized that: NLRP3 inflammasome activation, which is abrogated by NLRP3 inflammasome inhibitors in macrophages, leads to a pro-tumorigenic and immunosuppressive microenvironment favoring breast tumor growth. To this end, we demonstrated that the stimulation of NLRP3 inflammasomes in macrophages promoted an immunosuppressive phenotype shift that furthered tumor growth and increased stemness of breast tumor cells (Chapter 2). Next, we demonstrated that the tumor-promoting and immunosuppressive effect of NLRP3 inflammasome activation can be reduced by combination therapy of NLRP3 inflammasome specific inhibitor, MCC950, and chemotherapy, 5-fluorouracil, in a mouse model of breast cancer (Chapter 3). And, finally, we determined that reducing pro-inflammatory cytokine secretions by limiting NLRP3 inflammasome oligomerization and pore-mediated secretion, reversed the immunosuppressive phenotype associated with NLRP3 inflammasome activation in macrophages (Chapter 4).

## 1.6. Figures

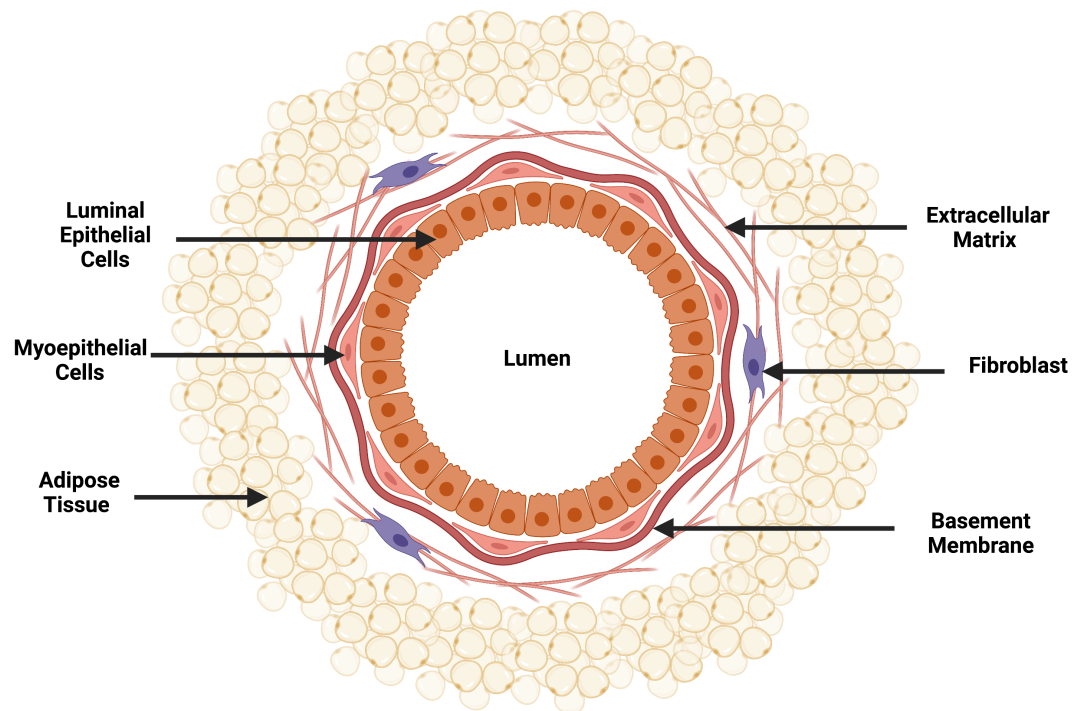


**Figure 1.1. Structure of Normal Mammary Gland Tissue.** A normal mammary gland duct contains a hollow lumen surrounded by a layer of luminal epithelial cells, followed by a layer of myoepithelial cells and the basement membrane. Beyond the basement membrane is a dense network of extracellular matrix maintained by fibroblasts and surrounded by adipose tissue (29, 246). Generated by KH using BioRender.com.

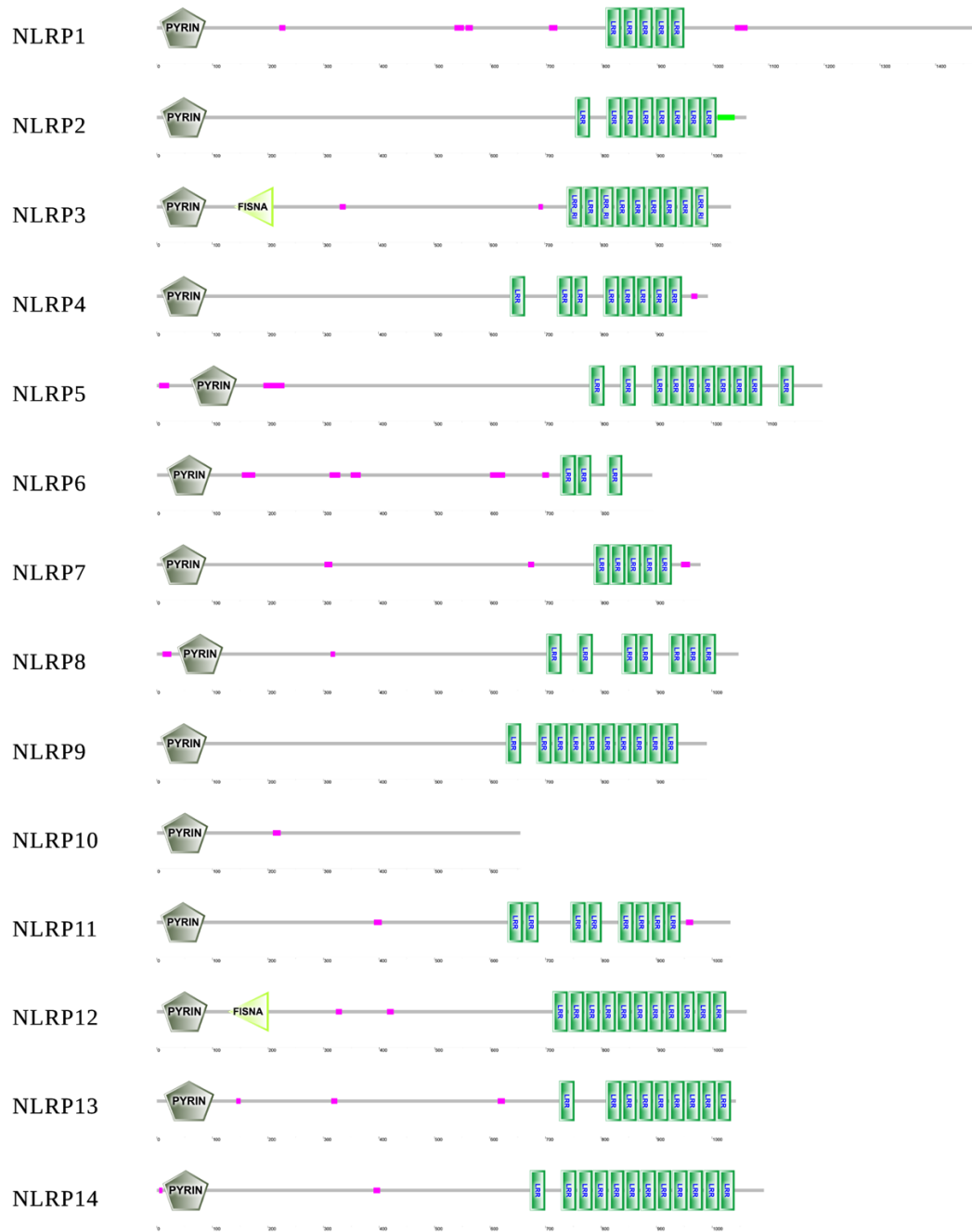
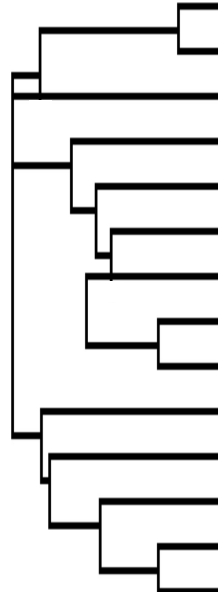


**Figure 1.2. Domains of the NLRP Family.** The NLRP family of pattern recognition receptors share a common structure. Each - except for NLRP10 which does not have a leucine-rich repeat domain - have an N-terminal pyrin (PYD) domain, central NACHT domain and a C-terminal leucine-rich repeat (LRR).



NLRP	UniProt Entry	Amplification			Deep Deletion		
		Incidence	OS (mo.)	p-value	Incidence	OS (mo.)	p-value
7	Q8WX94	1.59%	-21.1	n.s.	1.42%	-113.1	***
2	Q9NX02	1.61%	-20.4	n.s.	1.42%	-112.4	***
11	P59045	2.09%	-70.9	**	0.54%	-114.4	n.s.
5	P59047	2.15%	-67.0	**	0.56%	-113.8	n.s.
13	Q86W25	2.07%	-70.9	***	0.56%	-114.4	n.s.
8	Q86W28	2.15%	-70.3	***	0.56%	-113.8	n.s.
14	Q86W24	0.52%	-108.1	*	0.31%	-	n.s.
4	Q96MN2	2.09%	-70.9	**	0.54%	-114.4	n.s.
9	Q7RTR0	2.07%	-70.9	**	0.23%	-114.4	n.s.
1	Q9C000	0.12%	-	n.s.	0.35%	-	*
6	P59044	0.46%	-34.4	n.s.	0.63%	-	*
10	Q86W26	0.46%	68.9	n.s.	0.21%	-	n.s.
3	Q96P20	13.31%	5.5	n.s.	0.06%	-	-
12	P59046	1.59%	-20.7	n.s.	0.75%	-113.0	***

**Figure 1.3. Amplifications and Deletions of Phylogenetically Related NLRPs in Human Breast Cancer Impacts Patient Overall Survival (OS).** Genetic amplification of closely related NLRPs: 4, 5, 8, 9, 11, 13, and 14 in human breast cancer samples are associated with significantly decreased median overall survival. Conversely, homologous deletion (deep deletion) of closely related NLRP2 and NLRP7 reduced median overall survival. Patient data was acquired through cBioPortal (247-274) and phylogenetic data by BLAST alignment via UniProt. \*\*\*  $p < 0.001$ , \*\*  $p < 0.01$ , \*  $p < 0.05$

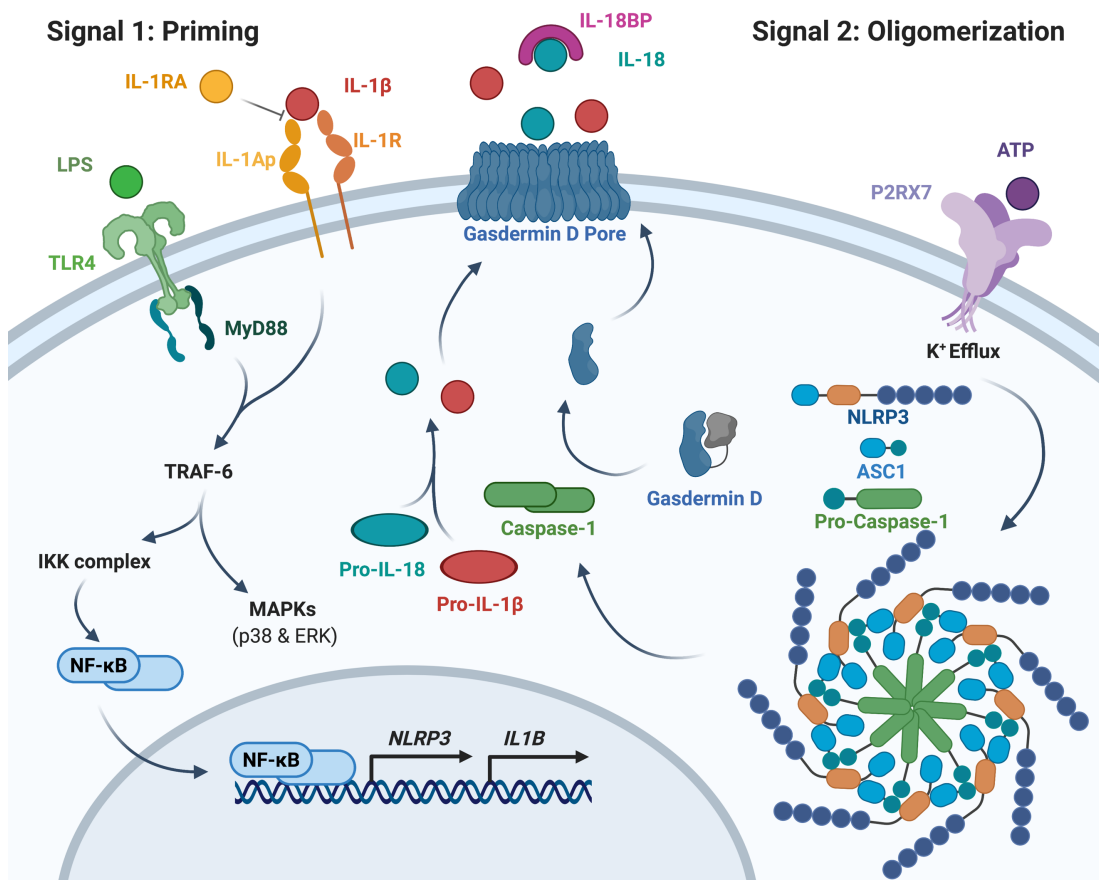


**Figure 1.4. NLRP3 Inflammasome Activation Occurs by Two Signals.** The first signal is a priming signal. Commonly, lipopolysaccharide (LPS) is used as priming signal to induce expression of *NLRP3* and *IL1B* (192, 275). The second signal leads to oligomerization of the NLRP3 inflammasome and subsequent activation of caspase 1 (276, 277). Active caspase 1 cleaves pro-inflammatory cytokines to their mature forms and cleaves gasdermin D; resulting in pore formation, from which IL-1β and IL-18 are secreted (6). The activities of secreted IL-1β and IL-18 can be limited by the presence of endogenous antagonists: IL-1 receptor antagonist (IL-1RA) and IL-18 binding protein (IL-18BP) (234, 278). Generated by KH using BioRender.com.

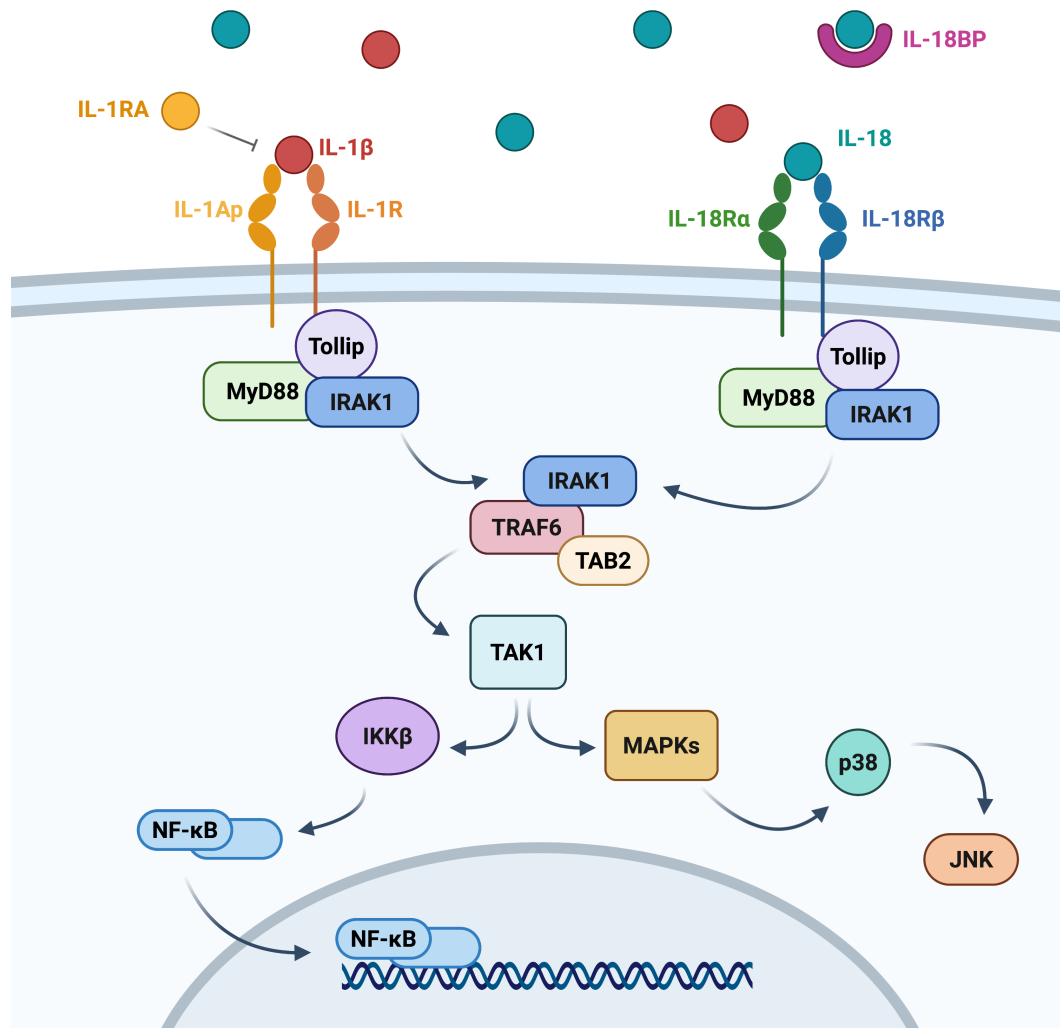


**Figure. 1.5. IL-1 $\beta$  and IL-18 Signaling Pathway.** Pro-inflammatory cytokines IL-1 $\beta$  and IL-18 interact with their respective receptor pairs: IL-1Ap/ IL-1R and IL-18 $\alpha$ / IL-18 $\beta$  (223, 224). The Tollip/ MyD88 and IRAK1 complex forms at the activated receptor leading to phosphorylation of IRAK1 (223). IRAK1 interacts with TRAF6 leading to activation of TAK1 (MAP3K7) which ultimately leads to NF- $\kappa$ B and JNK activation (223, 225). Generated by KH using BioRender.com

## 1.7. Tables

Commonly Prescribed Neoadjuvants and Adjuvants		
	Local	Advanced
<b>Taxanes</b>		
Paclitaxel (Taxol)	+	+
Docetaxel (Taxotere)	+	+
Albumin-bound Paclitaxel (Abraxane)		+
<b>Anthracyclines</b>		
Doxorubicin (Adriamycin)	+	+
Epirubicin (Ellence)	+	+
Pegylated Liposomal Doxorubicin		+
<b>Platinum Agents</b>		
Carboplatin (Paraplatin)	+	+
Cisplatin		+
<b>Antimicrotubular Antineoplastic Agents</b>		
Vinorelbine (Navelbine)		+
Ixabepilone (Ixemptra)		+
Eribulin (Halaven)		+
<b>Antimetabolite Antineoplastic Agents</b>		
5-Fluorouracil	+	
Capecitabine (Xeloda)	+	+
Gemcitabine (Gemzar)		+
<b>Alkylating Antineoplastic Agent</b>		
Cyclophosphamide (Cytosan)	+	

**Table 1.1. Commonly Prescribed Chemotherapies for the Treatment of Breast Cancer.** Breast cancer treatments depend on anatomical staging and molecular biomarkers. Single agent chemotherapy regimens can be used to treatment local (non-metastatic) or advanced (metastatic) disease (64).



Targeted Therapies for Breast Cancer					
	Targets:	ER	HER2/neu	Cell Cycle	Immune Anergy
<b>Selective Estrogen Receptor Modulator (SERM)</b>					
Tamoxifen		+			
Toremifene (Fareston)		+ $\alpha$ $\Phi$			
<b>Selective Estrogen Receptor Degradar (SERD)</b>					
Fulvestrant (Faslodex)		+ $\alpha$ $\Phi$			
<b>Aromatase Inhibitors</b>					
Letrozole (Femara), Anastrozole (Arimidex) and Exemestane (Aromasin)		+ $\Phi$			
<b>Monoclonal Antibodies</b>					
Trastuzumab (Herceptin, Ogivri, Herzuma, Ontruzant, Trazimera, Kanjinti)			+ $\alpha$ $\gamma$		
Trastuzumab and Hyaluronidase injection (Herceptin Hylecta)			+ $\gamma$		
Pertuzumab (Perjeta)			+ $\alpha$		
Trastuzumab, Pertuzumab, Hyaluronidase (Phesgo)			+		
Margetuximab (Magenza)			+ $\alpha$		
<b>Antibody-Drug Conjugates</b>					
Ado-Trastuzumab Emtansine (Kadcyla or TDM-1)			+ $\alpha$ $\gamma$		
Fam-Trastuzumab Deruxtecan (Enhertu)			+ $\alpha$ $\Psi$		
<b>Kinase Inhibitors</b>					
Lapatinib (Tykerb)				+ $\alpha$ $\gamma$	
Neratinib (Nerlynx)				+ $\alpha$ $\gamma$ $\Psi$	
Tucatinib (Tukysa)				+ $\alpha$ $\gamma$	
<b>CDK4/6 Inhibitors</b>					
Palbociclib (Ibrance), Ribociclib (Kisqali) and Abemaciclib (Verzenio)				+ $\alpha$ $\gamma$ $\Psi$ $\Phi$	
<b>mTOR Inhibitor</b>					
Everolimus (Afinitor)				+ $\alpha$ $\Psi$ $\Phi$	
<b>PI3K Inhibitor</b>					
Alpelisib (Piqray)				+ $\alpha$ $\Psi$ $\Pi$	
<b>PARP Inhibitors</b>					
Olaparib (Lynparza) and Talazoparib (Talzenna)				+ $\alpha$ $\Psi$ $\gamma$ $\Xi$	
<b>Antibody-Drug Conjugates</b>					
Sacituzumab Govitecan (Trodelvy)				+ $\tau$	
<b>PD-L1 Immunotherapy</b>					
Pembrolizumab (Keytruda) and Atezolizumab (Tecentriq)					+ $\alpha$ $\gamma$ $\tau$ $\lambda$

+ Indicates treatment target.

$\alpha$  Can be used to treat metastatic disease.

$\Phi$  Often combined with luteinizing-hormone releasing hormone (LHRH) agonist for ovarian ablation or used in post-menopausal women.

$\gamma$  Often combined with chemotherapy.

$\Psi$  Often used to treat HER2+ cancers.

$\Pi$  Used to treat patients with *PIK3CA* mutations.

$\Xi$  Used to treat patients with *BRC A* mutations.

$\tau$  Used to treat triple-negative cancers.

$\lambda$  Used to treat PD-L1 expressing cancers.

**Table 1.2. Targeted Therapies for Breast Cancer.** Therapies with molecular targets may be prescribed based on the patient's disease stage, age, therapeutic history, and disease biomarkers such as hormone receptor positivity and mutation status (61-63, 279-281).

NLRP	Activators	Requires ASC
1	NTPs (2)	Yes (6)
	Muramyl dipeptide (MDP) (2) Serine dipeptidase DPP8 and DPP9 inhibitors (Val-boroPro, aka PT-100, aka Talabostat) (3, 4) <i>Toxoplasma gondii</i> (5)	
2	$\alpha$ -CD3 and $\alpha$ -CD28 antibodies (8)	Yes (9)
	PMA/ionomycin (8) Exogenous ATP (9)	
3	<i>Listeria monocytogenes</i> (10)	Yes (56)
	<i>Staphylococcus aureus</i> (10)	
	<i>Vibrio cholera</i> (10)	
3	<i>Neisseria gonorrhoeae</i> (13)	
	<i>E. coli</i> (15)	
	<i>Candida albicans</i> (16)	
	<i>Saccharomyces cerevisiae</i> (16)	
	Adenovirus (17)	
	Influenza virus (18-20)	
	Sendai virus (18)	
	Encephalomyocarditis virus (EMCV) (24)	
	<i>Plasmodium malariae</i> (26, 27)	
	<i>Toxoplasma gondii</i> (5)	
	Alum (32, 33)	
	Asbestos (36, 37)	
	Silica (37)	
	Skin irritants (trinitrochlorobenzene, trinitrophenylchloride, and dinitrofluorobenzene) (41)	
	UVB radiation (42)	
	Monosodium urate crystals (MSU) monosodium urate crystals (MSU) and pyrophosphate dihydrate (CPPD) crystals (44)	
	Cholesterol (45, 46)	
	Amyloid deposits (45, 46)	
	Hydroxyapatite crystals (48)	
	Hyaluronan (50)	
	ATP (10)	
	High glucose (51)	
	Saturated fatty acids (53).	
	LPS (15)	
	Lipid A (15)	
	Pam3CysSerLys4 (Pam3CSK4) (15)	
	Peptidoglycan (PGN) (15)	
	Muramyl dipeptide (MDP) (15)	
	Lipoteichoic acid (LTA) (15)	
4	dsRNA or dsDNA (57)	No (58)
5	-	-

**Table 1.3. Known Activators of the NLRP Family. (Continued Below)**

6	Lipoteichoic acid (LTA) (1)	Yes (11)
	<i>Listeria monocytogenes</i> (1)	
	<i>Staphylococcus aureus</i> (1)	
	<i>Toxoplasma gondii</i> (5)	
	Rosiglitazone, a PPAR- $\gamma$ agonist (7)	
	LPS (7)	
	Muramyl dipeptide (MDP) (7)	
	$\gamma$ -D-Glu-mDAP (iE-DAP) (7)	
7	Pam3CysSerLys4 (Pam3CSK4) (7)	Yes (12)
	<i>Acholeplasma lailawii</i> (12)	
	<i>Legionella pneumophila</i> (12, 14)	
	<i>Staphylococcus aureus</i> (12)	
8	Diacylated lipoprotein FSL-1 (12)	-
	<i>Toxoplasma gondii</i> (5)	
9	Rotavirus (21, 22)	Yes (21, 23) and No (21)
	Poly(I:C) (23)	
10	LPS (25)	Yes (25, 28, 35)
	Phorbol myristate acetate (PMA) plus ionomycin (28)	
	<i>Shigella flexneri</i> (30)	
	<i>Fusobacterium nucleatum</i> (31)	
	<i>Streptococcus oralis</i> (31)	
	<i>Salmonella typhimurium</i> (25)	
11	Sendai virus infection (39)	No (43)
	Poly(I:C) (39)	
	IFN- $\beta$ (both mRNA and protein) (39)	
12	Nitrous Oxide (47)	-
	<i>Yersinia pestis</i> (49)	
13	<i>Toxoplasma gondii</i> (5)	-
14	-	No <sup>9</sup>

**Table 1.3. Known Activators of the NLRP Family.** NLRP family members are activated by an assortment of ligands. The NLRP3 receptor is the most extensively characterized and is demonstrated to interact with the adaptor protein, ASC1. Little is known about the activators or the structure on some NLRP family members such as NLRP5, NLRP12, NLRP13 and NLRP14.

## CHAPTER 2: NLRP3 Inflammasome Activation in Macrophages Promotes Breast Cancer Progression.

### 2.1. Introduction

Breast cancer is the most frequently diagnosed malignancy among women and mortality from this malignancy is associated with invasive disease (282). In breast cancer in particular, the tumor microenvironment - especially intra-tumor stroma cells including macrophages - promote tumor growth and dissemination (283). Mainly through secretions, macrophages promote tumor growth, angiogenesis, and extracellular matrix (ECM) remodeling. Indeed, clinically elevated infiltration of tumor-associated macrophages (TAMs) is associated with metastatic mammary carcinoma and poor overall survival (115, 123, 284). Through their high phenotype plasticity, macrophages, including TAMs, are distributed on a phenotype polarity spectrum from exerting pro-inflammatory and cytotoxic activities (M1-like) to displaying inflammation-resolving with tissue-repair and remodel activities (M2-like) (134).

Within the tumors, crosstalk between breast cancer cells and macrophages leads to macrophages with the M2-like phenotype (285). Among the many macrophage polarity markers (286-288), measuring arginine metabolism through the ratio arginase to inducible nitric oxide synthase (Arginase/iNOS) is commonly used to define the macrophage phenotype (289, 290). Indeed, cytotoxic, anti-tumor macrophages express more iNOS and MHC class II and participate in complement-mediated phagocytosis (289-291), whereas immunosuppressive, tumor promoting macrophages express elevated arginase (289, 290).

Additionally, innate immune cells, chiefly macrophages, regulate the inflammatory microenvironment in breast cancer through the secretion of multiple pro-inflammatory cytokines (130, 291-293). The maturation and secretion key pro-inflammatory cytokines from the IL1 superfamily i.e., IL-1 $\beta$  and IL-18 are mediated by the activities of inflammasomes, especially NLRP3 inflammasomes (184). Inflammasomes are intracellular, pattern recognition receptors activated by damage associated molecular patterns (adenosine triphosphate) and pathogen associated molecule patterns (lipopolysaccharide) (183, 184). Specifically, NLRP3 inflammasomes are multiprotein complexes which consist of a nucleotide-binding and oligomerization domain-like receptor (NLRP3), an adaptor protein (ASC1) and caspase-1 (183). While inflammasome activities have been mainly investigated in infections, more recent studies have demonstrated their critical role in cancer progression and in tumor response to treatments. For example, in hematopoietic cancers, NLRP3 inflammasomes promote migration of hematopoietic stem cells into bone marrow (294). Moreover, in colorectal cancer, large infiltration of macrophages with strong NLRP3 expression resulted in faster colorectal cancer migration and NLRP3 deficiency reduced visible liver metastasis *in vivo* (161). Furthermore, NLRP3 overexpression in lung adenocarcinoma and small-cell lung cancer is associated with higher grade cancers (161, 295). In human breast cancer, as well, NLRP3 inflammasome activation observed chiefly in stroma cells, mainly macrophages, is associated with advanced disease (296). Caspase-1 and NLRP3 knockout mice implanted with EO771 and PyT8 tumors experienced reduced tumor growth and less lung metastasis (161, 162). Additionally, IL-1 $\beta$ , a product of NLRP3 inflammasome activation, is associated with angiogenesis, tumor invasiveness and metastasis in breast cancer (184, 230, 231). While

NLRP3 inflammasome activation has been demonstrated to promote a more aggressive phenotype in breast cancer (90, 122, 161, 231), less is known about effect of NLRP3 inflammasome activation on tumor-associated macrophages.

Here, we assessed whether macrophage NLRP3 inflammasome activation promoted breast tumor progression in pre-clinical studies. Our results indicate that 1. 4T1 tumor cell secretions promoted macrophage NLRP3 inflammasome activation leading to IL-1 $\beta$  and IL-18 secretion *in vitro* and *in vivo*, which 2. Increased the presence of TAMs with immunosuppressive and tumor-promoting phenotypes and 3. Favored breast tumor stem cells and metastasis.

## **2.2. Methods**

### **Cell Culture**

RAW264.7 and J774A.1 (hereto forth abbreviated as RAW and J774 respectively) monocyte macrophages were purchased from ATCC (Manassas, VA). Bone marrow derived macrophages (BMDM) were harvested from C57BL/6 and CD1 mice as previously (297, 298). Briefly, after euthanasia, femurs and tibias were surgically cleaned, both bone heads excised, and the bone shaft flushed with sterile media. Collected cells were washed and plated in media supplemented with CSF-1 rich LADMAC conditioned media renewed thrice weekly and adherent and differentiated BMDMs were collected after a 7–9-day incubation (299). 4T1 cells are aggressive mammary cancer cells that mimic the later stage of breast cancer in humans (300). Cells were grown and cultured in DMEM supplemented with antibiotic, antifungal, and 10% of FBS (Atlanta biologic, Atlanta, GA). Prior to treatment with negative control (FBS-free media), positive control (LPS 5ug/ml + ATP 5mM) and 4T1 conditioned media, RAW, J774 and BMDM cells were incubated in FBS-free media (0% FBS) for 3 hours. Cells were then harvested for flow-cytometry and immunohistochemistry analyses. Additionally, both cell lysates and supernatants were collected and stored at -20°C until use in western blots and cytokine measurements.

### **Immunoblot Analyses**

For western dot-blots, *in vivo* tumor lysates, macrophage lysates and macrophage supernatants were combined with 10mM CTAB detergent and loaded onto 45mm nitrocellulose membranes (GE) using a dot-blot apparatus (ThermoFisher). Membranes were assessed for protein loading using Ponceau (Sigma) staining and then blocked in 5% milk TBS – Tween 20 buffer (Boston Biologicals). After blocking, blots were incubated

with primary antibodies against NLRP3 (1:1000; R&D Systems, Inc.), ASC1 (1:600; Santa Cruz Biotech.), cleaved caspase 1 (1:500; Santa Cruz Biotech.), arginase (1:500; Santa Cruz Biotech.), iNOS (1:500; Santa Cruz Biotech.), IL-1 $\beta$  (1:500; Santa Cruz Biotech.), IL-18 (1:500; Santa Cruz Biotech.) overnight at 4°C under gentle rocking. After removal of the primary antibody and washes in TBST buffer, blots were incubated with species-specific secondary HRP conjugated antibody for 1hr in similar conditions. After secondary antibody removal and multiple TBST buffer washes, the presence of the protein of interest was revealed following incubation with ECL substrate (Biorad) and detection using the MP Bioimager (Biorad). For each blot, protein signal was quantified using Image J and Protein Array Analyzer plugin (NIH). Protein expressions were normalized to protein loading defined by ponceau staining. In addition, protein expression detected in *in vivo* tumor lysates were normalized by average expression in control animals implanted with 4T1 cells alone and treated with saline (control conditions).

### **Phagocytosis Assay**

J774 cells were grown to confluency in a 96-well plate and treated with negative control (media alone), positive control (LPS 5 $\mu$ g/mL + ATP 5mM) and 4T1 conditioned media for 6 hours. Red fluorescent beads (10mm FluoroMax, ThermoScientific) and Hoechst (Molecular Probes) were added at ~6 hours after the initial treatment and washed after 30 minutes. Media was replaced with PBS and readings at both 360/460 and 530/580 excitation/emission wavelengths measured cell concentration and phagocytosis through Hoechst nuclear dye and red fluorescence, respectively. A phagocytosis index defined as the bead fluorescence relative to cell concentration / number (based on Hoechst nuclear intensity or number) normalized to control conditions was used to quantify phagocytosis.



Microphotographs were obtained using a IX71 microscope fitted with a DP70 camera and software (Olympus). Representative overlapping composite microphotographs were generated using ImageJ (NIH).

### **Tumor Cell Proliferation Assay**

4T1 cells were seeded and at 70-80% confluence, cells were incubated in FBS-free media for 6 hours, then treated with macrophage conditioned media (50% vol.). Macrophage conditioned media were collected following a 48hrs incubation of confluent macrophages in FBS-free media with macrophages, centrifugated using 0.2mm sterile filters (FisherScientific) and stored at -20°C until use. After a 24-hour incubation, 4T1 cell growth was determined using MTT assay. Briefly, MTT solution (Sigma) was added and after a 3-hour incubation, cell culture media was removed and 150uL of MTT solvent added. Following a 30-min incubation, proliferation determined as the 570nm (minus background at 630nm) absorbance using a microplate reader (Bio-Tek).

### ***In Vivo* Tumor Study**

*In vivo* experiments were conducted in the UNC Charlotte vivarium under veterinarian supervision and following approved IACUC protocols. Briefly, 4T1RFP (Imanis Inc), RAW and J774 cells (ATCC) were grown in sterile conditions collected, counted, and prepared for injection. Three different syngeneic cell implantations were tested: 4T1RFP cells alone, 4T1RFP cells + J774 cells (5:1) and 4T1RFP cells + RAW cells (5:1). Acclimated Balb/c female 6-week-old mice (Jackson Laboratory) (n=6 per treatment group) were orthotopically implanted in the mammary fat pad with one of the cells suspensions ( $10^5$  tumor cells without or with 20,000 J774 or RAW macrophages in 50 ml). Allocation to either injection group was random. Following implantation, primary

tumor growth was monitored weekly using both calipers and IVIS imaging as detailed previously (301).

Thirty-five (35) days post-tumor implantation, primary tumors and tissue including liver, spleen, lungs, bone (femurs and tibias) were collected and weighted. A part of each primary tumor was processed to generate tumor lysate through addition of T-PER (Thermo Scientific) lysis solution supplemented with a cocktail of protease inhibitors (Roche biologicals) and sonication on ice. The other primary tumor part was fixed in buffered formalin (4%) and then processed using classical histological techniques and 5-6 mm thick slides were used to assess the presence, location and abundance of specific proteins including active caspase 3, a marker of apoptosis. Whole or portions of the organs were similarly treated to generate lysates. For bones, after grinding in a mortar using a pestle. Grinded bone tissue, lungs, liver, and blood cells were mixed with the lysis buffer detailed above and sonicated on ice to generate lysates. All lysates that were stored at -20°C until use. For blood, after the draw in heparinized syringes, the blood was diluted with sterile PBS (0.5 vol), centrifugated and the plasma fraction collected and stored at -20°C until use. Blood cell pellets were combined with the lysis solution (see above) and sonicated before -20°C storage.

### **Cell Proliferation and Cell Apoptosis**

Both proliferation and apoptosis were assessed through using antibodies specific to the cell division proliferation marker, Ki67, and the apoptosis marker, active caspase 3. Both *in vitro* cell lysates and tumor lysates were assessed by Western Dot blots as described above. The expression of Ki67 and caspase 3 was determined and compared as above.

In addition, for each tumor paraffin embedded and formalin fixed tumor sections (5-6mm thick) were processed to remove paraffin, enhance antigen access through incubation in antigen retrieval solution (Dako) and, then, after a blocking incubation step (with BSA 1% in TBS Tween 20) incubated overnight in humidified chamber in the presence of either Ki67 (1:100 in blocking buffer, Santa Cruz Biotech.) or active caspase 3 (1:100 in blocking buffer, Santa Cruz Biotech.). Following wash, tissue slides were incubated with HRP-conjugated secondary antibody (Vector) following manufacturer's recommendations. After a wash step, the presence of the protein was revealed through incubation with DAB (Impact DAB stain, Vector). Tissue slides were lightly counterstained with hematoxylin (Vector), dehydrated through successive incubations in alcohol and xylene. Tissue slides mounted using a mounting solution (Vector) and slip covered (Fisher scientific). After hardening of the mounting media, tissue slides were assessed by microscopy. For each tumor, the entire tumor was microphotographed with overlapping edges and composite microphotograph obtained were assessed for DAB stain using Image J and DAB stain plugin. Both intensity and coverage (%) were recorded and normalized to tumor size. Necrotic regions were excluded.

### **Assessing Metastasis**

Metastasis was assessed first through gross anatomy visual evaluation of macro-metastases at euthanasia. In addition, the presence of dsRED protein was evaluated in organ lysates including blood, spleen, liver, lung and bone. Briefly, organ lysates centrifugated to remove debris and supplemented with SDS detergent (0.4% final) were loaded onto 45mm nitrocellulose using a dot blot apparatus (ThermoFisher). Western dot blots were evaluated for protein loading using the reversible Ponceau stain and blocked in 5% milk

TBST buffer. Blots were then incubated overnight anti-dsRED antibody (1:1000; MyBioSource Inc). After washing and incubation with a secondary HRP-conjugated antibody, the presence of dsRED was revealed following incubation with ECL substrate (Biorad) and chemiluminescence detection (MPchemi; Biorad). dsRED signals were quantified using Image J fitted with Protein Array Analyzer plugin (NIH). For each organ, signals 1.5-fold the average standard deviation was indicative of the presence of metastases and the frequency of metastases per tissues and group was recorded.

### ***In Silico* Genetic Alteration Analysis**

The open web-based database cBioPortal, that allows inquiries about clinical outcomes and specific genetic alterations, was used (247, 251). We assessed *in silico*, the effects of both amplification and deep deletion akin to overexpression and lack of expression, respectively. The cohort of patients assessed was limited to breast cancer and breast cancer invasive carcinoma (n=10,197 patients). Key genes associated with either cell type (macrophage, CD68), phenotype (M1 macrophage arginase, and M2 macrophages iNOS) as well as pro-inflammatory cytokines (IL-1 $\beta$ , IL-18) were assessed. Whether the genetic alteration was associated with a change in patient overall survival when comparing the cohort of patients without the genetic defect and the cohort of patients with the genetic defect was compared. Variations in median overall survival derived from Kaplan Meier curves (in months) and Log-rank test p value are reported.

### **Statistical Analysis**

All data are presented as mean  $\pm$  SEM. Graphs were obtained and statistical analyses conducted using Prism 9.0 (GraphPad). Differences between groups were analyzed using one-way ANOVAs and Fisher's LSD test unless noted. Survival patients'

data were assessed through Log rank test as determined through cBioPortal (247, 251). Correlation analyses were assessed using linear regression models. Significant differences between treatment groups are reported as (\*)  $p < 0.1$ , \*  $p < 0.05$ , \*\*  $p < 0.01$  and \*\*\*  $p < 0.001$ .

## 2.3. Results

### **NLRP3 Inflammasomes are Differentially Expressed by Macrophages.**

First, we determined expression of NLRP3 inflammasome protein sub-units and NLRP3 inflammasome activities of bone marrow-derived macrophages (BMDMs), J774 and RAW monocyte/macrophages. BMDMs, J774, RAW cells were treated with the combination LPS and ATP, known inflammasome activators (189, 275-277, 302), and 4T1 tumor cell conditioned media (4T1CM) and both the expression of NLRP3 inflammasome proteins and their activities i.e., the secretion of IL-1 $\beta$  and IL-18 cytokines were determined. All macrophages expressed NLRP3, regardless of LPS+ATP or 4T1CM treatment. However, NLRP3 expression was significantly lower in BMDMs compared to J774 and RAW macrophages (Fig. 2.1.A,  $p<0.05$ ). While expressed by all macrophages tested, the adaptor protein ASC1 was highly present in J774 compared to RAW or BMDM regardless of treatment (Fig. 2.1.B,  $p<0.001$ ). In contrast to J774 macrophages, ASC1 expression increased and decreased following incubation with LPS+ATP and tumor conditioned media in BMDM and RAW macrophages, respectively ( $p<0.05$ , Fig. 2.1.B). The expression of active caspase 1 was higher in J774 cells compared to the other macrophages tested ( $p<0.05$ , Fig. 2.1.C).

LPS and ATP treatment in all macrophages tested promoted the secretion of the pro-inflammatory IL-1 $\beta$  cytokine significantly in RAW cells ( $p<0.01$ , Fig. 2.2.A). Contrasting with IL-1 $\beta$  secretions, IL-18 secretions were only marginally altered regardless of treatment (Fig. 2.2.B). Moreover, LPS+ATP treatment led to significant decreases in IL-18 secretions by both BMDMs and J774 macrophages ( $p<0.05$ , Fig. 2.2.B). The endogenous antagonists to IL-1 $\beta$  and IL-18 were also measured. Interestingly, secretions

of IL-1RA by J774 macrophages and BMDMs were marginally increased in the presence of 4T1CM ( $p < 0.08$ , Fig. 2.2.C). IL-18BP secretions were unaffected by treatment, however, IL-18BP secretions by BMDMs were significantly lower than that of J774 and RAW cells ( $p < 0.01$ , Fig. 2.2.D).

### **NLRP3 Inflammasome Activation Promotes Pro-Tumorigenic Macrophages.**

Next, we assessed whether inflammasome activation led to pro-tumorigenic macrophages. In particular, the arginase : iNOS expression ratio, a marker of the M2 phenotype (286, 290), in macrophages treated with the NLRP3 inflammasome activator LPS + ATP or 4T1CM were assessed (Fig. 2.3.A). While in untreated conditions, arginase : iNOS expression ratios were similar regardless of the macrophages, following LPS and ATP inflammasome activation treatment, J774 macrophages displayed a significantly (3-fold) greater arginase : iNOS expression ratio compared to RAW and BMDM ( $p < 0.001$ , Fig. 2.3.A).

In addition, the phagocytic abilities of J774 macrophages, another marker of M2 macrophages (303), were assayed by determined the engulfing of 10mm fluorescent beads (Fig. 2.3.C). Treatment with both the inflammasome activator LPS and ATP and 4T1 CM led to a 2-fold reduction in J774 phagocytosis ( $p < 0.01$ , Fig. 2.3.D).

Moreover, as elevated arginase expression and decreased phagocytic activity were indicative of a more M2-like macrophage phenotype akin to a tumor-supporting phenotype for J774 macrophages, we assessed whether macrophage secretions (conditioned media) altered 4T1 tumor cell *in vitro* proliferation (Fig. 2.3.B). A 24hr incubation with CMs from BMDMs, J774 or RAW macrophages promoted 4T1 proliferation *in vitro* compared to control conditions (0% i.e., FBS-free media). Interestingly, both BMDM and J774

conditioned media more significantly promoted 4T1 proliferation compared to RAW conditioned media ( $p < 0.05$ , Fig. 2.3.B).

### **Tumor Growth Following Co-Implantation of Tumor Cells and Macrophages in the *In Vivo* Immunocompetent 4T1 Preclinical Breast Cancer Model.**

Given the low endogenous immune cell infiltration in mammary tumor preclinical models (304), to ascertain the effect of the macrophage presence within the 4T1 tumor mass, we assessed primary tumor growth following the orthotopic implantation of either 4T1 tumor cells alone or 4T1 tumor cells + J774 macrophages or + RAW macrophages in syngeneic immunocompetent Balb/c mice using calipers and by tumor weight after 35 days.

Regardless of the implantation: 4T1 tumor cells alone or combined with J774 or RAW macrophages, all tumors grew overtime ( $p < 0.001$ , Fig. 2.4.A). While no difference in wet tumor weight at euthanasia was observed ( $312.0 \pm 97.6$  vs.  $556.4 \pm 115.8$  vs.  $547.6 \pm 122.3$  mg for 4T1 alone, 4T1+RAW and 4T1+J774 implantation, respectively), analysis of the ratio Ki67/caspase 3, a measure of the net tumor proliferation, demonstrated that the presence of syngeneic J774 but not of RAW macrophages was associated with a significant decrease in proliferation ( $p < 0.05$ , Fig. 2.4.B and C) compared to controls (implantation of 4T1 cells alone).

### ***In Vivo* Co-Implantation of Macrophages and 4T1 Tumor Cells Led to a Pro-Tumorigenic Microenvironment.**

Next, we assessed the presence of macrophages (CD68+) in tumor lysates. As expected, co-implantations with either J774 or RAW syngeneic macrophages led to significant increase in CD68 expression in orthotopic 4T1 primary tumors ( $p < 0.05$ , Fig.



2.5.A). Interestingly, the Arginase : iNOS expression ratio, a marker of pro-tumorigenic macrophages was significantly increased (~8-fold higher) in the presence of J774 macrophages ( $p < 0.05$ , Fig. 2.5.B). Moreover, intra-tumoral IL-1 $\beta$  and IL-18 pro-inflammatory cytokine concentrations were increased in tumor masses derived from co-implantation with 4T1 tumor cells combined with J774 (but only marginally for IL-1 $\beta$  with RAW macrophages, Fig. 2.5.C) compared to tumors derived from orthotopic implantation of 4T1 tumor cells alone ( $p < 0.05$ ; Fig. 2.5.C and D).

Of note, the intra-tumoral expression of IL-1 $\beta$  and IL-18 was positively correlated with 35-days post inoculation tumor weight (Supplemental Fig. 2.1.A and B;  $R^2 = 0.48$ ,  $p < 0.001$  and  $R^2 = 0.35$ ,  $p < 0.001$ , respectively). Likewise, the arginase : iNOS expression ratio of was positively correlated with tumor weight (Supplemental Fig. 2.2.;  $R^2 = 0.09$ ,  $p < 0.04$ ). Lastly, intra-tumoral IL-1 $\beta$  and IL-18 expression was strongly associated with arginase expression (Supplemental Fig. 2.1.C and D;  $R^2 = 0.61$ ,  $p < 0.001$  and  $R^2 = 0.60$ ,  $p < 0.001$ , respectively).

### **Co-implantation of 4T1 Tumor Cells and Syngeneic Macrophages Promoted Tumor Stem-Like Characteristics *In Vivo*.**

Next, tumor stem-like characteristics, defined by cytokeratin 19, aldehyde dehydrogenase 1/2 and N-cadherin : E-cadherin ratio were determined in tumor mass following a 35-day tumor cell and macrophage co-injections.

Notably, cytokeratin 19 expression was elevated in tumor derived from 4T1 tumor cells co-implanted with J774 macrophages compared to 4T1 tumor cells alone or to 4T1 tumor cell co-implanted with RAW macrophages (Fig. 2.6.A,  $p < 0.05$ ). Additionally, elevations in cytokeratin 19 expression are strongly related to arginase expression within

the tumor (Supplemental Fig. 2.3.A,  $R^2=0.46$ ,  $p<0.001$ ). Additionally, expressions of aldehyde dehydrogenase 1/2 and the N-cadherin : E-cadherin expression ratio were marginally increased especially in tumors generated from co-implantation of 4T1 tumor cells with J774 macrophages compared to 4T1 cells alone ( $p<0.1$ , Fig. 2.6.B and C). Both aldehyde dehydrogenase 1/2 and the N-cadherin : E-cadherin expression ratio were correlated with arginase expression (Supplemental Fig. 2.3.B and C;  $R^2=0.30$ ,  $p<0.001$ ,  $R^2=0.18$ ,  $p=0.002$ , respectively).

### **Co-Implantation of 4T1 Tumor Cells with Macrophages Promoted Metastases.**

The presence of metastases in distant organs was determined based on both visual macroscopic inspection of organs and through assessment of the presence of dsRED protein in organ lysates. Macroscopically, both mesenteric and liver metastases were observed in only animals co-implanted orthotopically with 4T1 tumor cells and J774 macrophages (40% and 60%, respectively, Fig. 2.7.A) but not in mesenteric tissues and livers from animals implanted with 4T1 tumor cells alone or in combination with RAW macrophages (Fig. 2.7.A).

Furthermore, micro-metastases assessed through the presence of dsRED protein in organ lysates were detected in the liver and bones of mice co-implanted with 4T1 cells and J774 macrophages. Micro-metastases were also present in the lungs and spleen of animals implanted with 4T1 alone and the liver of mice implanted with 4T1 and RAW macrophages (Fig. 2.7.B).

## **Genetic Alterations in Macrophage Markers and Pro-Inflammatory Cytokines are Associated with Breast Cancer Patients' Overall Survival.**

To confirm the clinical relevance of the alterations observed *in vitro* and *in vivo* preclinical models, cohorts of human breast cancer patients with either amplification or deep deletion of genes associated with the presence macrophages and macrophage subtypes and IL-1 $\beta$  and IL-18 pro-inflammatory cytokines were analyzed (Table 2.1.) *in silico* through cBioPortal (247-274) .

Whereas genetic alterations of CD68 are rare; compared to patients without alteration in CD68 gene, breast patients with CD68 alterations shows a significant 10-year decrease in overall survival (Table 2.1.). Deep deletion akin to lack of CD68 expression specifically reduced breast cancer patient overall survival ( $p \sim 0.05$ , Table 2.1.). The genes associated with specific macrophage phenotypes were also assessed *in silico*. While no significant change in breast cancer patients' overall survival was associated with alterations in CD206 and only marginally with arginase deep deletion ( $p \sim 0.05$ , Table 2.1.), iNOS gene alterations both amplification and deep deletion were associated with significantly lower overall survival (by 3.3 and 7.6 months, respectively,  $p < 0.01$ , Table 2.1.)

Regarding the IL1 superfamily of pro-inflammatory cytokines, especially IL-1 $\beta$  and IL-18, no association between genetic alteration in IL-1 $\beta$  and survival was observed (Table 2.1.). However, IL-18 genetic alterations especially deep deletion of IL18 was associated with a significant 7.3-year decrease in breast cancer patients' overall survival.

## 2.4. Discussion

Tumor-associated macrophages (TAMs) are a prognostic indicator of invasive disease and poor overall survival in breast cancer (115, 123, 284). Elevated macrophage infiltration is associated with increased tumor growth, invasion, and metastasis (127, 305, 306). However, the mechanisms associated with the macrophage phenotype and activity alteration within the tumor microenvironment that support cancer growth is only partially understood. A better understanding of the macrophage switch toward a pro-inflammatory, pro-tumorigenic phenotype may uncover therapeutic targets to stir macrophages toward an anti-tumor phenotype (307, 308). Among the multiple mechanisms associated with macrophage alterations, in particular, toward a pro-tumorigenic phenotype, the activation of inflammasome especially NLRP3 inflammasome has garnered interest recently (286, 309). Indeed, NLRP3 activation within macrophages is associated with secretions of pro-inflammatory cytokines and the support of tumor cell growth, EMT transition, and migration (134, 310, 311). Here, *in vitro*, the effects of inflammasome activator combination LPS and ATP, and incubation with 4T1 tumor cell conditioned media were assessed on BMDMs, J774 and RAW macrophage phenotype and activities. In addition, *in vivo*, the effects of co-implantation of 4T1 tumor cells with macrophages on tumor phenotype and progression in an immunocompetent murine model was determined. Our data support that 1. *in vitro* macrophage NLRP3 inflammasome activation led to IL-1 $\beta$  and IL-18 secretion, 2. activation of macrophage NLRP3 *in vivo* led to TAMs with immunosuppressive and tumor-promoting phenotype that, in turn, 3. favored breast tumor stem cells and metastasis.

To more closely mimic the potential of macrophages in mammary tumor progression, we investigated the crosstalk between the aggressive 4T1 tumor cells and macrophages *in vitro* and *in vivo* and whether NLRP3 activation was associated with tumor progression. Beside syngeneic primary macrophages and J774 macrophages both with functional NLRP3 signaling, syngeneic RAW macrophages with defective NLRP3 inflammasome signaling were tested. As expected NLRP3 expression and activation was observed following *in vitro* incubation with the known NLRP3 inflammasome activator LPS+ATP in both J774 cells and BMDMs confirming prior observations (189, 276, 312). In contrast, RAW cells while expressing NLRP3, had much lower ASC1 expression and limited Caspase 1 expression supporting the demonstrated defect in RAW inflammasome signaling (313). Indeed, J774, RAW, and primary-derived monocytes (BMDM) differentially express the three major components of the NLRP3 inflammasomes: the cytosolic receptor (NLRP3), the adaptor (ASC1) and the effector caspase (caspase 1). ASC1 is an essential connector regulating NLRP3 inflammasome assembly and activation (167, 314). Consequently, active caspase 1 was lesser expressed in ASC1-deficient RAW macrophages compared to J774 macrophages. While active caspase 1 was, as expected, reduced in the NLRP3 signaling defective RAW cells, suggesting that those cells secreted the pro-inflammatory IL-1 $\beta$  likely through the non-canonical inflammasome activation by LPS via caspase 11 as demonstrated earlier (315).

Additionally, our data indicate that NLRP3 activation promotes a pro-tumorigenic macrophage phenotype as highlighted by the increase in the arginase (M2-type) to iNOS (M1-type) expression ratio in functional NLRP3 signaling, J774 macrophages following incubation with inflammasome activators. Moreover, the shift toward a tumor promoting

phenotype was associated with a decrease in phagocytic activity associated with pro-tumorigenic (M2-like) macrophages (135). Similar observations were made when comparing implantation of 4T1 cells alone and co-implantation with J774 macrophages. Indeed, arginase to iNOS expression ratio was greater in primary tumors obtained animals co-injected with 4T1 and J774 macrophages compared to tumor derived from implantation of 4T1 tumor cells alone. Moreover, elevated arginase expression was positively correlated with increased tumor weight while no correlation of tumor weight to intra-tumoral iNOS expression was detected. The overexpression of arginase observed here has been shown to induce T-cell anergy through the depletion of L-arginine and generation of toxic urea (316). Our data also indicate that pro-inflammatory IL-1 $\beta$  and IL-18 intra-tumoral expression polarized macrophages toward pro-tumor (M2-like) phenotype (317, 318), and was positively associated with arginase, but not iNOS expression. Congruent with our findings, IL-1 $\beta$  and TNF- $\alpha$  induced arginase expression through IL-33 secretion and recombinant IL-18 treatment increased arginase expression in monocytes (242, 319).

IL-1 $\beta$  and IL-18 expression were positively correlated with stem-like characteristics *in vivo*. Indeed, IL-1 $\beta$  signaling promotes epithelial-mesenchymal transition and increased expression of the IL-1 $\beta$  receptor, IL-1R1, and is associated with both proliferation and quiescent ALDH-positive stem cells in breast cancer (90, 320).

Moreover, compared to secretions from RAW macrophages, J774 conditioned media promoted the growth of 4T1 tumor cells *in vitro*. These data support the activation of NLRP3 triggering, or at least associated with, the pro-tumorigenic macrophage phenotype. Weight of tumors derived from co-implantation of 4T1 tumor cells with either J774 or RAW macrophages tended to be higher compared to tumor derived from 4T1 tumor

cells implantation alone supporting the effects of tumor-associated macrophages on tumor growth possibly through a shift toward M2-like, pro-tumor macrophages as the disease progresses (321). Interestingly, activation of NLRP3 inflammasome in tumor-associated macrophages has been correlated with invasion and metastasis (311). Our data following co-implantation of 4T1 tumor cells and J774 macrophages leading to increased liver and bone metastasis support the role of macrophage NLRP3 activation in metastasis.

The clinical relevance of NLRP3 inflammasome protein, macrophage phenotype marker and pro-inflammatory cytokine expression assessed *in silico* highlighted that overexpression (akin to gene amplification) and especially lack of expression (akin to gene deep deletion) of CD68, iNOS and IL-18 were associated with a worsening of overall survival.

Taken together our data support a role for macrophages in the promotion of breast cancer growth in part through the activation of the NLRP3 inflammasome by tumor cells leading to a phenotype change toward M2-like, pro-tumorigenic macrophages. Moreover, our data support further investigations of NLRP3 activation as a target to prevent the switch of macrophage phenotype toward a pro-inflammatory, pro-tumorigenic phenotype that promotes breast cancer progression.

## 2.5. Figures

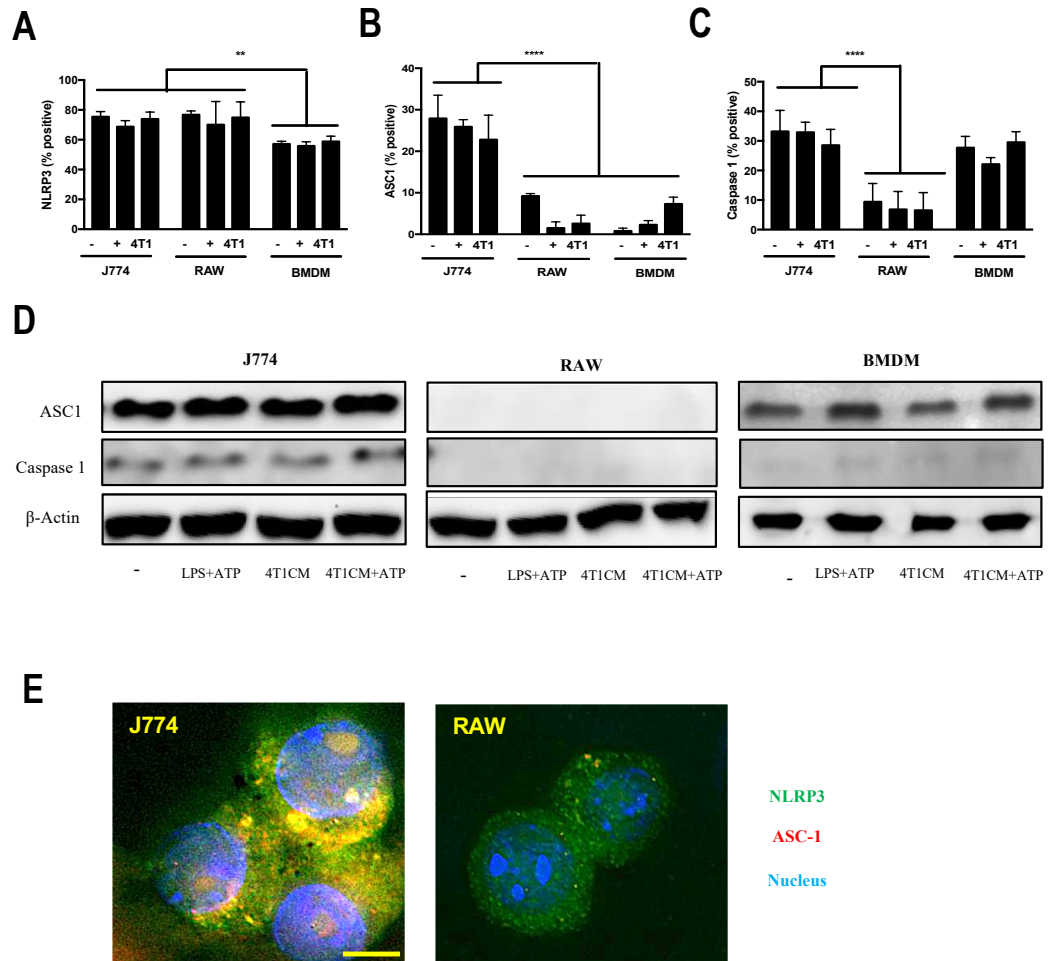


**Figure 2.1. NLRP3 Inflammasome Expression is Elevated in J774 Macrophages.** Flow cytometry analysis of **A**. NLRP3, **B**. ASC1, **C**. cleaved caspase 1 expression for J774, RAW, and bone marrow-derived macrophages (BMDM). **D**. ASC1 and cleaved caspase 1 expression as demonstrated by western blot was highest among J774 cells. **E**. Confocal microscopy shows that both J774 and RAW macrophages have diffuse NLRP3 expression, however, expression of ASC1 and colocalization with NLRP3 is significantly greater in J774 macrophages. \*\*\*  $p < 0.001$



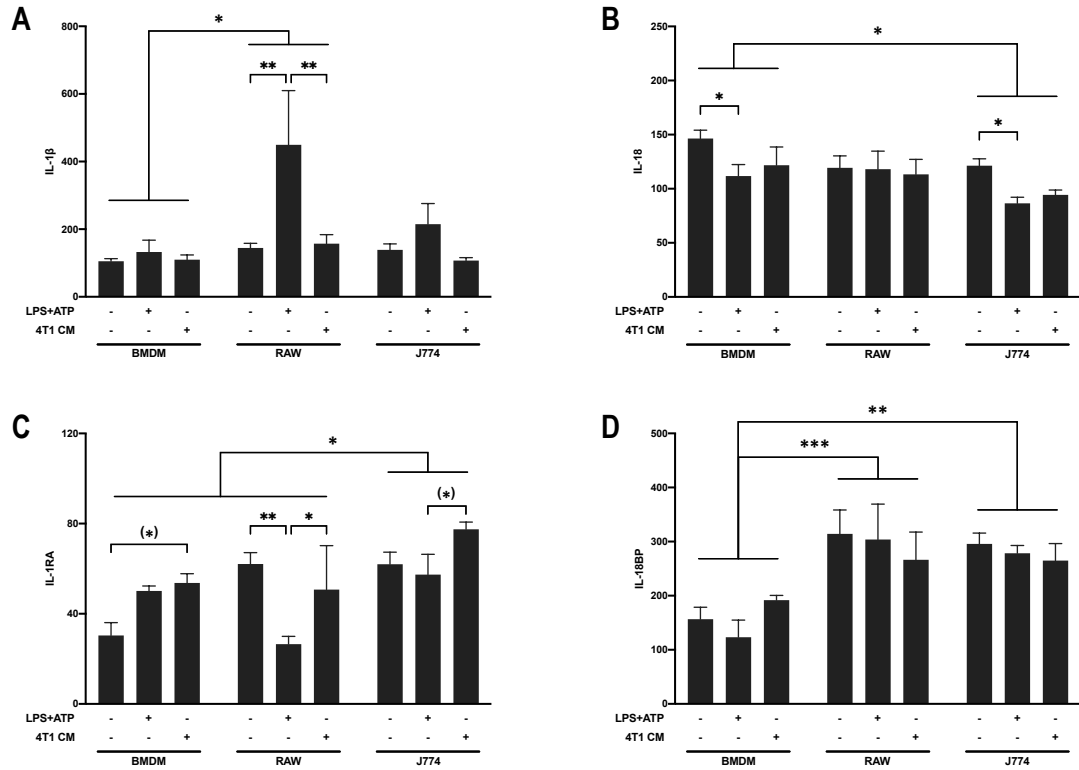


**Figure 2.2. Pro-Inflammatory Cytokine Secretion by Macrophages.** Immunoblot quantification relative to protein loading of **A.** secreted IL-1 $\beta$  by J774, RAW, and BMDM. Secretion of IL-1 $\beta$  was greater by RAW cells compared to BMDM. All macrophages secreted more IL-1 $\beta$  in response to LPS+ATP treatment compared to 4T1CM or No treatment. **B.** BMDM secreted more IL-18 compared to J774 cells. For both BMDM and J774, secretion of IL-18 was decreased following LPS+ATP treatment compared to control. **C.** IL-1 receptor antagonist (IL-1RA) was secreted most by J774 cells. In RAW cells, IL-1RA secretion was lowest following LPS+ATP treatment compared to control or 4T1CM treatment. **D.** Soluble antagonist to IL-18 (IL-18BP) secretion was lowest by BMDM. \*\*\*  $p < 0.001$ , \*\*  $p < 0.01$ , \*  $p < 0.05$ , (\*)  $p < 0.1$ .

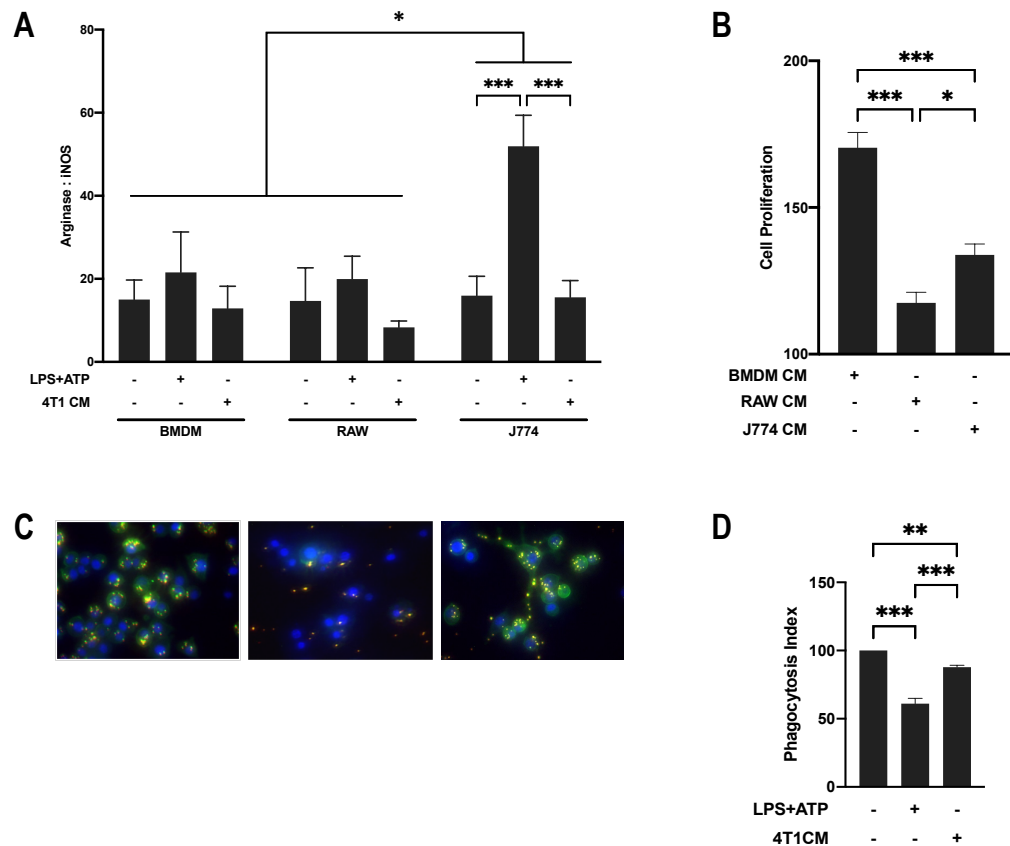


**Figure 2.3. NLRP3 Inflammasome Activation in Macrophages Results in Pro-Tumorigenic Macrophages.** **A.** Immunoblot quantification of Arginase : iNOS ratio relative to protein loading is highest in J774 compared to RAW and BMDM. For all cells, the expression of Arginase : iNOS is increased following LPS+ATP treatment. For J774 cells, this LPS+ATP induced increase is significant. **B.** MTT assay of 4T1 tumor cells treated with macrophage CM for 24hrs normalized to 0% FBS. Treatment with conditioned media from BMDM had the most positive effect on the proliferation of 4T1 cells. J774CM treatment increased 4T1 tumor cell proliferation compared to RAW cells. **C.** Representative microphotographs from the J774 phagocytosis assay depicting beads (yellow) to nuclei (blue) of no treatment (left), LPS+ATP (middle), and 4T1CM (right). **D.** Phagocytic activity of J774 macrophages normalized to no treatment was most decreased following LPS+ATP treatment.\*\*\*  $p < 0.001$ , \*\*  $p < 0.01$ , \*  $p < 0.05$ .

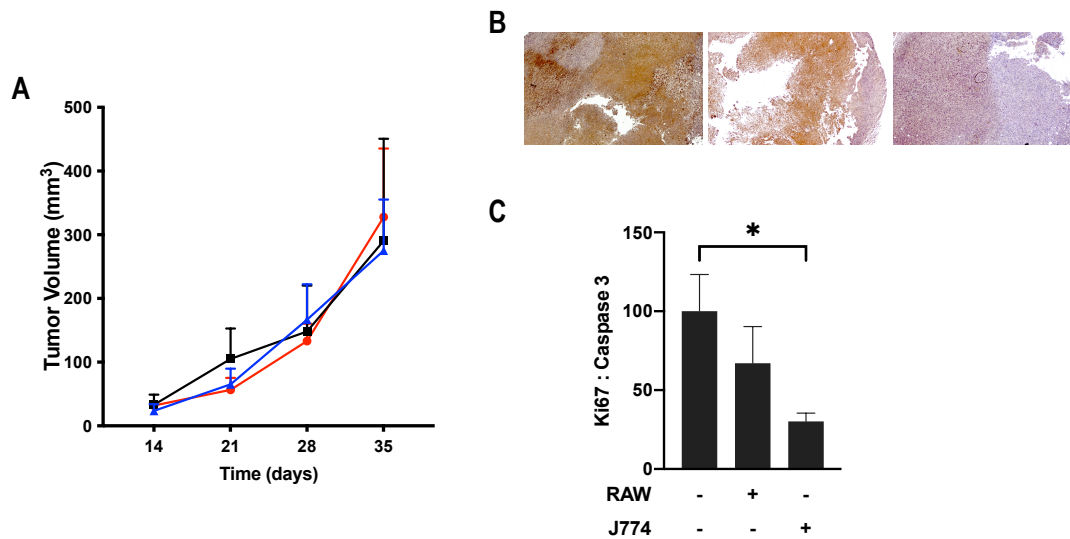


**Figure 2.4. NLRP3 Inflammasome Competent Macrophages Promote Tumor Growth.** Balb/c mice were implanted with 4T1 tumor cells with or with J774 or RAW macrophages. **A.** Tumor volume as measured by calipers weekly of mice implanted with 4T1 cells alone (black), 4T1 tumor cells and RAW macrophages (blue) and 4T1 tumor cells and J774 macrophages (red). At the 35-day endpoint, mice were sacrificed, and the tumors were excised. **B.** Immunohistochemistry of active caspase 3 expression in tumors from mice implanted with 4T1 alone (left), 4T1 and RAW cells (middle) and 4T1 and J774 cells (right). **C.** By immunoblot, the ratio of Ki67 to active caspase 3, or growth to apoptosis, was assessed. \* p<0.05

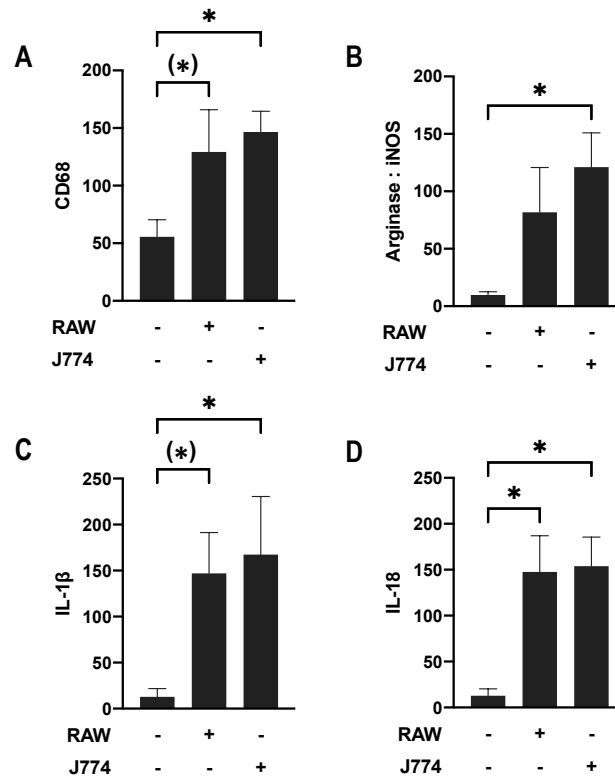


**Figure 2.5. Macrophage Infiltration is Associated with a Pro-Inflammatory Microenvironment *In Vivo*.** Intra-tumoral expression at 35-day post-implantation with 4T1 tumor cells with and without RAW and J774 macrophages. normalized to the 4T1 tumor cell alone group. **A.** CD68 expression, representative of macrophage infiltration, is elevated in mice co-implanted with RAW and J774 macrophages. **B.** The ratio of arginase to iNOS was elevated in the tumors of mice co-implanted with 4T1 and J774. **C.** IL-1 $\beta$  and **D.** L-18 intra-tumoral expression normalized relative to tumor mass and 4T1 tumor cell only control. Animals with J774 macrophages co-implanted into mammary tissue had elevated intra-tumoral expression of IL-1 $\beta$  and the co-implantation of either J774 and RAW macrophages lead to increased IL-18 expression. \* p<0.05, (\*) p<0.1.

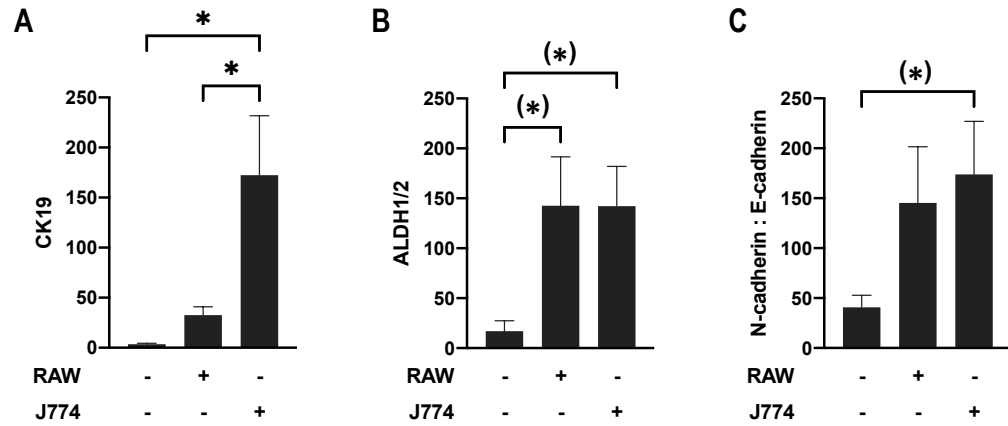


**Figure 2.6. Pro-Tumorigenic Macrophages Promote Tumor Growth and Stemness *In Vivo*.** Intra-tumoral expression at 35-day post-implantation with 4T1 tumor cells with and without RAW and J774 macrophages. normalized to the 4T1 tumor cell alone group. **A.** Cytokeratin 19 expression was greatest in tumors of mice implanted with J774 macrophages. **B.** Expression of aldehyde dehydrogenase (ALDH1/2) was greater in mice co-implanted with either RAW or J774 macrophages compared to tumors implanted with 4T1 cells alone. **C.** The ratio of N-cadherin to E-cadherin is marginally increased in mice co-implanted with 4T1 and J774 cells compared to 4T1 cells alone. \*  $p < 0.05$ , (\*)  $p < 0.1$

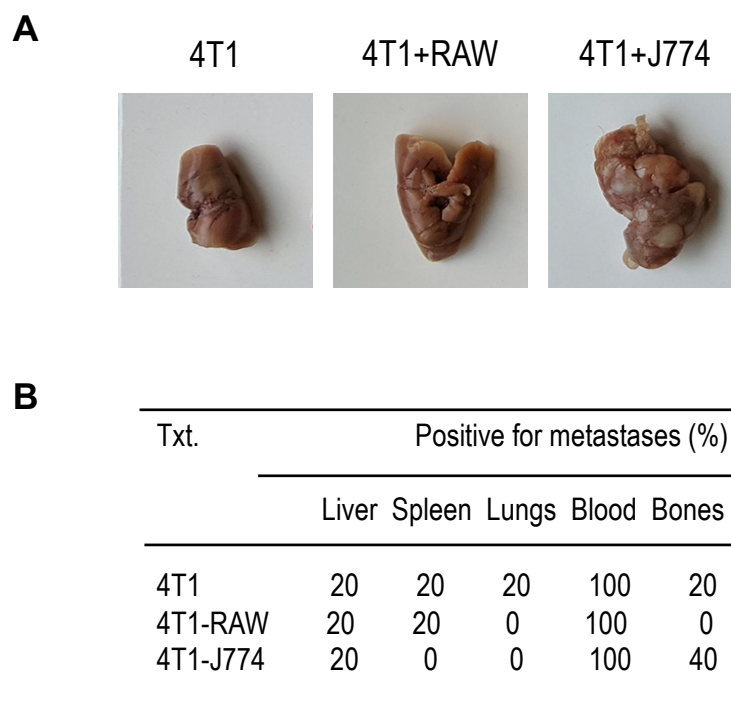


**Figure 2.7. Co-Implantation with J774 Macrophages Promotes Metastasis. A.** Representative photos of liver metastasis from animal implanted with 4T1 tumor cells alone (left), 4T1 and RAW cells (middle) and 4T1 and J774 cells (right). **B.** The rate of organ metastasis quantified by immunoblot detection of dsRED expression in distant organs. Metastasis to the liver and bone was dependent on macrophage implantation.

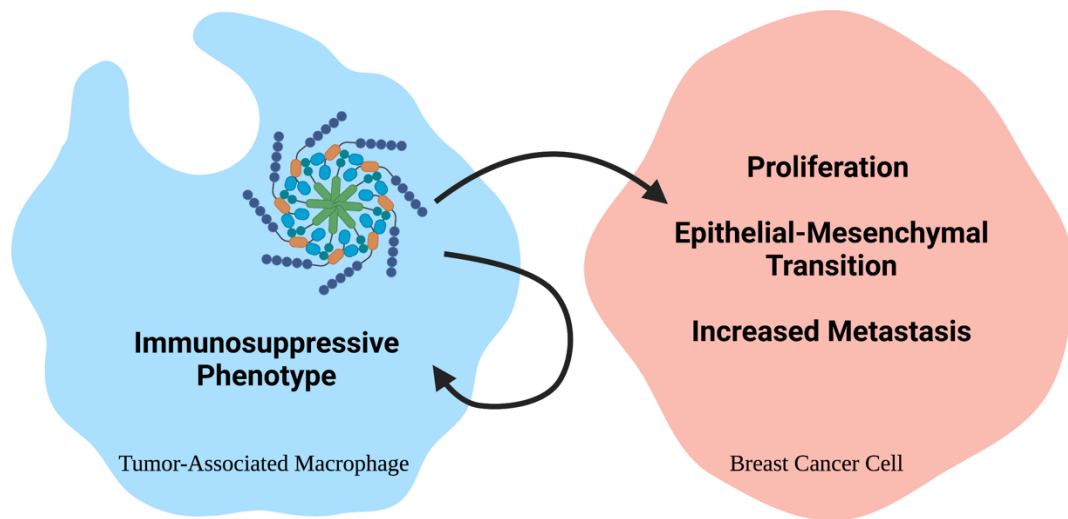


**Figure 2.8. Schema of the Proposed Effects of NLRP3 Inflammasome Activation on Breast Cancer Cells.** NLRP3 inflammasome activation in macrophages is associated with an immunosuppressive and pro-tumorigenic phenotype that promotes the proliferation, stemness and metastasis of tumor cells. Generated by KH using BioRender.com

## 2.6. Tables

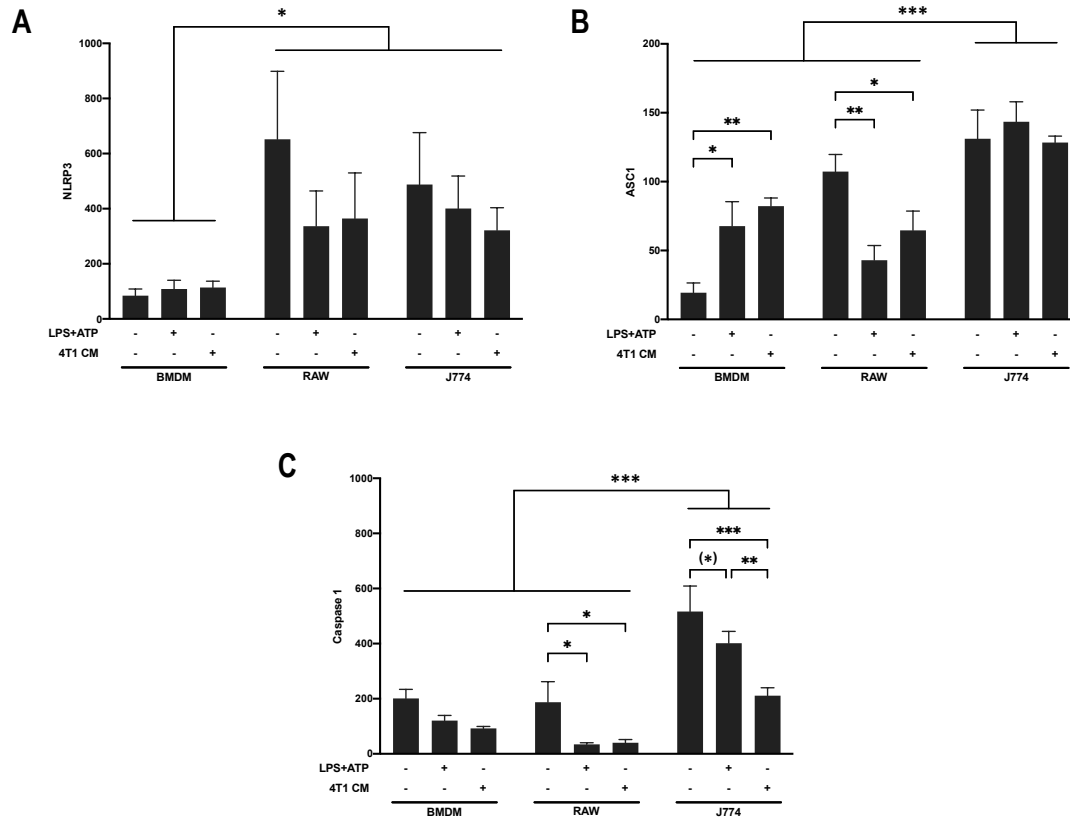
Gene	Overall Incidence	OS	Amplification		Homologous Deletion	
			Incidence	OS	Incidence	OS
CD68	0.84%	-121.49 ***	51.19%	— n.s.	41.17%	-13.47 (*)
MRC1 <sup>^</sup>	2.23%	-13.96 n.s.	91.03%	-0.13 n.s.	1.79%	— n.s.
ARG1 <sup>#</sup>	1.80%	-15.03 n.s.	83.33%	-30.37 n.s.	10.56%	— (*)
NOS2 <sup>&gt;</sup>	4.05%	-51.40 ***	91.85%	-39.73 **	2.47%	-91.81 ***
IL1B	0.26%	— n.s.	100.00%	— n.s.	—	— n.s.
IL18	0.73%	-87.20 ***	17.81%	-130.47 n.s.	73.97%	-87.20 ***

<sup>^</sup> CD206; <sup>#</sup> Arginase 1; <sup>></sup> iNOS; Overall Survival (OS) is presented as difference in months compared to median overall survival of patients without alterations. \*\*\* p<0.001, \*\* p<0.01, \* p<0.05, (\*) p<0.1

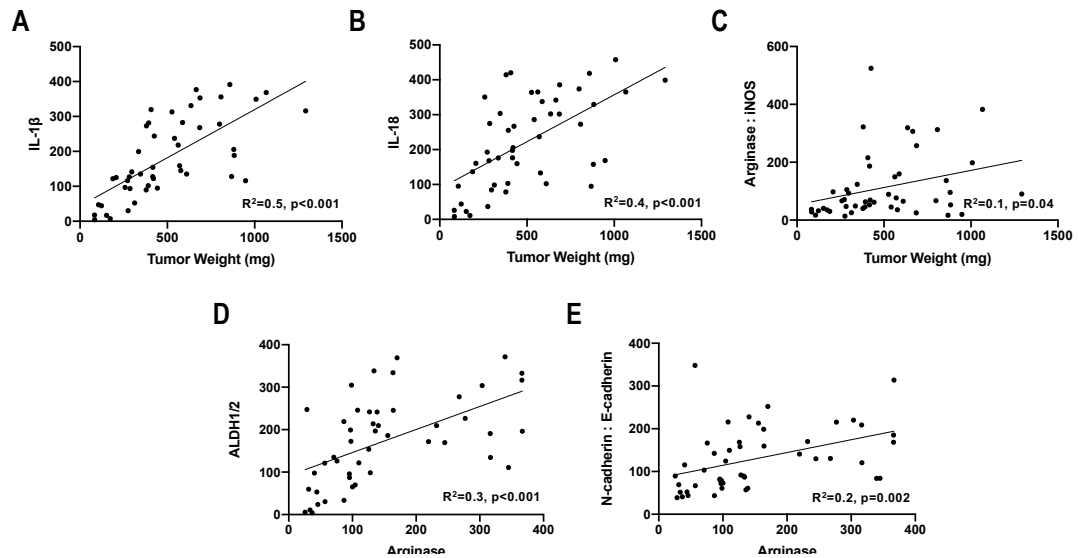
**Table 2.1. Genetic Alterations of Macrophage Polarization Markers and Cytokines Impact Overall Survival in Human Breast Cancer.** Patient data using cBioPortal (247-274) demonstrates that both amplification and homologous deletion of iNOS results in a 3.3 to 7.6 year reductions in median overall survival. Alteration of pro-inflammatory cytokine genes is less frequent and homologous deletion of IL-18 reduces overall survival by 7.3 years.



## 2.7. Supplemental Figures



**Supplemental Figure 2.1. NLRP3 Inflammasome Expression is Elevated in J774 Macrophages.** Immunoblot quantification normalized to protein loading of **A.** NLRP3 expression for J774, RAW, and bone marrow-derived macrophages (BMDM). NLRP3 receptor expression was greatest by J774 and RAW cells with no treatment responsive change in expression. **B.** ASC1 expression was highest in J774 cells but not treatment dependent. **C.** Similar to ASC1 expression, cleaved caspase 1 expression was highest among J774 cells. \*\*\*  $p < 0.001$ , \*\*  $p < 0.01$ , \*  $p < 0.05$ , (\*)  $p < 0.1$ .



**Supplement Figure 2.2. Pro-Inflammatory Cytokine Secretion is Positively Associated with Tumor Growth and Pro-Tumorigenic Macrophages.** 4T1 tumor cells were implanted alone or with RAW or J774 macrophages into the mammary fat pad of Balb/c mice. At the 35-day endpoint, the mice were sacrificed, and the tumors excised. Intra-tumoral **A.** IL-1 $\beta$  and **B.** IL-18 expression are positively correlated with tumor weight. **C.** Intra-tumoral ration of arginase to iNOS expression ratios are positively correlated with tumor weight. **D.** aldehyde dehydrogenase 1/2 and **E.** N-cadherin to E-cadherin ratio are positively correlated with arginase expression.

## CHAPTER 3. COMBINING 5-FU AND THE NLRP3 INFLAMMASOME INHIBITOR, MCC950, TO PREVENT BREAST TUMOR PROGRESSION.

### 3.1. Introduction

Among women, breast cancer is the most frequently diagnosed malignancy with breast cancer deaths accounting for 15% of cancer-related deaths (282). Despite progress in treatment approaches, the development of metastatic disease remains a challenge. Moreover, in contrast with other cancers, neither targeting angiogenesis or immune responses has yielded clinical breakthroughs although clinical benefits were demonstrated (322-324). Current standards of care rely on mainly on targeting the estrogen and epidermal growth factor pathways following molecular tumor classification (325). Chemotherapy alone or in combination regimen are routinely used (for more details, see Chapter #1)

In particular, the antimetabolite drug 5-Fluorouracil (5-FU) that inhibits thymidylate synthase to impede DNA replication (326) remains given intravenously (327, 328). 5-FU also promotes single base C(T>C)T or C(T>G)T mutations in CTT trinucleotides (329). As with any chemotherapy treatment, in particular, with anti-mitotic agents, resistance has been demonstrated and remains a major clinical limitation to successful treatment (75, 79, 222, 323, 330). Interestingly, resistance to anti-mitotic agents is in large part driven by tumor-associated macrophages (330, 331).

Macrophage infiltration in the primary tumor is a prognostic marker of poor clinical outcome in breast cancer (115, 284, 332). In contrast, increased CD45<sup>+</sup> leukocyte infiltration is indicative of a more positive clinical outcome, even when high proportion of the CD45<sup>+</sup> are CD68<sup>+</sup> macrophages (333). Macrophages promote migration, angiogenesis

and metastasis of breast cancer and participate in immunosuppression (127, 289, 306, 332, 334). Through tissue remodeling and the promotion of a pro-inflammatory tumor microenvironment, macrophages facilitate breast cancer progression (310, 335-337). Intratumoral inflammation is associated with an increase in pro-inflammatory cytokines mainly driven by tumor-associated macrophages that promotes cancer progression (159, 166, 338-341).

Multiple mechanisms promote the secretion of pro-inflammatory cytokines (159, 215, 302, 342). In particular, the activation of inflammasomes, especially NLRP3 inflammasomes, in macrophages has been shown to lead to the secretions of IL-1 $\beta$  and IL-18 proinflammatory cytokines. Like most inflammasomes, the NLRP3 inflammasome is comprised of three protein subunits: the internal receptor, NLRP3, the adaptor protein, ASC1, and the effector caspase, caspase 1 (178). NLRP3 inflammasomes are activated through pathogen-associated or damage-associated molecular patterns (163, 187, 208). Notably, NLRP3 is an internal receptor that does not interact directly with the activating ligand but relies on upstream signaling proteins, such as RACK1 (Receptor of Protein Kinase C Isoform  $\beta$ II) and the intercessor NEK7 (NIMA-associated kinase 7) (168). NEK7 (c-terminal lobe) interacts between the LRR and NACHT domains of NLRP3, joining adjacent NLRP3, in response to ATP-triggered potassium efflux (172, 173). The joining of adjacent NLRP3 receptors triggered ASC1 interaction and the cleavage of pro-caspase 1 and activation of caspase 1 (178). Caspase 1 then cleaves pro-inflammatory cytokines into mature IL-1 $\beta$  and IL-18, which in turn are secreted via pore formation or released into the extracellular space by pyroptosis (6, 193, 215, 216).

Interestingly, pharmacological inhibition of the NLRP3 inflammasome using MCC950 limited head and neck and pancreatic cancer progression in preclinical models (312, 343-345). While the detailed mechanisms of actions of MCC950 remain unclear, MCC950 is viewed as a specific NLRP3 inhibitor (346). Studies suggest that the binding of MCC950 to NLRP3 forces the receptor into a closed and inactive conformation by interacting at a hydrophobic pocket of the Walker B ATP-hydrolysis motif of NLRP3 preventing ATP hydrolysis needed for the conformational shift to an open position (347, 348). This conformational constraint by MCC950 prevents a critical conformational change in NLRP3 necessary for NLRP3 and NEK7 interaction and subsequent oligomerization (347) and thereby limiting caspase activity and the production of mature IL-1 $\beta$  and IL-18. Remarkably, inflammasome activation participates to cancer chemotherapy resistance in cancer. Indeed, chemotherapy induced NLRP3 inflammasome activation in myeloid cells promoted immunosuppression (349-351).

Here, we assessed the inhibitory potential of the combination of the antimetabolite, 5-Fluorouracil, and the NLRP3-specific inhibitor, MCC950, on tumor growth and immune cell infiltration in the 4T1 immunocompetent orthotopic preclinical murine model. Tumor growth and the presence of intra-tumoral immune cells was determined following MCC950 and 5-FU treatment of syngeneic mice implanted with 4T1 tumor cells alone or co-implanted with 4T1 tumor cells and syngeneic J774 macrophages. Our data indicate that macrophages supported tumor growth, and that tumor growth was significantly reduced in animals receiving the treatment combination of NLRP3 inflammasome inhibitor, MCC950, and 5-Fluorouracil. Moreover, intratumorally, the MCC950 and 5-FU treatment was associated with a reduction in pro-inflammatory cytokine production, changes in

immune cell infiltration and a reduction of the pro-tumorigenic phenotype of infiltrating macrophages.

### **3.2. Methods**

#### **Cell Culture**

J774 monocyte macrophages were purchased from ATCC (Manassas, VA). 4T1 cells (ATCC) are aggressive mammary cancer cells that mimic the later stage of breast cancer in humans (300). Cells were grown and cultured in DMEM supplemented with antibiotic, antifungal, and 10% of FBS (Atlanta biologic, Atlanta, GA).

#### **Macrophage Protein Expression**

Seeded in 6-well plates (Greiner), once cells at confluence, the media was changed, and cells incubated in FBS-free media for 3 hours. J774 macrophages were then incubated for 6 hours with either negative control (FBS-free media alone), positive control (LPS 5ug/ml + ATP 5mM) and 4T1 conditioned media. Afterwards, cells and supernatants were collected. Cells were fixed and used in flow-cytometry analyses. Both cell lysates and supernatants were processed as previously, and lysates and supernatants stored at -20°C until Western blots and cytokine measurements.

#### **Macrophages and Tumor Cell *In Vitro* Co-Cultures**

For co-cultures 4T1 tumor cells and J774 macrophages (5:1) were seeded in 6-well plates. Following a 3-hr incubation in FBS-free media, co-cultures were incubated with MCC950 (10μM; Selleckchem) and/or 5-Fluorouracil (1 μM, Sigma) for 6hrs and both supernatants and cell lysates collected. To assess cell proliferation, 4T1-dsRED (Ex:556nm, Em: 586nm) tumor cells and J774 macrophages (5:1) were seeded in a 96-well plate and treated with MCC950 (0, 1 or 10 μM) and/or 5-Fluorouracil (0, 0.5, 5 μM), Hoechst 33342 (Ex:350nm; Em:461nm) vital nuclear stain (1:2000) added. Changes in nuclear and dsRED (specific to 4T1 tumor cells) fluorescence were determined

immediately post-treatment and 4 days later using ID5 Spectramax reader (Molecular Device). Changes in 4T1dsRED proliferation was measured by dsRED fluorescence 4-days post-treatment normalized to control (0 hour) .

### ***In Vivo Tumor Study***

Immunocompetent Balb/c female 5-6 week-old mice (Jackson Laboratory) were implanted orthotopically in the mammary fat pad with syngeneic 4T1-RFP ( $0.1-10^6$ ; Imanis Life Sci) with or without syngeneic J774 cells (ATCC) at a ratio tumor cells : macrophages of 5:1. Animals were then randomized and were administered IP either vehicle (sterile saline solution), the NLRP3 inflammasome inhibitor MCC950 (15 $\mu$ g/kg three time/weekly for three weeks) or the combination 5-Fluorouracil (daily for 4 days during the 1<sup>st</sup> week only) and MCC950 (15 $\mu$ g/kg three time/weekly for three weeks) (345, 346, 352, 353). Primary tumor growth was monitored twice weekly through IVIS fluorescence imaging and physical caliper measurements. On day 35 post-tumor implantation, primary tumors, blood, bones (femurs and tibias), spleen, liver, lungs were collected for further analyses. Obtained by cardiac puncture, blood samples were processed to obtain both plasma and blood cells. Plasmas were stored at -20°C until use, blood cell pellets, portions of primary tumors, liver, spleen, lungs were mechanically dissociated and sonicated in lysis buffer (T-PER, ThermoFisher) supplemented with protease inhibitors (Roche Biologics). Bones were also mechanically grinded and associated proteins solubilized in lysis buffer. All lysate samples were stored at -20°C until use. A fraction of primary tumors was fixed in neutralized formalin embedded in paraffin and 5-6mm thick tissue slides obtained and utilized in histological and immunohistochemistry analyses as previously (354-357).



## **Immunohistochemistry**

Paraffin embedded and formalin fixed tumor sections (5-6mm thick) were processed to remove paraffin, enhance antigen access through incubation in antigen retrieval solution (Dako). After a blocking incubation step (with BSA 1% in TBS Tween 20) tumor tissues were incubated overnight in humidified chamber in the presence of either Ki67 (1:100 in blocking buffer, Santa Cruz Biotech.) or active Caspase 3 (1:100 in blocking buffer, Santa Cruz Biotech.) as previously (354). Following wash, tissue slides were incubated with HRP-conjugated secondary antibody and the presence of the protein was revealed through incubation with DAB (Impact DAB stain, Vector) following manufacturer's recommendations. Tissue slides were lightly counterstained with hematoxylin (Vector), dehydrated through successive incubations in alcohol and xylene and then mounted using a mounting solution (Vector) and slipcovers (Fisher scientific). After hardening of the mounting media, tissue slides were assessed by microscopy (IX70 and imaging system with mounted DP70 camera, Olympus). For each tumor, the entire tumor tissue was microphotographed with overlapping edges and composite microphotograph obtained. Composite microphotographs were analyzed for active caspase 3 expression through assessments of DAB staining using Image J and DAB stain plugin (NIH). Both intensity and distribution (tumor area covered in %) were recorded and normalized to tumor size. Necrotic regions were excluded.

## **Immunoblots**

Further, expressions of specific proteins associated with tumor growth, and macrophage phenotype and NLRP3 signaling pathways were determined using Western dot-blot immunodetection. Briefly, lysate samples were diluted with the cationic detergent,

cetyltrimethylammonium bromide (CTAB, 10mM) (355) and then loaded onto a nitrocellulose membrane (GE healthcare) using a dot-blot apparatus (ThermoFisher). After ponceau staining (Sigma) to verify and estimate protein loading, membranes were blocked in 5% fat-free milk in Tris buffer (25mM Tris HCl, 137mM NaCl, 2.7mM KCl pH= 7.4, Boston Bioproducts) supplemented with 0.1% Tween 20 (Sigma). All antibodies used were diluted in the blocking buffer. Variations in protein contents in *in vivo* tumor lysates (4ml per dot), *in vitro* cell lysates (10ml/dot) and *in vitro* cell supernatants (50ml per dot) were assessed with following primary antibodies with specificity to NLRP3 (1:1000 R&D Systems, Inc.), ASC1, cleaved caspase 1, Gasdermin D, arginase, iNOS, IL-1 $\beta$ , IL-18, cytokeratin 19, CD68, CD45, Ki67 and active caspase 3, respectively. All primary antibodies were obtained from Santa Cruz Biotechnology (San Cruz, CA) and diluted 1/500 in blocking buffer unless noted. Secondary conjugated with HRP were from Jackson Immunological Laboratories and were diluted 1/2000 in blocking buffer. Following the blocking step, membranes were incubated overnight with the primary antibody (4°C, under gentle shaking), then after multiple washes, membranes were incubated with the appropriate specie secondary HRP-conjugated antibody for 1-2 hrs in the same conditions. After washes, the presence of protein of interest was revealed using ECL (Biorad) and chemiluminescence signal recorded using the MP Imaging system (Biorad). Protein expression was normalized to protein loading and quantified using FIJI Image J and the Protein Array Analyzer plugin (NIH). For *in vivo* tumor samples, data are presented as percent of the expression observed in the control group.

## Statistical Analysis

All statistical analyses were completed using Prism 9.0 (GraphPad). Data are presented as mean  $\pm$  SEM. Differences between groups were analyzed using two-way ANOVAs and Fisher's LSD test to compare drug and cell co-culture effects. Significance is reported as \*\*\*  $p < 0.001$ , \*\*  $p < 0.01$ , \*  $p < 0.05$ , (\*)  $p < 0.1$ .

### 3.3. Results

#### **The NLRP3 Inhibitor MCC950 Alone or Combined with 5-FU Prevented *In Vitro* 4T1 Tumor Cell Growth.**

The growth of 4T1-dsRED tumor cells alone or co-cultured with syngeneic J774 macrophages (tumor : macrophage at a 5:1 ratio) was determined based on the constitutive expression of dsRED by 4T1 cells in the presence of increasing doses of MCC950 (0-10 $\mu$ M) and 5-FU (0-5 $\mu$ M). Growth of 4T1 tumor cells cultured alone was dose-dependently and significantly reduced following treatment with 10 $\mu$ M MCC950 ( $p < 0.01$ , Fig. 3.1.A). Notably, incubation with 5-FU regardless of the concentrations tested (0-5 $\mu$ M) had no significant effect on the growth of 4T1 tumor cells (Fig. 3.1.A).

Proliferation of 4T1 tumor cells when in co-culture with J774 macrophages was similarly reduced when treated with MCC950 (Fig. 3.1.B,  $p < 0.1$ ). However, no dose-dependent decrease in tumor growth was detected (Fig. 3.1.B). Moreover, the decrease in 4T1 growth tended to be blunted in the presence of J774 macrophages. Separately, the proliferation of J774 macrophages was assessed when treated with either MCC950 and/or 5-FU in similar conditions (Supplemental Fig. 3.1.) and was only marginally decreased ( $< 10\%$ , Supplemental Fig. 3.1.).

#### **MCC950 and 5-FU Treatment Decreased NLRP3 Inflammasome Protein Complex Expression 4T1 Tumor Cells Alone and in Co-Culture with J774 Macrophages.**

To address whether the MCC950 and 5-FU treatments modulated NLRP3 inflammasome activation in 4T1 tumor cells, 4T1 cells alone were incubated with MCC950 and 5-FU and NLRP3 inflammasome protein expression assessed. NLRP3 receptor expression was reduced treated with MCC950 (Fig. 3.2.A,  $p < 0.05$ ). Intriguingly, when 4T1

tumor cells were treated with 5-FU alone, the expression of the NLRP3 receptor was increased compared to control (Fig. 3.2. A,  $p < 0.05$ ). Neither the ASC1 nor the active caspase-1 expression were significantly altered regardless of MCC950 and 5-FU dose tested in the 4T1 tumor cells cultured alone (Fig. 3.2.BC).

In co-culture with J774 macrophage (tumor : macrophage ratio 5:1) NLRP3 expression was also reduced in the presence of MCC950 whereas 5-FU treatment promoted NLRP3 expression (Fig 3.2.A,  $P < 0.05$ ). ASC1 expression also tended to be higher when co-cultures were treated with 5-FU (Fig 3.2.B, n.s.). Both MCC950 and 5-FU promoted active caspase 1 expression (Fig. 3.2.C,  $p < 0.05$ ).

#### **MCC950 and 5-FU Treatment of 4T1 Tumor Cells Alone and in Co-Culture with J774 Macrophages Decreased Pro-Inflammatory Cytokine Secretions.**

Regardless of MCC950 or 5-FU treatment, IL-1 $\beta$  secretions *in vitro* culture 4T1 tumor cells alone or co-culture of 4T1 tumor cells with J774 macrophages were not altered (Fig. 3.3.A, n.s.). In contrast, IL-18 secretions were decreased following MCC950 treatments in both culture of 4T1 tumor cells alone or in combination with J774 macrophages (Fig. 3.3.B). Interestingly, in the presence of 5-FU, the decrease in IL-18 secretion associated with MCC950 treatment was blunted (Fig. 3.3.B).

#### **In the 4T1 Pre-Clinical, Immunocompetent, Murine Model the Combination MCC950 and 5-FU Regimen Reduced Primary Tumor Growth.**

The potential of a MCC950 and 5-FU regimen in the orthotopic 4T1 pre-clinical immunocompetent murine model implanted with 4T1 cells alone or with the mix 4T1 tumor cells (Fig. 3.4.AC) and syngeneic J774 macrophages (Fig. 3.4.BD) at a tumor cell : macrophage 5:1 ratio was assessed. J774 macrophages present a functional NLRP3

inflammasome (313). Treatment with MCC950 alone tended to increase tumor growth regardless of whether 4T1 tumor cells were implanted alone or combined with syngeneic J774 macrophages (at a 5:1 ratio) compared to vehicle control (saline) (Fig. 3.4.ABCD). Notably, the combination 5-FU (20 µg/kg) and MCC950 (15µg/kg) significantly reduced tumor growth, especially compared to MCC950 alone treatment (Fig. 3.4.ABCD,  $p<0.05$ ). Interestingly, Kaplan-Meier plots associated with tumor mass reaching 150 mm<sup>3</sup> confirm that with 4T1 cell alone, MCC950 treatment was associated with 4T1 tumor mass reaching 150 mm<sup>3</sup> earlier than in either saline (control) or MCC950+5-FU treatment groups ( $p=0.04$ , log rank Fig. 3.4.E)). In animals implanted with the 5:1 mix of 4T1 tumor cells and J774 macrophages, both saline and MCC950 treatment led to rapid increase in tumor weights compared to animals receiving the MCC950+5-FU combined regimen ( $p=0.02$ , log rank Fig. 3.4.F). Importantly, in mice treated with saline, the co-implantation with J774 macrophages led to significant increased tumor growth ( $p=0.05$ , log rank Supplemental Fig. 3.2.).

Immunostaining tumors for caspase 3, a marker of apoptosis, showed diffuse apoptosis and a dense apoptotic core in tumors from animals treated with the combination regimen (Fig. 3.5.AB). The net tumor cell growth evaluated through the Ki67 to active caspase 3 ratio tended to increase in animals co-implanted with 4T1 and J774 and treated with MCC950 alone or in combination with 5-FU (Fig. 3.5.D, n.s.).

#### **The MCC950 + 5-FU Combination Reduced Cytokeratin 19 and Total Leukocyte Infiltration in Mice Co-Implanted with 4T1 Tumor Cells and J774 Macrophages.**

As expected, expression of cytokeratin 19 (CK19) a marker of 4T1 tumor cells was associated with tumor weight ( $R^2=0.29$ ,  $p<0.001$ ; Supplemental Fig. 3.3.) especially in

mice co-implanted with 4T1 tumor cells and J774 macrophages. Most notably, the MCC950 + 5-FU regimen led to a drastic decrease in the tumor mass in the co-implanted mice whereas the MCC905+ 5-FU regimen had no effect on CK19 expression in animal implanted with 4T1 tumor cells alone (Fig. 3.6A).

The presence of immune cells was also determined. CD45 expression was high in tumor derived from co-implantation of 4T1 tumor cells and J774 (CD45+) macrophages in the control group but decreased significantly following treatment with the combination MCC950±5-FU ( $p<0.05$ ; Fig. 3.6.B). Moreover, CD68 expression, a marker of mainly macrophages was high regardless of treatment in tumors derived from co-implantation of 4T1 cells and J774 macrophages regardless of treatment (Fig. 3.7.A). Notably, in tumors derived from the implantation of 4T1 cells alone, MCC950 treatment led to a significant increase in CD68<sup>+</sup> expression not observed following the combination treatment (Fig. 3.7.A,  $p<0.05$ ). No change was detected in the CD206 mannose receptor expression, mainly associated with the M2 macrophage phenotype, in tumors derived from the implantation of 4T1 cells alone regardless of treatment. In tumors derived from the co-implantation of 4T1 tumor cells + J774 macrophages the dual MCC950±5-FU treatment led to a significant decrease in CD206 expression ( $p<0.05$ , Fig. 3.7.B).

Moreover, the ratio CD68/CD45 tended to be decreased by MCC950 alone or in combination with 5-FU treatments in tumor derived from 4T1 tumor cells alone (Fig. 3.7.C). In contrast, the CD68/CD45 ratio assessing the proportion of macrophages tended to be increased in tumor derived from co-implantation of 4T1 and J774 cells by MCC950 alone or in combination with 5-FU treatments (Fig. 3.7.C). Lastly, arginase : iNOS expression ratio, a marker of macrophage phenotype tended to be decreased following the

MCC950+5-FU combination but only in tumor derived from the co-implantation of 4T1 and J774 cells (Fig. 3.7.D).

**The MCC950 + 5-FU Combination Reduced Intra-Tumoral Secretions of Pro-Inflammatory IL-1 $\beta$  and IL-18 Cytokines in Mice Co-Implanted with 4T1 Tumor Cells and J774 Macrophages.**

Inflammasomes including NLRP3 inflammasomes participate in the secretion of IL-1 $\beta$  and IL-18 pro-inflammatory cytokines (141, 186). No difference in either IL-1 $\beta$  or IL-18 expression was detected in the tumors derived from 4T1 tumor cells orthotopic implantation regardless of treatment (Fig. 3.8.AB). In contrast, expression of IL-1 $\beta$  and IL-18 tended to be higher in the tumor derived from co-implantation of 4T1 and J774 cells following control (saline) and MCC950 alone treatment. Interestingly, the combination MCC950 $\pm$ 5-FU treatment led to significant decreases in both IL-1 $\beta$  and IL-18 expressions in tumor resulting from the co-implantation of 4T1 and J774 cells (Fig. 3.8.AB,  $p < 0.05$ ),



### 3.4. Discussion

Breast cancer progression is favored by a pro-inflammatory, pro-tumorigenic tumor microenvironment (121, 130, 357-359). In particular, the presence of macrophages with activated NLRP3 inflammasome that trigger secretion of pro-inflammatory cytokines especially IL-1 $\beta$  and IL-18 has been associated with primary tumor growth and metastases (159, 230, 231, 243, 311, 360). Decreasing local inflammation has been associated with reduced tumor growth including in breast cancer preclinical models (361, 362).

Here, we investigated the effects of the combination of a specific NLRP3 inflammasome inhibitor, MCC950, and the chemotherapeutic, 5-Fluorouracil on 4T1 orthotopic growth in an immunocompetent murine model (352, 357). As the 4T1 murine model is associated with limited macrophage infiltration, co-implanted 4T1 and syngeneic J774 macrophages to more closely mimic macrophage infiltration in breast tumor. In addition, we assessed 4T1 tumor cell and J774 macrophage proliferation and NLRP3 inflammasome activation *in vitro* following treatment with MCC950 and 5-FU *in vitro* as previously (345, 346, 352, 353). Strikingly, our data indicate that the NLRP3 inhibitor MCC950 alone or in combination with 5-FU decreased NLRP3 inflammasome protein complex expression and prevented 4T1 tumor cell growth *in vitro* whereas 5-FU alone did not. The MCC950 and 5-FU combination treatment also decreased the pro-inflammatory cytokine secretions of 4T1 tumor cells as well as when in co-culture with J774 macrophages. *In vivo*, the growth of the primary mammary tumor derived from orthotopically co-implanted 4T1 cells alone or in combination with 20% of syngeneic macrophages was decreased by MCC950 and 5-FU combination treatment. In 4T1 and J774 co-implanted mice only, the combined treatment also reduced cytokeratin 19 and

CD45<sup>+</sup> leukocyte intra-tumoral infiltration as well as intra-tumoral secretions of pro-inflammatory IL-1 $\beta$  and IL-18 cytokines.

*In vitro*, 5-FU treatment at the doses tested had no significant effect on the proliferation of either macrophages or 4T1 tumor cells or of co-culture of 4T1 tumor cells with J774 macrophages. Interestingly, tumor cells cultured alone were more susceptible to MCC950 treatment than when co-cultured with J774 macrophages. 5-FU has been shown to activate the NLRP3 inflammasome through cathepsin B release and ROS generation blunting the anticancer efficacy (350, 363-365). Our data indicate that 5-FU treatment promoted the expression of active caspase 1 activation in an *in vitro* co-culture of 4T1 and J774 cells. However, of the pro-inflammatory cytokine associated with NLRP3 activation, only IL-18, but not IL-1 $\beta$  secretions, were affected possibly because, in contrast with IL-1 $\beta$ , IL-18 is constitutively produced (211-214).

*In vivo*, treatment with MCC950 alone promoted tumor growth whereas the combination MCC950 and 5-FU treatment led to marginally reduced apoptosis. Our data confirm the prior observation that NLRP3 inflammasome inhibition with andrographolide sulfonate combined with 5-FU inhibited tumor growth *in vivo* (363). Moreover, only animals co-implanted with J774 macrophages experienced decreased tumor growth when treated with the NLRP3 specific inflammasome inhibitor MCC950, combined with 5-FU confirming that inhibition of the NLRP3 inflammasome in myeloid lineage cells, specifically myeloid-derived suppressor cells, limited tumor growth (363).

Our data also highlights that tumors derived from mice co-implanted with 4T1 tumor cells and J774 macrophages following the combination MCC950 and 5-FU treatment displayed significantly reduced leukocyte infiltration although with an elevated

macrophage proportion. That observation mimics the effects of NLRP3 inflammasome inhibition using BAY 11-7082 and MCC950 leading to reduced leukocyte infiltration – an effect lost when myeloid lineage cells were depleted (366, 367). Furthermore, in an *in vivo* model of head and neck small cell carcinoma, MCC950 NLRP3 inflammasome blocking reduced infiltrating MDSCs, regulatory T cells and tumor-associated macrophages and, lead to smaller tumors (343). This may explain why the decrease in intra-tumoral CD45 expression is observed in tumors derived from the co-implantation of 4T1 tumor cells and J774 macrophages, but not in tumors derived from the implantation of 4T1 tumor cells alone, treated with both MCC950 and 5-FU, but in the MCC950 only treatment arm remains unaffected. Although not investigated here, immune checkpoint alterations following MCC950 or 5-Fluorouracil treatment have been demonstrated previously (338, 353, 368) and may actively participate in the tumor progression noted here possibly through immune checkpoint inhibition and anergy.

Overall, our studies demonstrated that the combination of the NLRP3 inflammasome inhibitor MCC950 and the chemotherapeutic 5-Fluorouracil at a relatively low dose altered inflammasome activation, leukocyte infiltration and limited tumor growth in an immunocompetent, orthotopic, breast cancer, pre-clinical model modified to include syngeneic macrophages with functional NLRP3 inflammasomes.

### 3.5. Figures

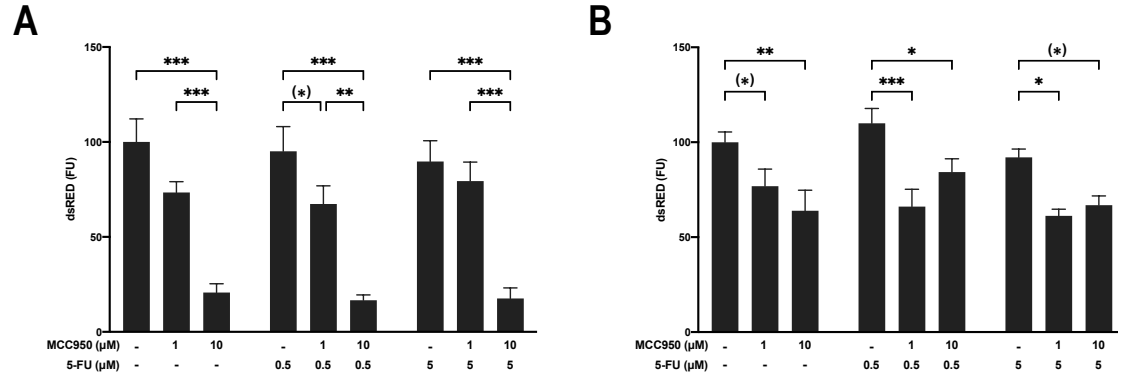


**Figure 3.1. 4T1 Tumor Cells are Less Sensitized to MCC950 when Co-Cultured with J774 Macrophages.** 4T1 tumor cells and J774 macrophages were co-cultured for 4 days with NLRP3 Inflammasome inhibitor, MCC950, and chemotherapeutic, 5-Fluorouracil (5-FU). Fluorescence of dsRED (4T1 tumors) and Hoechst (nuclei) normalized to the media alone control of **A**. 4T1 tumor cells alone and **B**. 4T1 and J774 co-culture. 4T1 were more sensitive to higher dose MCC950 when cultured alone and less sensitive when cultured with J774 macrophages. \*\*\*  $p < 0.001$ , \*\*  $p < 0.01$ , \*  $p < 0.05$ , (\*)  $p < 0.1$ .

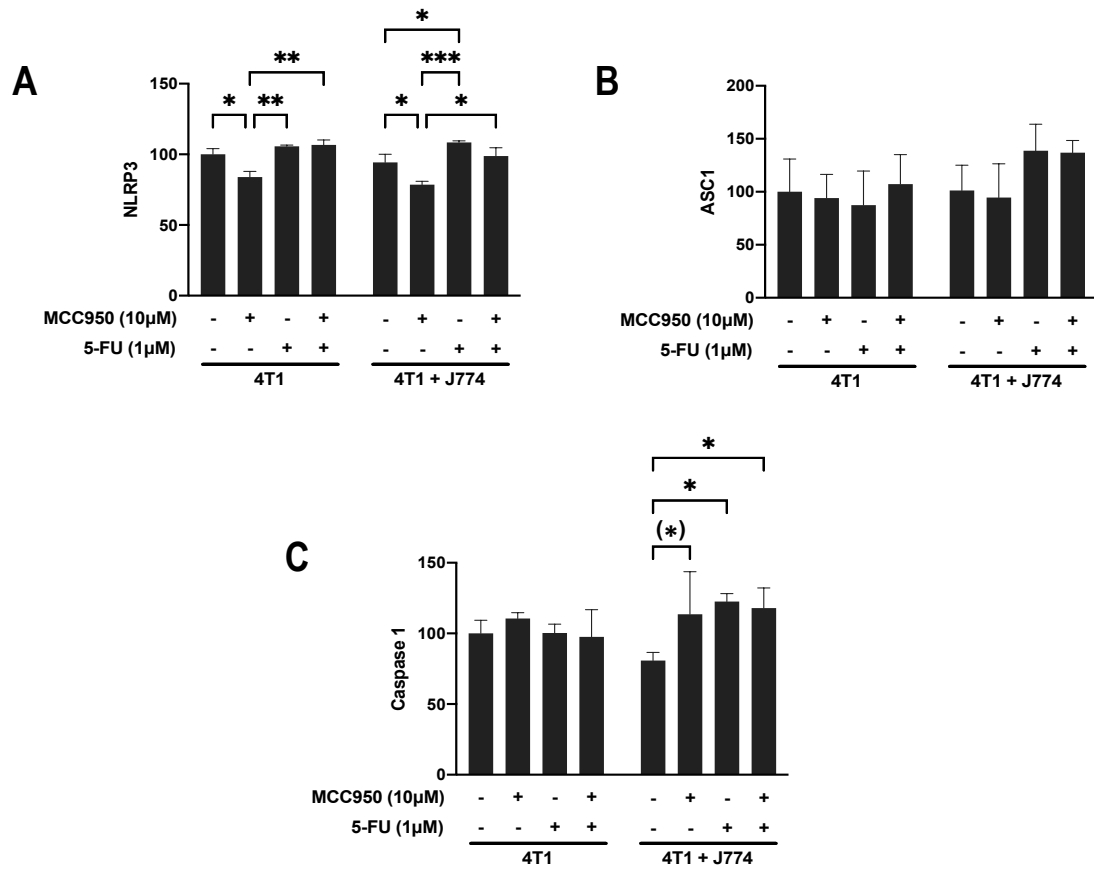


**Figure 3.2. Co-Cultures of 4T1 Tumor Cells and J774 Macrophages Expressed Less NLRP3 Receptor When Treated with MCC950 and the Addition of 5-Fluorouracil is Inflammasome Activating.** Immunoblot quantification normalized to the 4T1 tumor cell alone negative control of **A. NLRP3**, **B. ASC1** and **C. caspase 1** of 4T1 tumor cells cultured alone or in a 5:1 co-culture with J774 macrophages and treated with MCC950 or 5-Fluorouracil (5-FU) for 6 hours. \*\*\*  $p < 0.001$ , \*\*  $p < 0.01$ , \*  $p < 0.05$ , (\*)  $p < 0.1$ .

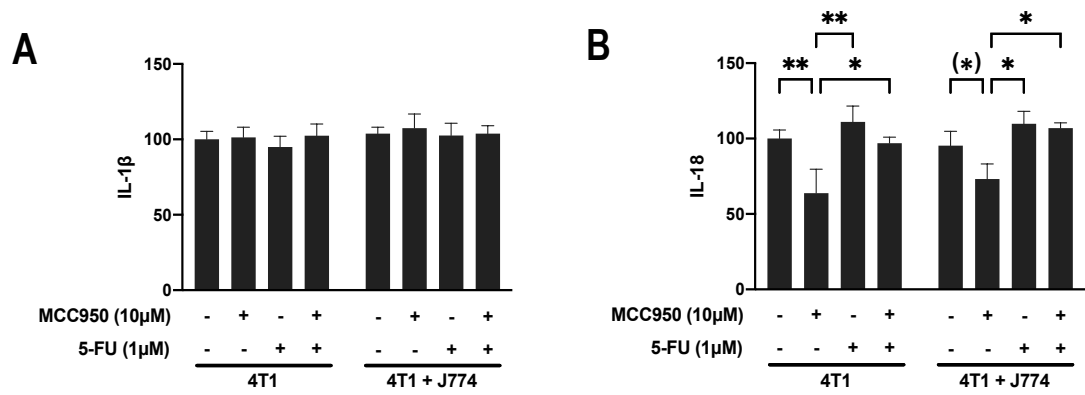


**Figure 3.3. Co-Cultures of 4T1 Tumor Cells and J774 Macrophages Secreted Less IL-18 When Treated with MCC950 and the Addition of 5-Fluorouracil is Inflammasome Activating.** Immunoblot quantification normalized to the 4T1 tumor cell alone negative control of **A**. IL-1 $\beta$  and **B**. IL-18 of 4T1 tumor cells cultured alone or in a 5:1 co-culture with J774 macrophages and treated with MCC950 or 5-Fluorouracil (5-FU) for 6 hours. \*\*\*  $p < 0.001$ , \*\*  $p < 0.01$ , \*  $p < 0.05$ , (\*)  $p < 0.1$

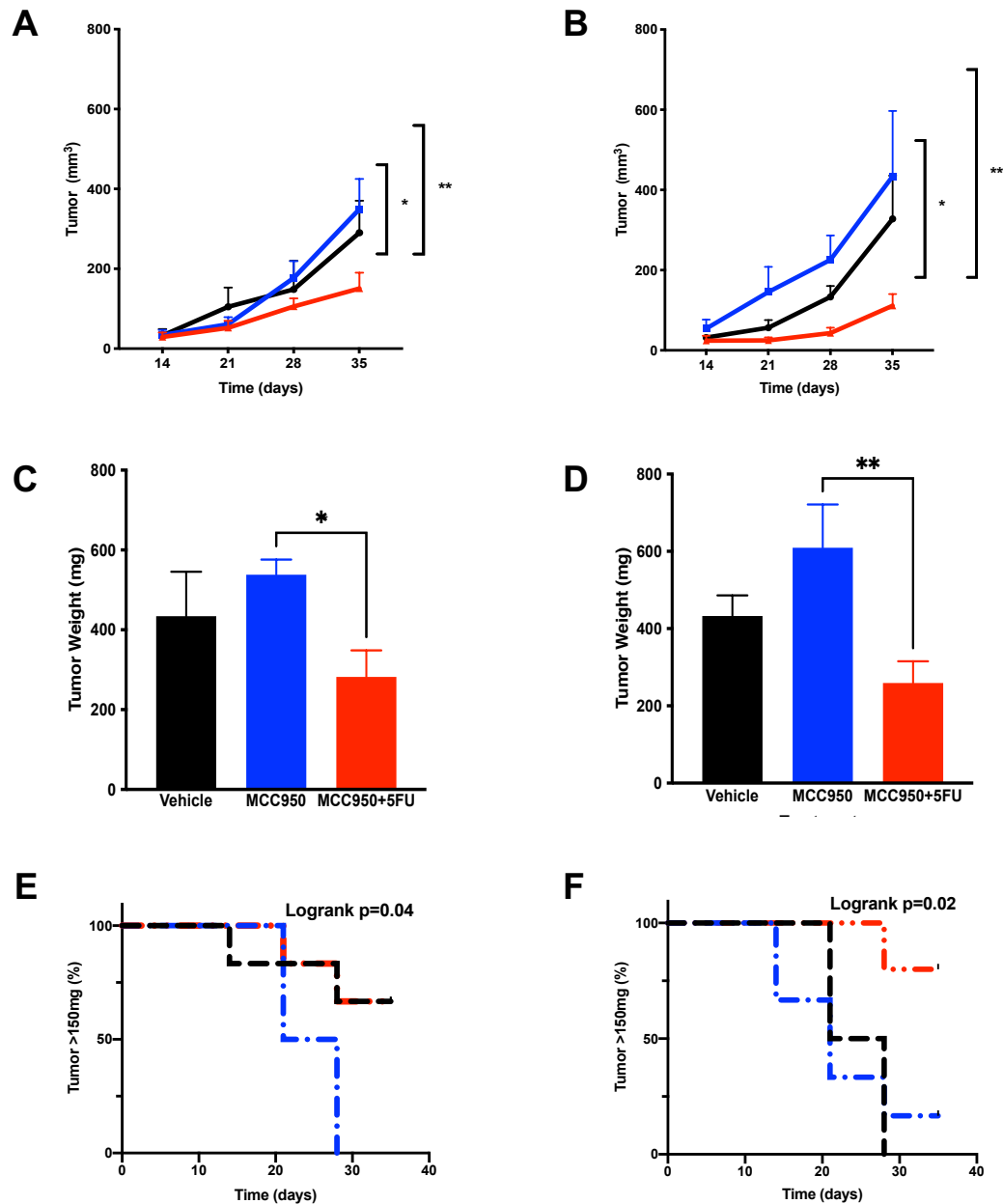


**Figure 3.4. In an Immunocompetent Mouse Model, the Combination of MCC950 and 5-Fluorouracil Decreased 4T1 Tumor Growth.** Tumor size by caliper measurement of **A.** the 4T1 tumor cells alone and **B.** 4T1 tumor cell co-implanted with J774 macrophages and treated with PBS (black), MCC950 (blue) and MCC950 and 5-Fluorouracil (red). 35-day endpoint tumor weight **C.** of mice implanted with 4T1 tumor cells alone and **D.** 4T1 tumor and J774 cells co-implanted. And time (days) to reach a minimum tumor size of 150mg for **E.** 4T1 alone and **F.** 4T1 co-implanted with J774 macrophages. The lowest tumor weight is in mice co-implanted with 4T1 tumor cells and J774 macrophages and treated with the combination of MCC950 and 5-Fluorouracil (5-FU). \*\*\*  $p < 0.001$ , \*\*  $p < 0.01$ , \*  $p < 0.05$

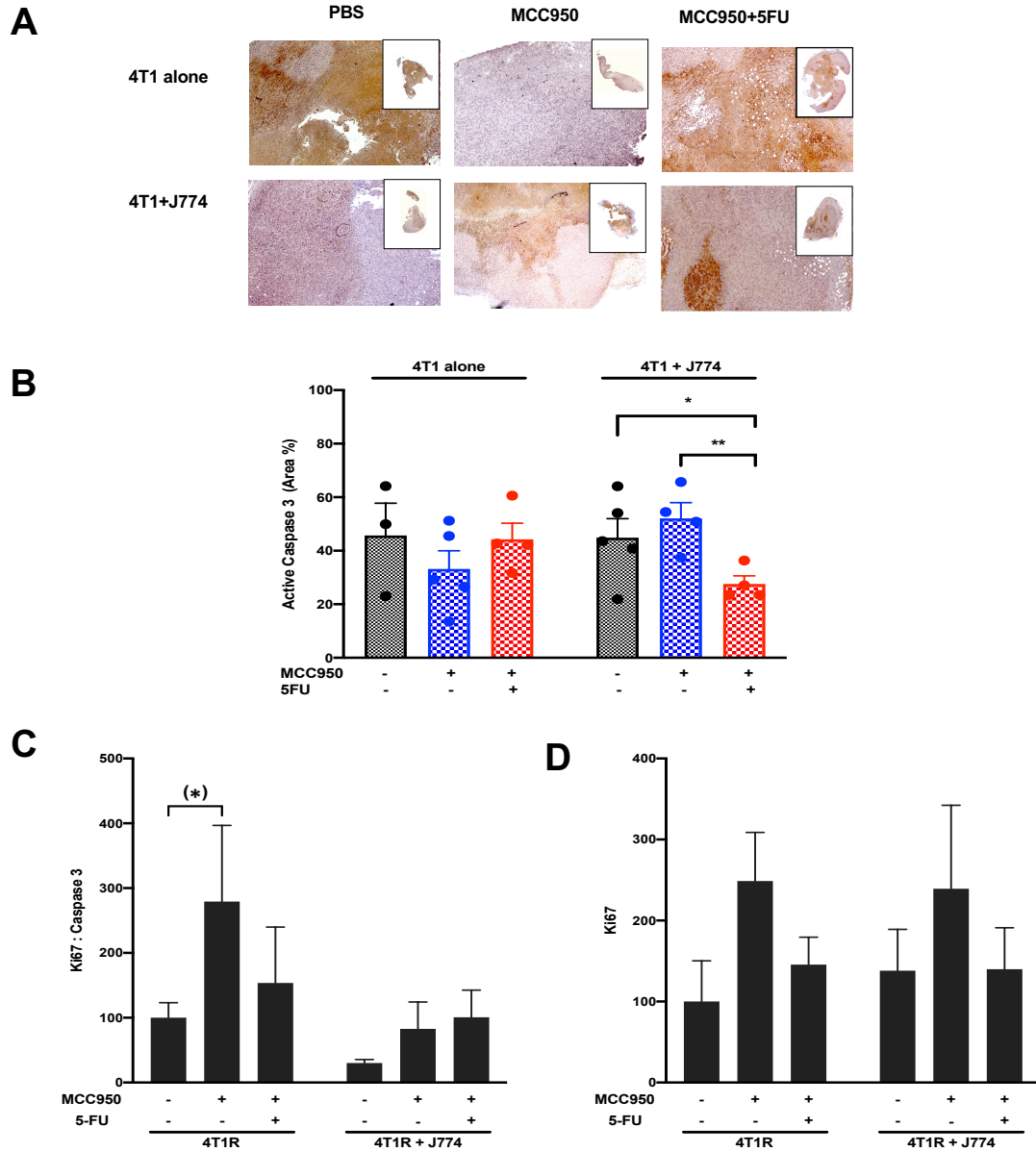


**Figure 3.5. Cell Death is Elevated When Mice Implanted with 4T1 Tumor Cells Alone are Treated with MCC950 and 5-FU, an Effect Opposite of That Demonstrated in 4T1 and J774 Co-Implanted Mice.** **A.** Microphotographs of active caspase 3 expression (red) representative of 4T1 and 4T1 and J774 co-implanted animals treated with MCC950 and MCC950 combined with 5-Fluorouracil (5-FU) and **B.** Microphotograph quantification of active caspase 3 expression relative to area showing reduced caspase 3 expression in co-injected animals treated with MCC950 and 5-FU. Immunoblot quantification normalized to the saline-treated, 4T1 alone control of **C.** Ki67 and **D.** Caspase 3 of mice implanted with 4T1 tumor cells alone or with J774 macrophages (5:1) and treated with MCC950 or MCC950 and 5-Fluorouracil (5-FU) in combination. \*\*  $p < 0.01$ , \*  $p < 0.05$ , (\*)  $p < 0.1$



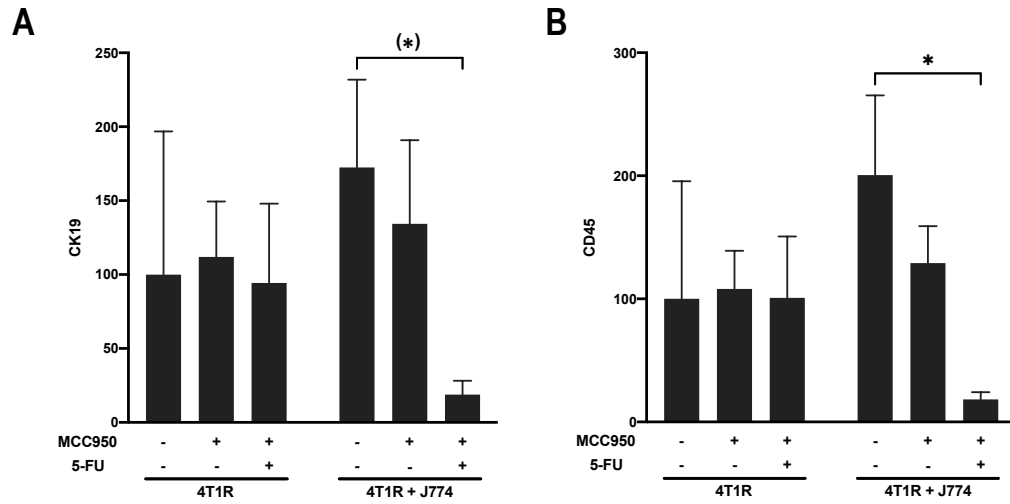


**Figure 3.6. Immune Cell Infiltration of Tumors is Altered by Macrophage Co-Implantation and MCC950 and 5-FU Treatment.** Immunoblot quantifications normalized to the saline-alone, 4T1 tumor cell only treatment group of **A.** cytokeratin 19 and **B.** leukocyte marker CD45 in tumor lysates collected at the 35-day endpoint of mice implanted with 4T1 tumor cells alone or with J774 macrophages and treated with MCC950 or MCC950 and 5-Fluorouracil (5-FU). \*  $p < 0.05$ , (\*)  $p < 0.1$

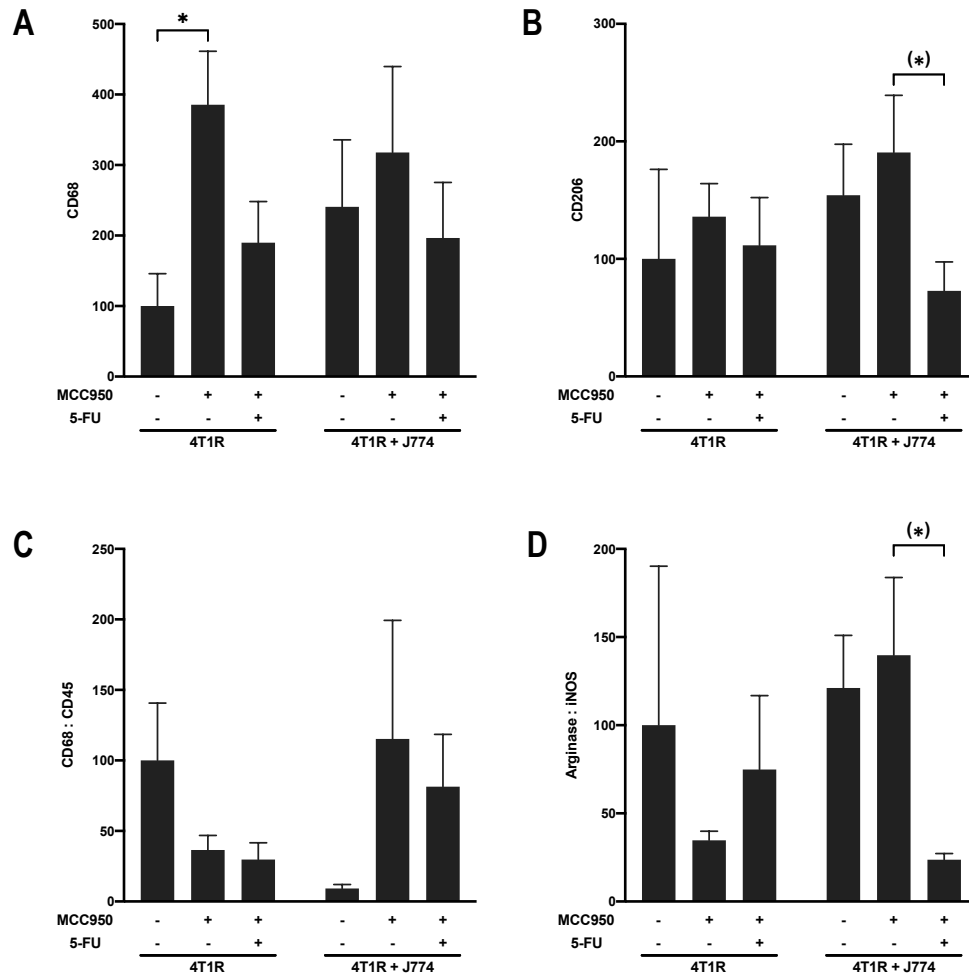


**Figure 3.7. The MCC950 and 5-Fluorouracil Combination Reduced the Pro-Tumorigenic Phenotype of Tumor Infiltrating Macrophages.** Immunoblot quantifications normalized to the saline-alone, 4T1 tumor cell only treatment group of **A.** macrophage marker, CD68, **B.** pro-tumorigenic marker CD206, **C.** the ratio of macrophages to total leukocytes and **D.** the arginase to iNOS expression ratio in tumor lysates collected at the 35-day endpoint of mice implanted with 4T1 tumor cells alone or with J774 macrophages and treated with saline, MCC950 or MCC950 and 5-Fluorouracil (5-FU). \*  $p < 0.05$ , (\*)  $p < 0.1$

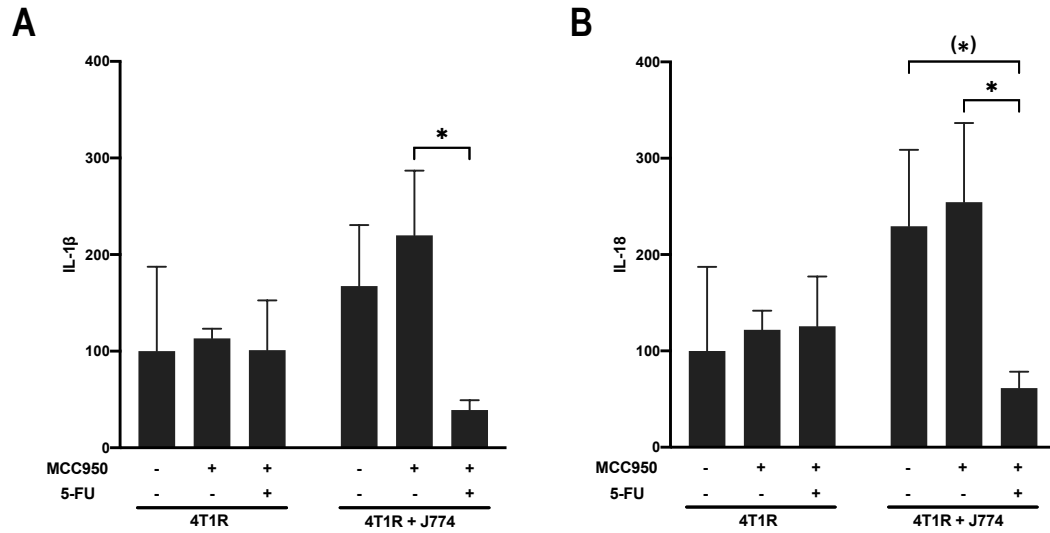
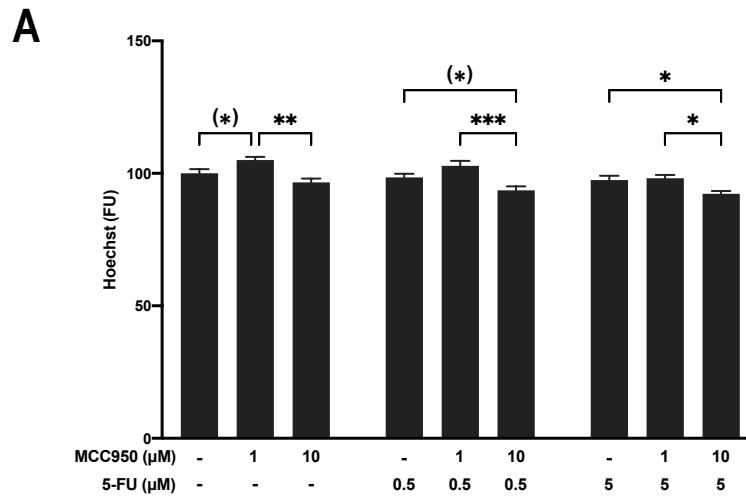
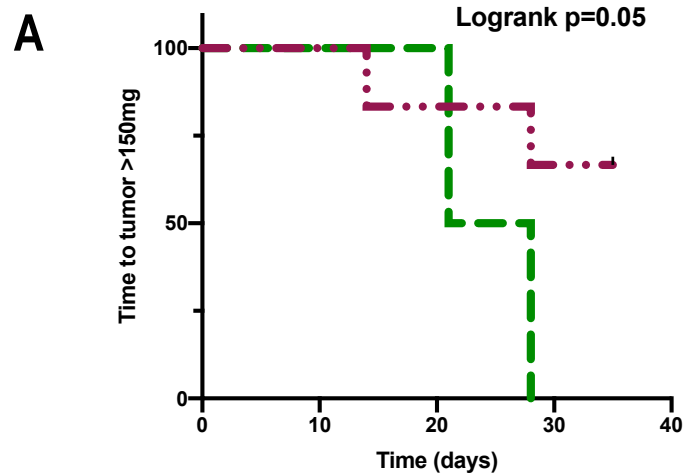


**Figure 3.8. The MCC950 and 5-Fluorouracil Combination Reduced the Pro-Inflammatory Cytokine Secretion.** Immunoblot quantifications normalized to the saline-alone, 4T1 tumor cell only treatment group of **A**. IL-1 $\beta$  and **B**. IL-18 in tumor lysates collected at the 35-day endpoint of mice implanted with 4T1 tumor cells alone or with J774 macrophages and treated with saline, MCC950 or MCC950 and 5-Fluorouracil (5-FU). \*  $p < 0.05$ , (\*)  $p < 0.1$

### 3.6. Supplemental Figures



**Supplemental Figure 3.1. J774 Macrophage Proliferation was Reduced by the Combination of MCC950 and 5-Fluorouracil.** J774 macrophages were treated with MCC950 and 5-Fluorouracil (5-FU) and cultured for 4-days. Hoechst nuclear stain was used to assess macrophage proliferation. Data was normalized to the Hoechst reading at 0 hours and is displayed as mean $\pm$  SEM. Analysis conducted on Prism by 2-way ANOVA and Fisher's LSD \*\*\*  $p < 0.001$ , \*\*  $p < 0.01$ , \*  $p < 0.05$ , (\*)  $p < 0.1$ .



**Supplemental Figure 3.2. 4T1 Tumor Cell Growth is Accelerated by the Co-Implantation of J774 Macrophages.** 4T1 tumor cells were injected into the mammary fat pad of Balb/c mice alone or with J774 macrophages. Tumors of mice co-injected with J774 macrophages (green) reached a median minimum size of 150mg by 20 days, while mice injected with 4T1 tumor cells alone (purple) failed to reach the median minimum size of 150mg by the 35-day endpoint. Log rank test p value derived from Prism statistical analysis.

## CHAPTER 4. BLOCKING P2RX7 ATP RECEPTOR SIGNALING AND GASDERMIN D PORE FORMATION LIMITS NLRP3 INFLAMMASOME-INDUCED PRO- TUMORIGENIC MACROPHAGE POLARIZATION.

### 4.1. Introduction

One in every 8 women will be diagnosed with breast cancer in their lifetime (282). Elevated infiltration of macrophages into breast tumors is associated with decreased overall survival (115, 123, 284). Tumor-macrophage crosstalk promotes growth and dissemination of tumors by a variety of processes including secretions promoting tumor growth, angiogenesis, and extracellular matrix (ECM) remodeling (112, 130, 134, 289, 332). Macrophages display a highly plastic phenotype associated with a spectrum of functions ranging from inflammation promotion with cytotoxic activities (M1-like) to inflammation-resolution with tissue-repair and remodeling activities (M2-like) (134).

Tumor-macrophage crosstalk shifts macrophages toward a tumor-supporting, M2-like phenotype (285). Several markers have been proposed to characterize macrophage phenotype and, of them, the metabolism of arginine by arginase or inducible nitric oxide synthase (iNOS) is the most widely accepted (289, 290). Cytotoxic, anti-tumor macrophages express more iNOS and MHC class II and participate in complement-mediated phagocytosis (289-291). Conversely, immunosuppressive, tumor promoting macrophages express elevated arginase (289, 290). Additionally, innate immune cells such as macrophages regulate the inflammatory microenvironment in breast cancer through the secretion of cytokines.

NLRP3 inflammasome activation is one of the mechanism by which an inflammatory microenvironment is achieved (345). The NLRP3 inflammasome consists of

an internal receptor (NLRP3), an adaptor (ASC1) and an effector caspase (caspase 1) (172) and is activated in response to variety of stimuli, such as lipopolysaccharide and extracellular ATP (179, 276, 341). Extracellular ATP interacts with the ATP-ligand-gated cationic channel receptor, P2RX7 and the binding triggers the opening of the channel and the flux of sodium and calcium ions (369). P2RX7 receptor activation drives the recruitment of pannexin-1 and the formation of hemi-channel responsible for potassium efflux that induces NLRP3 inflammasome activation (184). Following NLRP3 inflammasome oligomerization, caspase 1 becomes activated and cleaves IL-1 $\beta$  and IL-18 into their active mature forms (159).

Beside cytokine maturation, caspase 1 also activates gasdermin D (GSDMD) through cleavage at Asp276 in mice (Asp275 in humans). The N-terminal fragment (GSDMD-NT) oligomerizes at the membrane to form pores through interactions with the inner leaflet of the plasma membrane (216, 217). Electrochemical interactions within the GSDMD pore favors the secretion of mature IL-1 $\beta$  and IL-18, preventing pro-IL-1 $\beta$  and pro-IL-18 secretions (218). Gasdermin D amplification occurs in 14.36% of breast cancers and is associated with a 15.31-month reduction in median overall survival (247-274).

Pharmacological inhibition of NLRP3 inflammasome-derived cytokine secretion may be achieved by inhibiting ATP signaling leading to cytokine maturation and by limiting secretion via gasdermin D inhibition. For example, the chemical inhibitor A438079 functions by competitively blocking ATP interaction with P2RX7. Indeed, incubation with A438079 prior to activation with LPS treatment was demonstrated to impair NLRP3 activation by limiting potassium flux in monocytes (341, 369).

Additionally, *in vivo* A438079 treatment reduced IL-18-inducible IFN- $\gamma$  serum levels (277).

Disulfiram is clinically approved for the treatment of chronic alcoholism (370). Continuous use of disulfiram for the treatment of alcohol dependency is associated with a 34% reduction in cancer death rate compared to those who discontinued disulfiram use (371) supporting the therapeutic potential of disulfiram in cancer (372, 373). Interestingly, disulfiram targets Cys192 of mouse GSDMD (i.e., Cys191 of human GSDMD) – a critical AA residues for the pore formation – and prevents the cleavage of GSDMD (374).

Previously, we demonstrated that NLRP3 inflammasome components were differentially expressed by macrophages and that NLRP3 inflammasome activation is associated with a pro-tumorigenic macrophage phenotype *in vivo*. Whether reducing NLRP3 inflammasome-driven cytokine secretion through either blocking ATP-induced cytokine maturation and inhibiting GSDMD-mediated cytokine secretion would alter macrophage polarization is unclear. Here, we demonstrate that both A438079 and disulfiram alter the macrophage secretion of IL-1 $\beta$  and IL-18 and limit the NLRP3 inflammasome activation driven pro-tumorigenic macrophage phenotype.



## **4.2. Methods**

### **Cell Culture**

J774 monocyte macrophages were purchased from ATCC (Manassas, VA). Cells were grown and cultured in DMEM supplemented with antibiotic, antifungal, and 10% of FBS (Atlanta biologic, Atlanta, GA). Prior to treatment with negative control (FBS-free media), positive control (LPS 5 $\mu$ g/mL + ATP 5mM) and 4T1 conditioned media, with or without 100 $\mu$ M A438079 (Selleckchem) or 10 $\mu$ M disulfiram (Selleckchem), J774 cells were incubated in FBS-free media (0% FBS) for 3 hours. Cells were then harvested for flow-cytometry and immunohistochemistry analyses. Additionally, both cell lysates and supernatants were collected and stored at -20°C until use in Western blots and cytokine measurements.

### **Immunoblots**

For western dot-blots, *in vivo* tumor lysates, macrophage lysates and macrophage supernatants were diluted in a loading buffer with 10mM CTAB detergent and loaded onto 45 $\mu$ m nitrocellulose membranes (GE) using a dot-blot apparatus (ThermoFisher). Membranes were assessed for protein loading using Ponceau (Sigma) staining and then blocked in 5% milk TBS – Tween 20 buffer (Boston Biologicals). After blocking, blots were incubated with primary antibodies against NLRP3 (1:1000; R&D Systems, Inc.), ASC1 (1:600; Santa Cruz Biotech.), cleaved caspase 1 (1:500; Santa Cruz Biotech.), arginase (1:500; Santa Cruz Biotech), iNOS (1:500; Santa Cruz Biotech), IL-1 $\beta$  (1:500; Santa Cruz Biotech.), IL-18 (1:500; Santa Cruz Biotech.) overnight at 4°C under gentle rocking. After removal of the primary antibody and washes in TBST buffer, blots were incubated with species-specific secondary HRP conjugated antibody for 1hr in similar

conditions. After secondary antibody removal and multiple TBST buffer washes, the presence of the protein of interest was revealed following incubation with ECL substrate (Biorad) and detection using the MP Bioimager (Biorad). For each blot, protein signal was quantified using Image J and Protein Array Analyzer plugin (NIH). Protein expressions were normalized to protein loading defined by ponceau staining. In addition, protein expression detected in *in vivo* tumor lysates were normalized average expression in control animals implanted with 4T1 cells alone and treated with saline (control conditions).

### **Phagocytic Assay**

J774 cells were grown to confluency in a 96-well plate and treated with negative control (media alone), positive control (LPS 5 $\mu$ g/mL + ATP 5mM), 4T1 conditioned media and 100 $\mu$ M A438079 or 10 $\mu$ M disulfiram for 6 hours. Red fluorescent beads (10 $\mu$ m FluoroMax, ThermoScientific) and Hoechst (Molecular Probes) were added at ~6 hours after the initial treatment and washed after 30 minutes. Media was replaced with PBS and readings at both 360/460 and 530/580 excitation/emission wavelengths measured cell concentration and phagocytosis through Hoechst nuclear dye and red fluorescence, respectively. A phagocytosis index defined as the bead fluorescence relative to cell concentration / number (based on Hoechst nuclear intensity or number) normalized to control conditions was used to quantify phagocytosis. Microphotographs were obtained using a IX71 microscope fitted with a DP70 camera and software (Olympus). Representative overlapping composite microphotographs were generated using ImageJ (NIH).

## Statistical Analysis

All statistical analysis was completed using GraphPad Prism. Data are presented as mean  $\pm$  SEM. Differences between groups were analyzed using one-way ANOVAs and Fisher's LSD test. Significant differences between treatment groups are reported as (\*) $p < 0.1$ , \* $p < 0.05$ , \*\*  $p < 0.01$  and \*\*\*  $p < 0.001$ .

### 4.3. Results

#### **J774 Macrophages Expressed Inducible and Functional NLRP3 Inflammasomes.**

NLRP3 inflammasomes are expressed by J774 macrophages. The expression of the internal receptor, NLRP3 and cleaved caspase 1 were slightly increased following treatment with known NLRP3 inflammasome activators, LPS and ATP, and tumor conditioned media, 4T1 conditioned media (Fig. 4.1.AC, n.s.). Additionally, expression of ASC1 and IL-18 secretion were both marginally increased with 4T1CM treatment (Fig. 4.1.BF,  $p<0.1$  and  $p<0.05$  respectively).

Furthermore, the expression of pore-forming gasdermin D is remarkably increased following LPS and ATP treatment (Fig. 4.1. D,  $p<0.05$ ). Consequentially, the secretion of IL-1 $\beta$  was elevated by LPS and ATP (Fig. 4.1. E,  $p<0.01$ ).

#### **NLRP3 Inflammasome Activation was Associated with Pro-Tumorigenic Macrophage Phenotype.**

NLRP3 inflammasome activating treatments shifted macrophages toward a tumor-promoting phenotype. Inflammasome activating LPS+ATP led to a 4-fold increase arginase expression by J774 macrophages (Fig. 4.2. A,  $p<0.001$ ). Meanwhile, both LPS and ATP and 4T1 conditioned media moderately increased iNOS expression (Fig. 4.2. B,  $p<0.01$  and  $p<0.05$  respectively). Importantly, the arginase to iNOS expression ratio increased 2-fold following LPS+ATP treatment (Fig. 4.2. C,  $p<0.001$ ).

Pro-tumorigenic macrophages also exhibited impaired phagocytosis. Following LPS and ATP treatment, which increased IL-1 $\beta$  secretion, bead phagocytosis was reduced 2-fold compared to the negative control (Fig. 4.2. D,  $p<0.001$ ). Moreover, 4T1CM also reduced phagocytosis by roughly 25% compared to media alone (Fig. 4.2. D,  $p<0.01$ ).

### **The P2RX7 Antagonist, A438079, Altered Macrophage Pro-Inflammatory Cytokine Secretions.**

Treatment of macrophages with the P2RX7 antagonist, an inhibitor of NLRP3 inflammasome activating  $K^+$  efflux (375), had limited effects on LPS+ATP treatment driven ASC1 expression or caspase-1 activation, with expression of both marginally increased (Fig. 4.3.BC). Additionally, LPS+ATP treatment marginally increased GSDMD macrophage expression regardless of P2RX7 inhibition (Fig. 4.3.E,  $p<0.1$ ). While intracellular IL-1 $\beta$  expression remained unaltered following LPS+ATP treatment combined with P2RX7 inhibition, IL-1 $\beta$  secretion was increased in response to LPS+ATP treatment (Fig. 4.4.A,  $p<0.05$ ). Furthermore, the IL-1 $\beta$  intracellular to IL-1 $\beta$  secreted ratio was elevated following combination treatment with LPS+ATP and A438079 (Fig. 4.4.C, n.s.). Similarly, the ratio of IL-18 intracellular to IL-18 secreted ratio was marginally increased following P2RX7 antagonist treatment (Fig. 4.4.D,  $p<0.1$ ).

### **P2RX7 Antagonist, A438079, Limited the NLRP3 Inflammasome Activation Driven Pro-Tumorigenic Macrophage Phenotype.**

P2RX7 antagonist treatment increased iNOS expression by 50% compared to LPS+ATP treatment alone (Fig. 4.5.B,  $p<0.05$ ). While arginase expression was not significantly altered by A438079 treatment, the arginase to iNOS expression ratio was reduced when treatment with A438079 was added to LPS+ATP NLRP3 inflammasome activation driven macrophages compared to LPS+ATP, NLRP3 inflammasome activation driven macrophages (Fig. 4.5.C,  $p<0.001$ ). Moreover, the P2RX7 inhibition by A438079, partially abrogated the LPS+ATP, NLRP3 inflammasome activation driven reduction in phagocytosis (Fig. 4.5.D,  $p<0.01$ ).

### **Disulfiram Reduces Cytokine Secretion without Limiting NLRP3 Inflammasome Expression.**

Disulfiram, a drug that prevent gasdermin D pore formation (374), was assayed on macrophages with NLRP3 inflammasome activated with either the LPS and ATP mix or 4T1 conditioned media. Disulfiram did not reduce the expression of macrophage NLRP3 expression even when treated with the NLRP3 inflammasome activator LPS and ATP treatment (Fig. 4.6.A). However, disulfiram treatment led to reduced ASC1 expression when compared to media alone and LPS+ATP treatment (Fig. 4.6.B,  $P<0.05$ ). Disulfiram also tended to promote active caspase 1 expression compared to treatment with the NLRP3 inflammasome activator LPS and ATP and media alone (Fig. 4.6.C, n.s.). Disulfiram treatment of LPS+ATP-driven, NLRP3 inflammasome activated macrophages led to with marginal increases in gasdermin D and P2RX7 expression compared to LPS+ATP-driven, NLRP3 inflammasome activated macrophages and control macrophages (Fig. 4.6.DE,  $p<0.1$ ).

Disulfiram treatment reduced the LPS+ATP-driven, NLRP3 inflammasome activated macrophage secretions of IL-1 $\beta$  (Fig. 4.7.A,  $p<0.001$ ). Furthermore, the intracellular IL-1 $\beta$  to secreted IL-1 $\beta$  ratio was increased 3-fold compared to LPS+ATP-driven, NLRP3 inflammasome activated macrophage secretions (Fig. 4.7.C,  $p<0.001$ ). Additionally, disulfiram treatment also increased macrophage intracellular expression IL-18 compared to control (not shown,  $p<0.05$ ). However, the secretion of IL-18 and the intracellular IL18 to secreted IL-18 ratio were unaltered following treatment with disulfiram (Fig. 4.7.BD).

### **Disulfiram Limits the Pro-Tumorigenic Phenotype of NLRP3 Inflammasome Activated Macrophages.**

Treatment of LPS and ATP driven NLRP3 inflammasome activated macrophages treated with disulfiram led to increased arginase expression compared to untreated LPS and ATP-driven, NLRP3 inflammasome activated macrophages (Fig. 4.8.A,  $p < 0.01$ ). Additionally, the treatment of LPS and ATP-driven, NLRP3 inflammasome activated macrophages treated with disulfiram increased iNOS expression compared to untreated LPS and ATP-driven, NLRP3 inflammasome activated macrophages (Fig. 4.8.B,  $p < 0.01$ ). The arginase to iNOS expression ratio was decreased following treatment of LPS and ATP-driven, NLRP3 inflammasome activated macrophages treated with disulfiram (Fig. 4.8.C,  $p < 0.001$ ). Moreover, the decline in macrophage phagocytic activity driven by LPS and ATP-induced NLRP3 inflammasome activation was partially reduced by disulfiram treatment (Fig. 4.8.D,  $p < 0.05$ ).

#### 4.4. Discussion

Breast cancer remains a deadly disease that is exacerbated by tumor-associated macrophages (TAMs) (115, 123, 284). TAMs present a unique phenotype that promotes breast cancer proliferation and immunosuppression (127, 305, 306). The mechanisms by which macrophages become polarized to a tumor-promoting phenotype in breast cancer are poorly understood although studies have demonstrated that NLRP3 inflammasome signaling skewed macrophages toward a pro-tumorigenic phenotype (309, 317, 340, 343, 376, 377). In the present study, we investigated the potential of targeting ATP activation and gasdermin D pore formation, both associated with NLRP3 inflammasome activation in preventing the generation of M2-like pro-tumorigenic macrophages. Our results indicate that NLRP3 inflammasome activation is associated with pro-tumorigenic macrophage polarization and that pharmacological blocking of pro-inflammatory cytokine maturation and secretion limits pro-tumorigenic polarization *in vitro*.

Importantly, our data indicate that the macrophage NLRP3 inflammasome activated not only by the canonical NLRP3 inflammasome LPS+ATP combination, but also by the mammary 4T1 tumor cell secretome - supporting the activation of macrophage NLRP3 inflammasomes once macrophages are within the tumor microenvironment. In turn, NLRP3 inflammasome activation led to macrophage pro-inflammatory cytokine secretions (50, 195). Notably, our data indicate that IL-18 secretions were triggered by tumor secretome. Interestingly, in lung cancer, tumor cell-derived exosomes containing TRIM59 was demonstrated to activate NLRP3 inflammasomes of tumor-associated macrophages (378). And, physiologically relevant to breast cancer, which forms adjacent



to mammary fat, adipocyte-derived leptin activates macrophage NLRP3 inflammasomes (379).

Interestingly, our data support the switch in macrophage polarization as assessed by the arginase (M1) to iNOS (M2) expression ratio that closely mimic the IL-1 $\beta$  secretion flux. Previously, cytokine secretions also led to macrophage arginase expression associated with a pro-inflammatory cytokine-driven polarization including IL-1 $\beta$  and TNF- $\alpha$  secretions inducing arginase expression through IL-33 secretion and recombinant IL-18 treatment increasing arginase expression in monocytes (242, 319). Moreover, our data shows that the shift toward a tumor promoting phenotype was associated with a decrease in phagocytic activity associated with pro-tumorigenic (M2-like) macrophages (135).

Neither antagonizing P2XR7 nor inhibiting gasdermin D inhibitor reduced NLRP3 inflammasome activation, likely because of purigenic receptors redundancy (380) and multi-modal activities of disulfiram. Nevertheless, antagonizing P2RX7 signaling led to a marginal cytoplasmic cytokine retention. Disulfiram also increased IL-1 $\beta$  retention and decrease IL-1 $\beta$  secretion, but had no effect on IL-18 secretion. In other studies, disulfiram treatment inhibited both caspase 1 and caspase 11 activation (381). Our data point, especially the increase in intracellular to secreted cytokines, to an inhibition of the gasdermin D activation and thus the blocking of the pore formation partially trapping the mature cytokine in the cytoplasm (374, 381).

Our data reveal that macrophage NLRP3 inflammasome-driven IL-18 secretions were not significantly altered by disulfiram treatment and may be driving the increase in arginase expression this despite disulfiram treatment (242). Although neither A438079 nor disulfiram interfere with inflammasome priming or NF- $\kappa$ B activity, both antagonizing

P2RX7 ATP receptor signaling and gasdermin D inhibition increased macrophage iNOS expression promoting an anti-tumorigenic (M1-like) macrophage phenotype. Inhibition of macrophage NF- $\kappa$ B halted iNOS induction increase (382, 383) . We also assessed the effects of inhibiting NF- $\kappa$ B using the proteasome inhibitor MG-132 (384). Following MG-132 treatment, NLRP3 inflammasome activated macrophages had reduced arginase to iNOS expression ratios, but the decrease in phagocytic activity associated with inflammasome activation remained unchanged (Supplemental Fig. 4.1.).

Our data also highlight that NLRP3 inflammasome activated macrophage reduced phagocytosis activity was rescued by treatment with a P2RX7 ATP receptor antagonist or an inhibitor of gasdermin D cleavage supporting a shift toward an anti-tumorigenic phenotype (179, 276, 341). The P2RX7 ATP receptor antagonist used, A438079, induced a greater shift in phagocytic activity than inhibitor of gasdermin D cleavage disulfiram. Our result support the role of P2RX7 ATP receptor as a scavenger receptor and the positive effect A438079 on macrophage phagocytosis following treatment with ATP (385). Inhibition of gasdermin D pore-formation and pro-inflammatory cytokine secretion by disulfiram also increased the phagocytic activity of J774 macrophages. This observation is in line with the repolarization of tumor-associated macrophages to an anti-tumor M1 phenotype following co-delivery of disulfiram and copper in an *in vivo* glioma preclinical model (386). On the other hand, *in vitro* disulfiram treatment (10 $\mu$ M) of primary monocytes led to a markedly increased phagocytosis (387).

Overall, our data indicate that targeting P2RX7 signaling and the gasdermin D pore formation altered the NLRP3 inflammasome activated pro-tumorigenic macrophage phenotype shifting it to a more phagocytic M1-like phenotype. Validating studies

confirming M2-polarizing effects of NLRP3 inflammasome activation and of pro-inflammatory cytokines on macrophages are required. Furthermore, studies supporting the disulfiram effects on gasdermin D cleavage and not caspase 1-mediated cytokine maturation are needed.

Our data report that macrophage NLRP3 inflammasome activation is associated with an increase in pro-inflammatory cytokine secretion and a pro-tumorigenic (M2-like) phenotype characterized by increased arginase expression and decreased phagocytic activity. In NLRP3 inflammasome activated macrophages, inhibiting either P2RX7 ATP receptor signaling or gasdermin D cleavage and subsequent pore formation altered the secretion of pro-inflammatory cytokines but not NLRP3 inflammasome formation and activity including active caspase 1 expression. Furthermore, in NLRP3 inflammasome activated macrophages, treatment with inhibitors of either P2RX7 ATP receptor signaling or gasdermin D cleavage and subsequent pore formation rescued phagocytic activities suggesting a shift toward a more anti-tumorigenic macrophage phenotype. Our data support further investigations in NLRP3 inflammasome activation, P2RX7 ATP receptor and gasdermin D cleavage as adjuvant therapeutic targets for breast cancer.

## 4.5. Figures

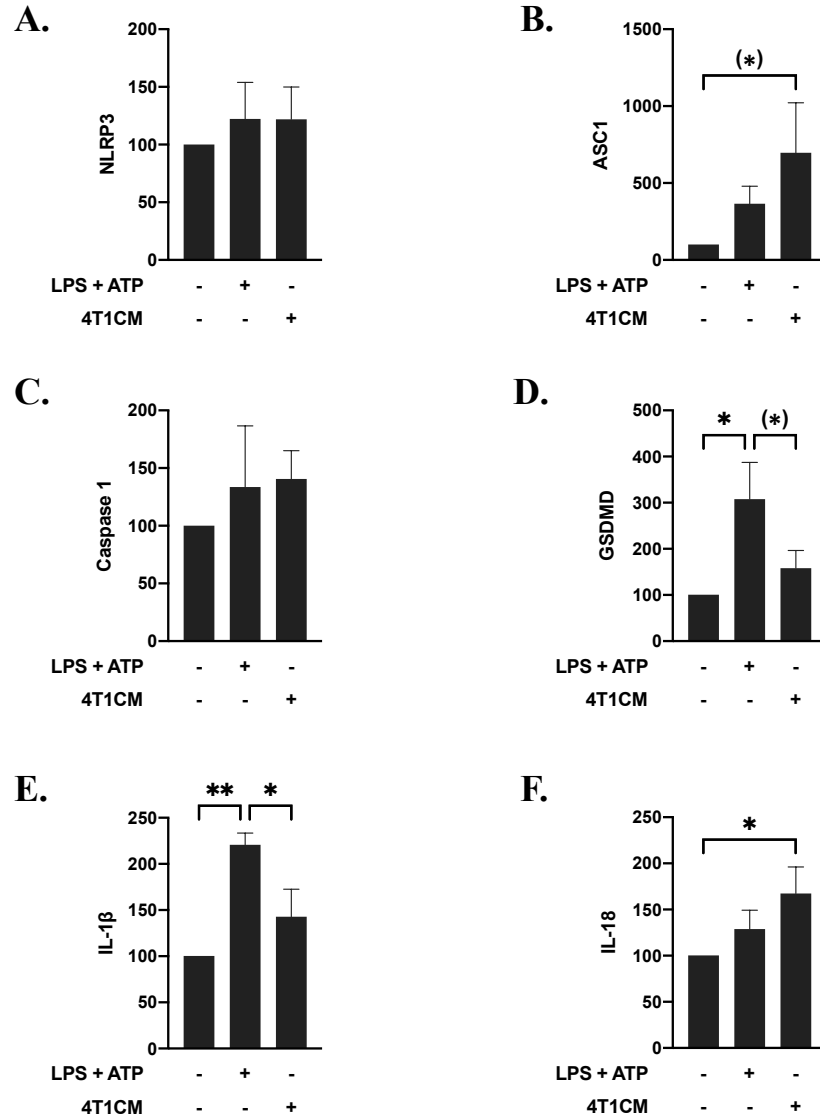


**Figure 4.1. NLRP3 Inflammasomes are Activated by LPS and ATP and Tumor Conditioned Media Treatment in J774 Macrophages.** Immunoblot quantifications normalized to the negative control of **A.** NLRP3, **B.** ASC1, **C.** Caspase 1, **D.** Gasdermin D and cytokines, **E.** IL-1 $\beta$  and **F.** IL-18, by J774 macrophages. Expression is increased following LPS+ATP and 4T1CM treatments. \*\* p<0.01, \* p<0.05, (\*) p<0.1.

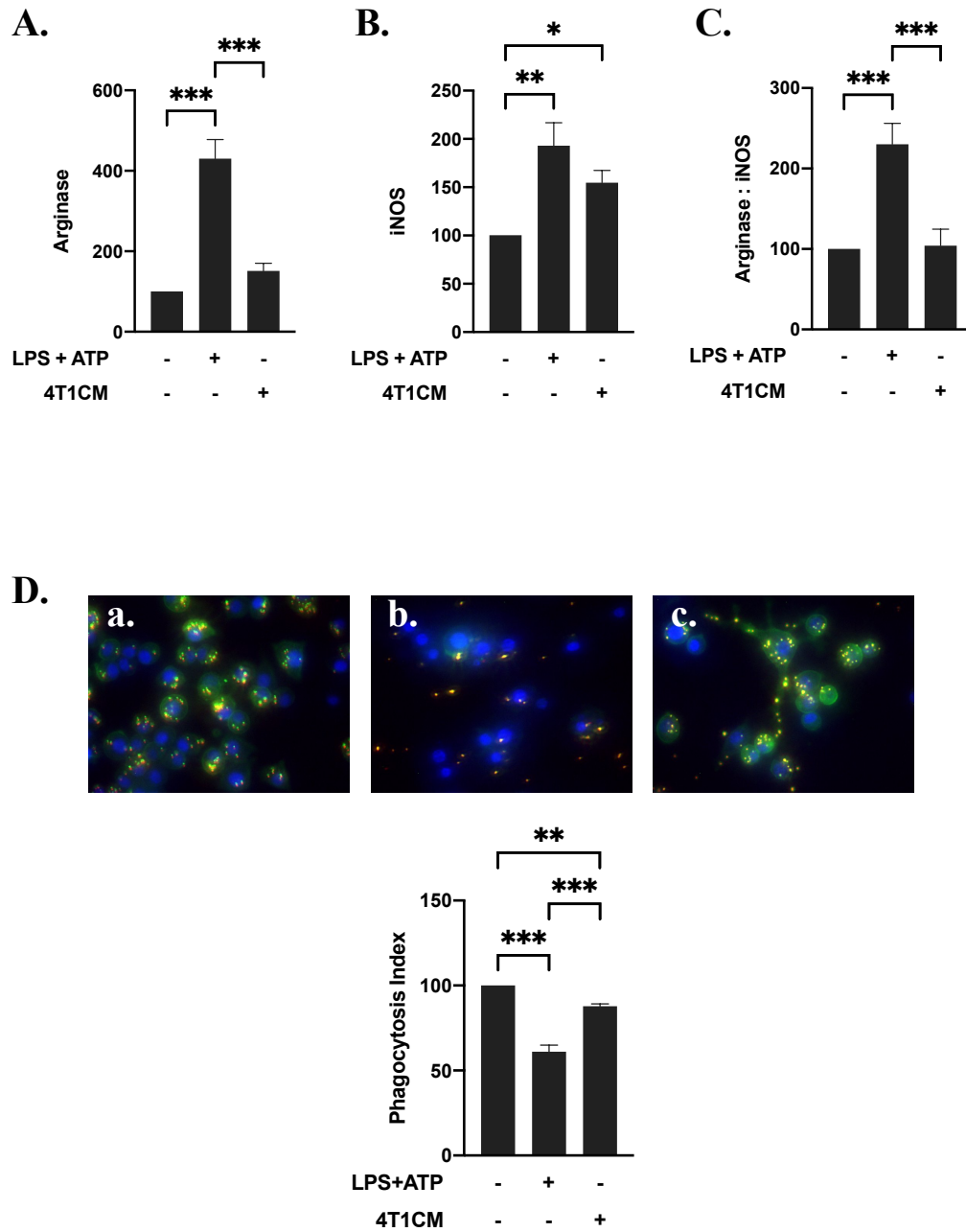


**Figure 4.2. NLRP3 Inflammasome Activating Treatments are Associated with a Pro-Tumorigenic Macrophage Phenotype.** Immunoblot quantifications normalized to the negative control of **A.** arginase, **B.** iNOS and **C.** arginase : iNOS expression ratio by J774 macrophages following LPS+ATP and 4T1CM treatment. **D.** Phagocytosis by J774 macrophages is reduced compared to **a.** control following **b.** LPS+ATP and **c.** 4T1CM. In the representative images, beads are yellow, and nuclei are blue. \*\*\*  $p < 0.001$ , \*\*  $p < 0.01$ , \*  $p < 0.05$ , (\*)  $p < 0.1$ .

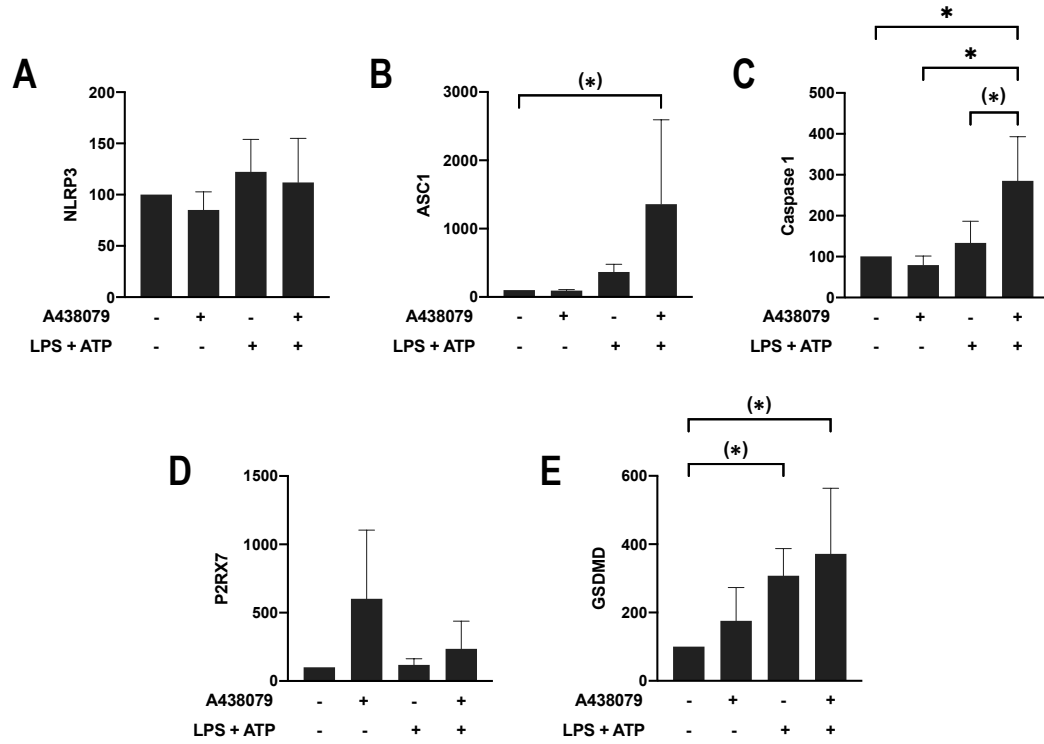


**Figure 4.3. NLRP3 Inflammasome Activation is not Inhibited by the P2RX7 Antagonist, A438079, in J774 Macrophages.** Immunoblot quantifications normalized to the negative control of **A.** NLRP3, **B.** ASC1, **C.** cleaved caspase 1, **D.** P2RX7, and **E.** Gasdermin D by J774 macrophages following LPS+ATP and A438079 treatment. \*  $p < 0.05$ , (\*)  $p < 0.1$ .

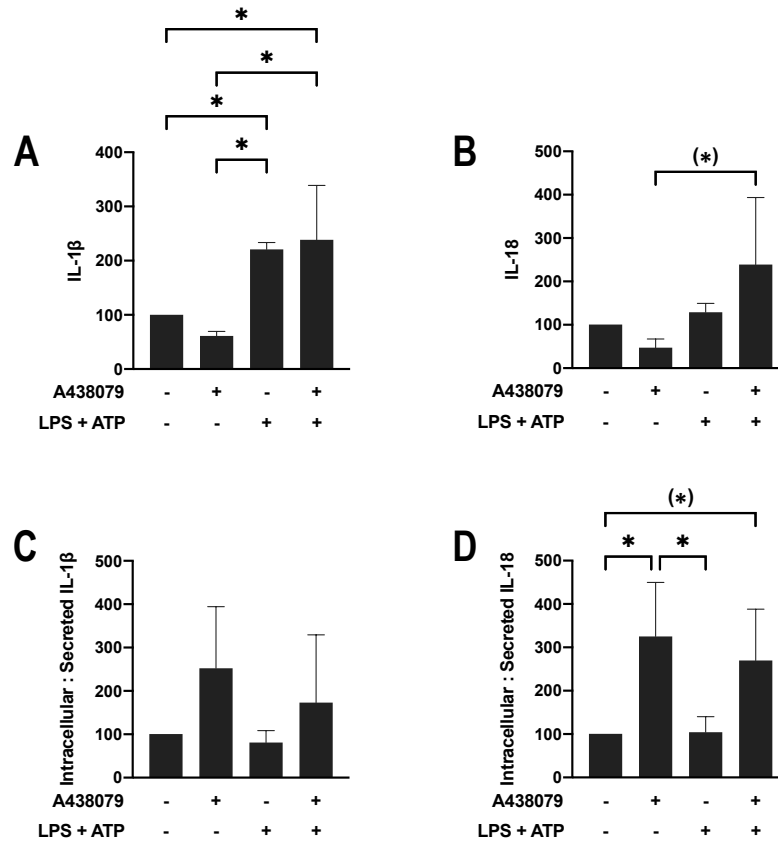


**Figure 4.4. Pro-Inflammatory IL-1 $\beta$  Secretion is Altered by A438079 Treatment in J774 Macrophages.** Immunoblot quantifications normalized to the negative control of **A.** IL-1 $\beta$  and **B.** IL-18 secretion and the ratio of **C.** intracellular to secreted IL-1 $\beta$  and **D.** intracellular to secretion IL-18 by J774 macrophages following LPS+ATP and A438079 treatment. \*  $p < 0.05$ , (\*)  $p < 0.1$ .

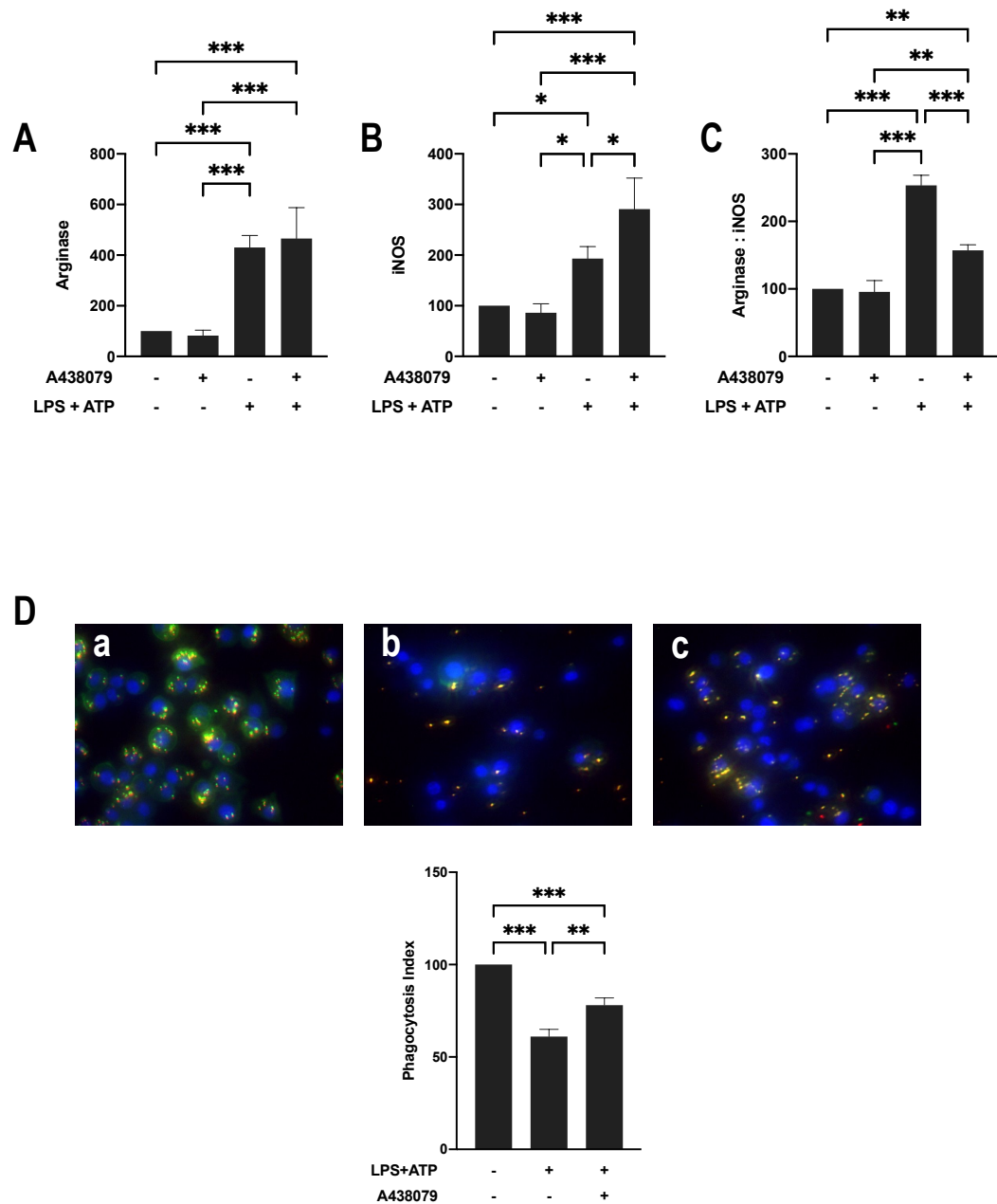


**Figure 4.5. Pro-Tumorigenic Phenotype is Reduced Following Treatment with P2RX7 Antagonist, A438079.** Immunoblot quantifications normalized to the negative control of **A.** arginase, **B.** iNOS, **C.** the ratio of arginase to iNOS expression and **D.** the phagocytic activity of J774 macrophages in **a.** control conditions and treated with **b.** LPS+ATP and **c.** LPS+ATP combined with A438079. \*\*\*  $p < 0.001$ , \*\*  $p < 0.01$ , \*  $p < 0.05$ .



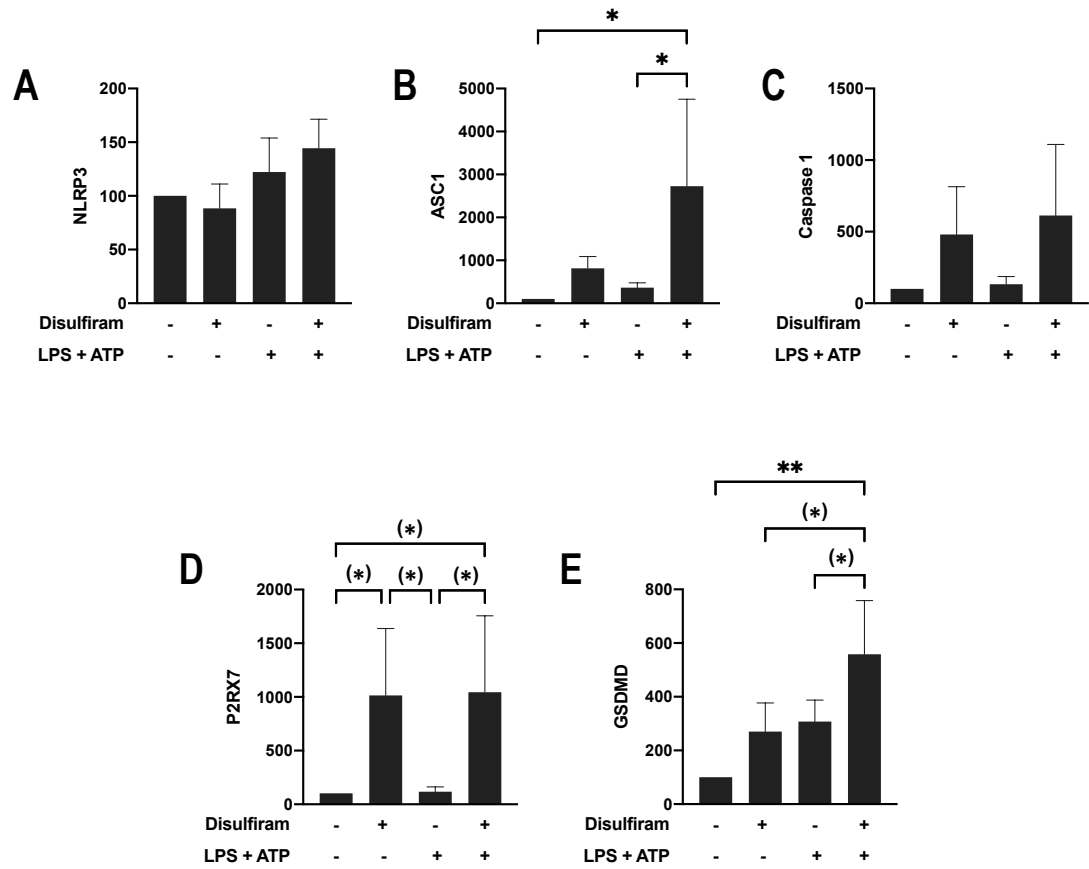


**Figure 4.6. NLRP3 Inflammasome Activation is not Inhibited by Gasdermin D Inhibitor, Disulfiram, Treatment in J774 Macrophages.** Immunoblot quantifications normalized to the negative control of **A.** NLRP3, **B.** ASC1, **C.** cleaved caspase 1, **D.** P2RX7, and **E.** Gasdermin D by J774 macrophages following LPS+ATP and disulfiram treatment. \*\*  $p < 0.01$ , \*  $p < 0.05$ , (\*)  $p < 0.1$ .

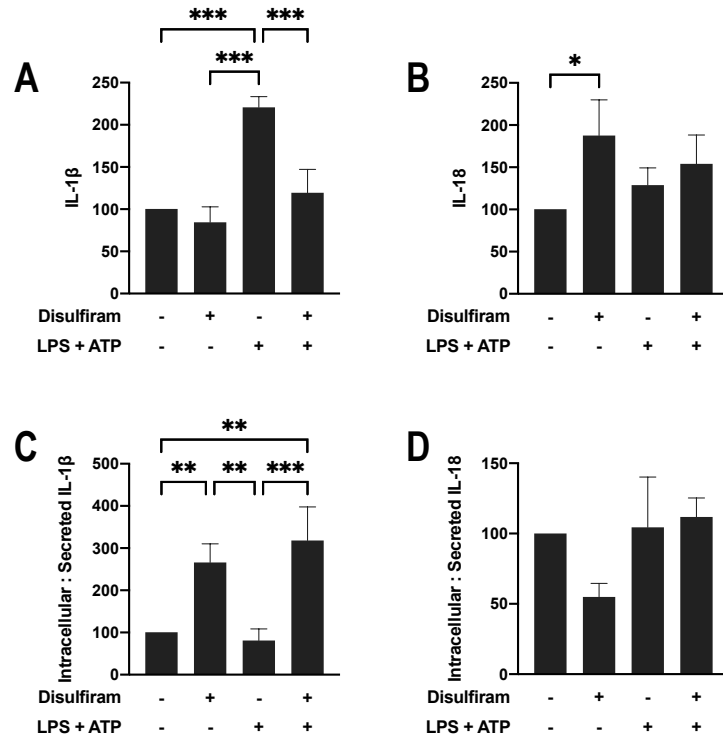


**Figure 4.7. Pro-Inflammatory IL-1 $\beta$  Secretion is Inhibited by Disulfiram Treatment in J774 Macrophages.** Immunoblot quantifications normalized to the negative control of **A.** IL-1 $\beta$  and **B.** IL-18 secretion and the ratio of **C.** intracellular to secreted IL-1 $\beta$  and **D.** intracellular to secretion IL-18 by J774 macrophages following LPS+ATP and disulfiram treatment. \*\*\*  $p < 0.001$ , \*\*  $p < 0.01$ , \*  $p < 0.05$ , (\*)  $p < 0.1$ .

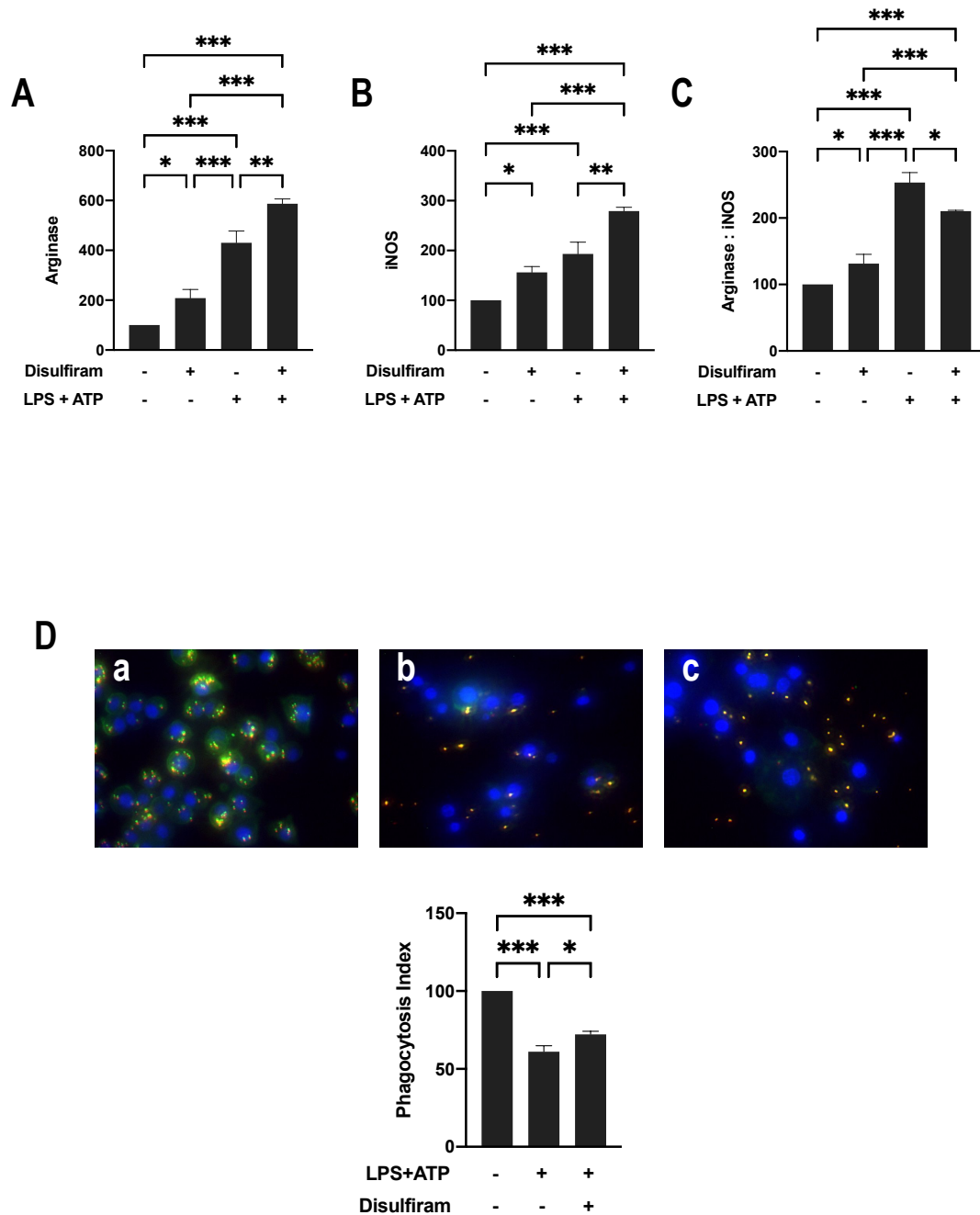


**Figure 4.8. Pro-Tumorigenic Phenotype is Reduced Following Treatment with Gasdermin D Inhibitor, Disulfiram.** Immunoblot quantifications normalized to the negative control of **A.** arginase, **B.** iNOS, **C.** the ratio of arginase to iNOS expression and **D.** the phagocytic activity of J774 macrophages in **a.** control conditions and treated with **b.** LPS+ATP and **c.** LPS+ATP combined with disulfiram. \*\*\*  $p < 0.001$ , \*\*  $p < 0.01$ , \*  $p < 0.05$ .

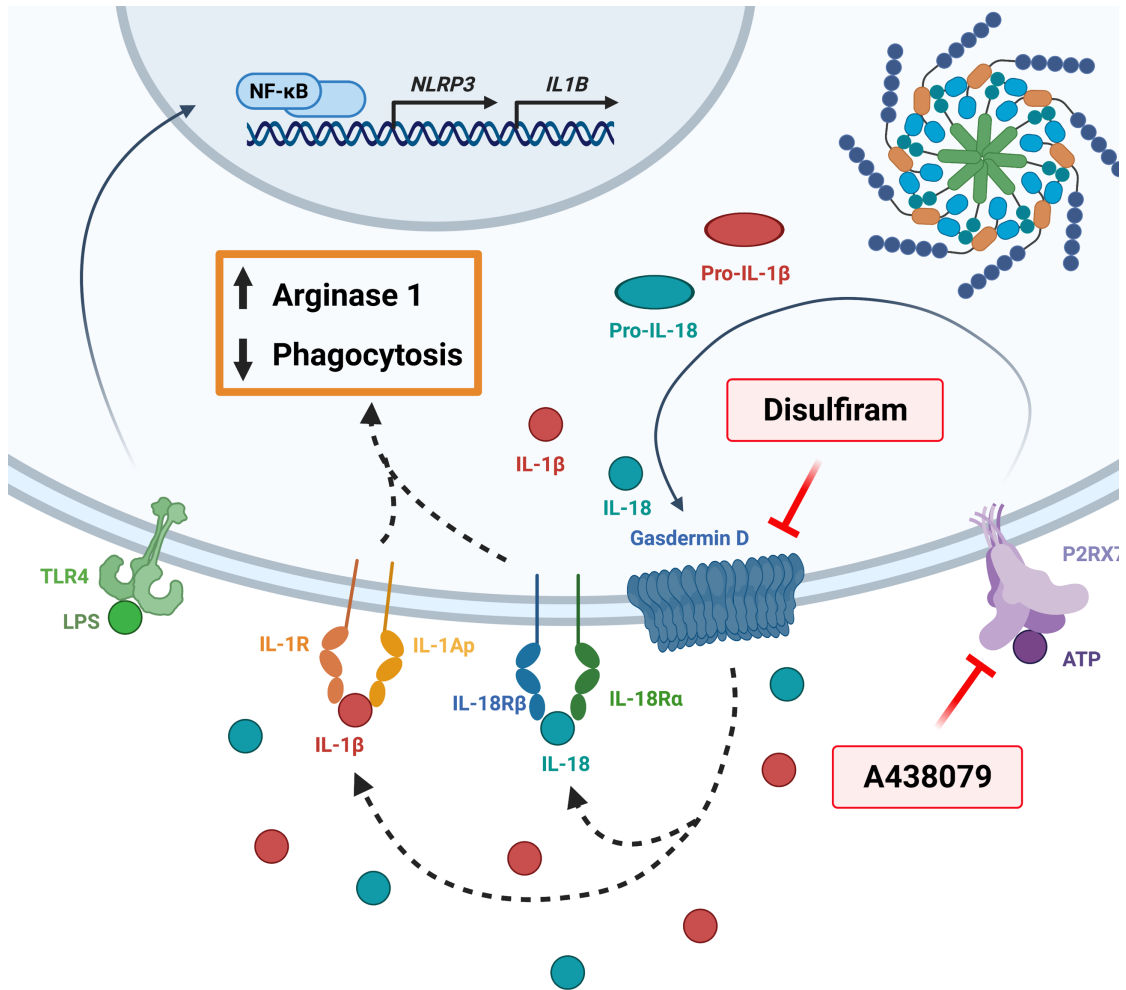
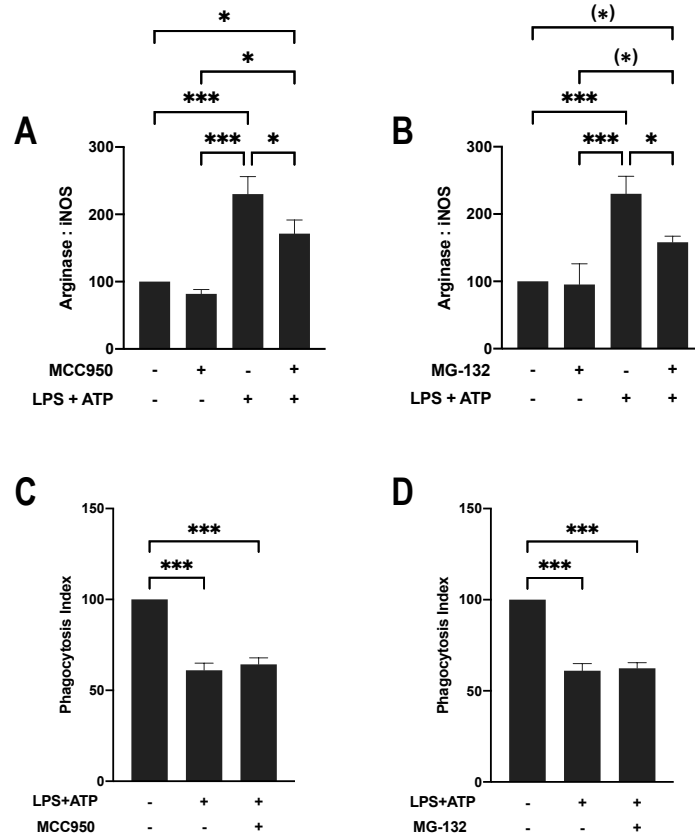


**Figure 4.9. Graphical Representation of the Pro-Tumorigenic Effect of the NLRP3 Inflammasome.** The NLRP3 inflammasome is activated by LPS and ATP through TLR4 and P2RX7 respectively (179, 276, 341). P2RX7 activation results in a  $K^+$  efflux that leads to the oligomerization of the NLRP3 inflammasome – A438079 blocks this activation (375). Following NLRP3 inflammasome oligomerization, gasdermin D is cleaved and moves to the membrane to form a pore through which IL-1 $\beta$  and IL-18 are secreted (215, 216, 218, 219). Disulfiram inhibits the cleavage and subsequent pore formation of gasdermin D (374). Pro-inflammatory cytokine signaling, in an autocrine or paracrine manner, results in increased arginase expression and decreased phagocytosis. Generated by KH using BioRender.com

#### 4.6. Supplemental Figure



**Supplemental Figure 4.1. NLRP3-Specific Inflammasome Inhibitor, MCC950, and NF- $\kappa$ B Inhibitor, MG-132, Reduced the Ratio of Arginase to iNOS, But Did Not Reverse the Reduced Phagocytic Activity Associated with NLRP3 Inflammasome Activation.** Immunoblot quantifications normalized to the negative control of the arginase to iNOS expression ratio following treatment with **A.** MCC950 and **B.** MG-132. Phagocytic activity of J774 macrophages following treatment with **C.** MCC950 and **D.** MG-132. \*\*\*  $p < 0.001$ , \*\*  $p < 0.01$ , \*  $p < 0.05$ , (\*)  $p < 0.1$ .

## CHAPTER 5. CONCLUSIONS AND FUTURE DIRECTIONS.

### 5.1. Conclusions

Despite the steady decline in breast cancer-related deaths since the 1980s, breast cancer remains the second-leading cause of malignant deaths among women (282). Breast cancer-associated mortality is concomitant with malignant dissemination to distant organs such as the brain, liver, lungs, and bones (388, 389) as highlighted by the three-fold reduction in 5-year survival for women with metastatic breast cancer compared to non-metastatic disease (390). Increased infiltration of macrophages, specifically of pro-inflammatory macrophages, correlates with breast cancer metastases (112, 126, 306, 334, 335). Indeed, inflammatory crosstalk between macrophages and tumor cells promotes tumor progression through increased proliferation, angiogenesis, and epithelial-mesenchymal transition (159, 230, 235, 236, 238, 311). In particular, inflammation generated by NLRP3 inflammasomes has been linked to breast cancer progression (159, 160, 311, 339, 344).

Our work demonstrates that macrophages with activated NLRP3 inflammasomes have elevated active caspase 1 expression and become skewed toward a pro-tumorigenic, M2 phenotype that promotes breast tumor proliferation, metastasis, and immunosuppression. *In vitro*, the secretome of macrophages J774 with functional and activated NLRP3 inflammasomes enhanced 4T1 tumor cell proliferation. In addition, J774 macrophages treated with NLRP3 inflammasome activators, displayed an increased arginase : iNOS expression ratio, a marker of the M2 pro-tumorigenic macrophage phenotype. Moreover, NLRP3 inflammasome activation in macrophages led to reduced phagocytic activity. These observations confirm the relationship between NLRP3

inflammasome activation and the tumor-promoting macrophage (M2-like) phenotype (242, 319).

*In vivo*, co-implantation of 4T1 tumor cells and syngeneic J774 macrophages resulted in elevated 4T1 tumor cell stem characteristics and increased metastasis compared to implantation of 4T1 tumor cells alone or co-implantation of 4T1 cells with the syngeneic NLRP3 inflammasome-deficient RAW macrophages. Indeed, the *in vivo* syngeneic orthotopic co-implantation of 4T1 cells with J774 macrophages that have functional NLRP3 inflammasomes promoted increased tumor cell stemness as highlighted by significantly higher cytokeratin 19 expression and higher N-cadherin to E-cadherin expression ratios. These findings are congruent with previous data showing that NLRP3 inflammasome activation in macrophages promotes stemness, invasiveness and metastasis (90, 311, 320).

Next, we assessed the potential of the NLRP3 inflammasome-specific inhibitor MCC950 to alter the macrophage tumor-promotion alone or combined with a chemotherapy regimen. *In vitro*, 4T1 tumor cells treated with increasing doses of the NLRP3 inflammasome inhibitor, MCC950, alone or in combinations with chemotherapeutic drug, 5-Fluorouracil (5-FU), demonstrated a significant reduction in 4T1 tumor cell proliferation following exposure to 10 $\mu$ M of MCC950 alone. While similar observations were made in *in vitro* co-cultures of 4T1 tumor cells with J774 macrophages, the effects of MCC950 with or without 5-FU were significantly reduced.

Interestingly, *in vivo* in the orthotopic immunocompetent 4T1 breast cancer model with implantation of 4T1 cells alone or co-implantation of 4T1 tumor cells and syngeneic J774 macrophages, the MCC950 and 5-FU combination regimen led to significantly

reduced tumor burden compared to mice receiving MCC950 alone. The MCC950 and 5-FU combination regimen was especially potent in animals co-implanted with 4T1 and macrophages with functional NLRP3 inflammasomes. These observations are consistent with a prior demonstration highlighting that NLRP3 inflammasome inhibition in combination with chemotherapy reduced tumor growth (363).

Additionally, in mice co-implanted with both 4T1 tumor cells and J774 macrophages, leukocyte (CD45+) infiltration was significantly reduced in tumor derived from mice treated with MCC950 and 5-FU combination compared to tumors isolated from vehicle-treated mice. In particular, the reduced leukocyte infiltration may be indicative of a decline in myeloid lineage suppressor cells and regulatory T-cells - both of which are positive prognostic outcomes in human breast cancer (343, 366, 367). Intriguingly, 5-Fluorouracil has been demonstrated to induce cathepsin B-mediated NLRP3 inflammasome activation that promotes a pro-tumorigenic Th17 response (350). However, analogous to our findings, 5-FU treatment in NLRP3- and caspase 1- null mice, restrained the tumor promoting immune response (350).

Mechanisms of NLRP3 inflammasome activation and pro-inflammatory cytokine release were also investigated through pharmacological inhibition of ATP-induced activation and pore-mediated cytokine release (276, 374, 391). To assess whether NLRP3 inflammasome oligomerization or autocrine pro-inflammatory cytokine signaling was driving the pro-tumorigenic phenotype associated with NLRP3 inflammasome activation in macrophages, we inhibited NLRP3 inflammasome mediated cytokine maturation using a P2RX7 inhibitor and blocked gasdermin D pore-mediated cytokine secretion.



Our results indicate that the P2RX7 inhibition of ATP-induced NLRP3 inflammasome activation did not significantly reduce macrophage active caspase 1 expression or IL-1 $\beta$  or IL-18 pro-inflammatory cytokine secretions. However, P2RX7 inhibition of ATP-induced NLRP3 inflammasome activation significantly reduced the macrophage arginase to iNOS expression ratio and phagocytic activity. This observation highlights the association between P2RX7-mediated NLRP3 inflammasome activation and the M2-like, pro-tumorigenic macrophage phenotype (392). Moreover, disulfiram inhibition of the formation of gasdermin D transient pores increased macrophage pro-inflammatory IL-1 $\beta$  intracellular retention and limited its secretion. Interestingly, in those conditions, the macrophage arginase to iNOS expression ratio was minimally reduced with an unchanged arginase expression and an increased iNOS expression. Additionally, disulfiram treatment, gasdermin D pore inhibition, significantly prevented the macrophage phagocytic activity reduction driven by NLRP3 inflammasome activation. Disulfiram treatment has been shown to reduce macrophage immunosuppressive responses (387, 393). Interestingly, our data indicate that intra-tumoral pro-inflammatory cytokine expression was positively correlated with arginase expression whereas IL-1 $\beta$  and IL-18 expression was not correlated with iNOS expression (Fig. 5.2.). Taken, together we suggest that autocrine pro-inflammatory cytokine signaling may induce a tumor-promoting, immunosuppressive shift in tumor-associated macrophages (Fig. 5.3.).

This dissertation highlights the role of NLRP3 inflammasome activation in macrophages to promote tumor growth and generate an immunosuppressive microenvironment. Our results establish that the NLRP3 inflammasome is associated with an immunosuppression macrophage phenotype defined by arginase and CD206 expression

and reduced phagocytosis. Investigations of other mechanisms of immune evasion present in cancers (394-398) including the anergic interactions between PD-1 and PD-L1 (399-401) are warranted.

## 5.2. Future Directions

Inflammation plays a major role in the transition from differentiated to dedifferentiated state of cancer stem-like cells as shown in breast cancer mouse models (88). High IL-1 $\beta$  intra-tumoral concentrations are associated with worse prognosis, likely because IL-1 $\beta$  autocrine/paracrine signaling promotes growth and metastasis (89). Indeed, in breast cancer cells, IL-1 $\beta$  signaling activation promotes a transition toward a mesenchymal phenotype and epithelial to mesenchymal transition (EMT) in cancer is associated with tumor growth and metastasis (90, 159, 230, 231). Moreover, EMT also leads to elevated expression of the programmed death receptor ligand (PD-L1) by tumor cells thus hindering host immune cell cytotoxicity (79, 90, 402-406). Interestingly, tumor-intrinsic NLRP3 inflammasome activation also promotes PD-L1 upregulation by tumor cells in gastric cancer, melanoma, and lymphoma cancers (323, 338, 402). Whether similar mechanisms prevent efficient host immune responses in breast cancer remains to be demonstrated.

Expression of PD-1 on macrophages and the effect of NLRP3 inflammasome on PD-1 expression by macrophages are only beginning to be uncovered. We demonstrated that when NLRP3 inflammasomes are activated in macrophages, the phagocytic activity of macrophages declines. Likewise, phagocytosis of tumor cells by macrophages is reduced when macrophages express PD-1 (407). Although, this is likely due to PD-1/PD-L1 interactions preventing phagocytosis, the connection between NLRP3 inflammasome activation and PD-1 expression warrants further investigations.

Overall, our work highlights that macrophages through functional NLRP3 inflammasome activation promote tumor proliferation and tumor cell stemness. In addition,

NLRP3 inflammasome activation in macrophages is associated with a measurable shift in tumor-promoting characteristics and this shift is, in part, driven by autocrine, pro-inflammatory cytokine signaling. Among the various NLRP3 inflammasome inhibitors available, as highlighted in figure 5.1., the combination of the NLRP3-specific inhibitor MCC950 and of the chemotherapeutic drug 5-FU demonstrated efficacy in reducing tumor burden, metastasis, and immune cell infiltration. Future investigations will further our understanding of the immunosuppressive shift driven by NLRP3 inflammasome activation in macrophages and the potential of altering inflammasome-driven immune responses to improve breast cancer treatments.

### 5.3. Figures

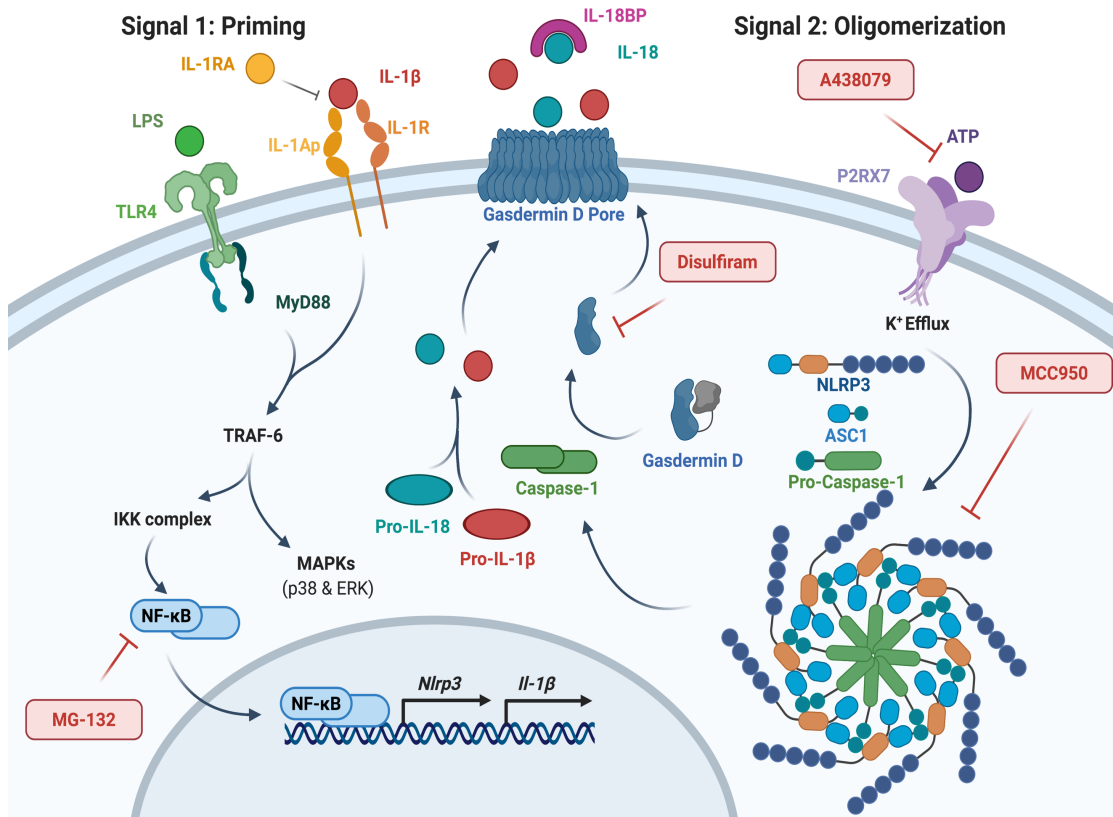


**Figure 5.1. NLRP3 Inflammasome Pharmacological Inhibitors Target Both Priming and Activation Steps.** NLRP3 inflammasome activation occurs by two signals: the first which increases the expression of receptor protein, NLRP3, and immature cytokine, pro-IL-1β, and the second which promotes the oligomerization of the NLRP3 inflammasome (181, 185). NLRP3 inflammasome inhibitors targeting both steps exist. Proteasome inhibitor, MG-132, reduces the activity of NF-κB resulting in diminished priming or *NLRP3* and *IL1B* transcription (384). P2X7 receptor antagonist, A438079, blocks the activity of ATP and inhibits oligomerization (369). The precise mechanism of MCC950 is unclear, but literature suggests the MCC950 fixes the NLRP3 receptor into an inactive conformation, thus preventing oligomerization (347). Finally, disulfiram neither inhibits priming nor oligomerization, but blocks the pore formation necessary for cytokine secretion (374, 381). Generated by KH using BioRender.com

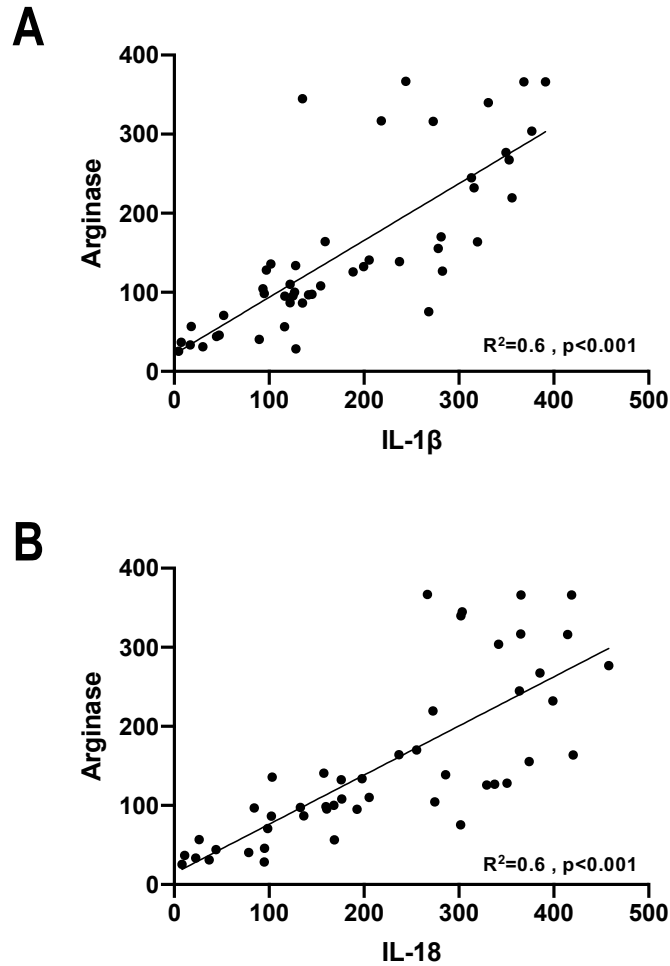


**Figure 5.2. Pro-Inflammatory Cytokines Production Within Tumors is Associated with Pro-Tumorigenic Immune Response.** Immunoblot quantification of arginase expression normalized relative to tumor mass and 4T1 tumor cell injected and saline administered control. Intra-tumoral arginase expression is positively associated with **A.** IL-1 $\beta$  and **B.** IL-18 intra-tumoral expression. Simple regression analysis was conducted in Prism.

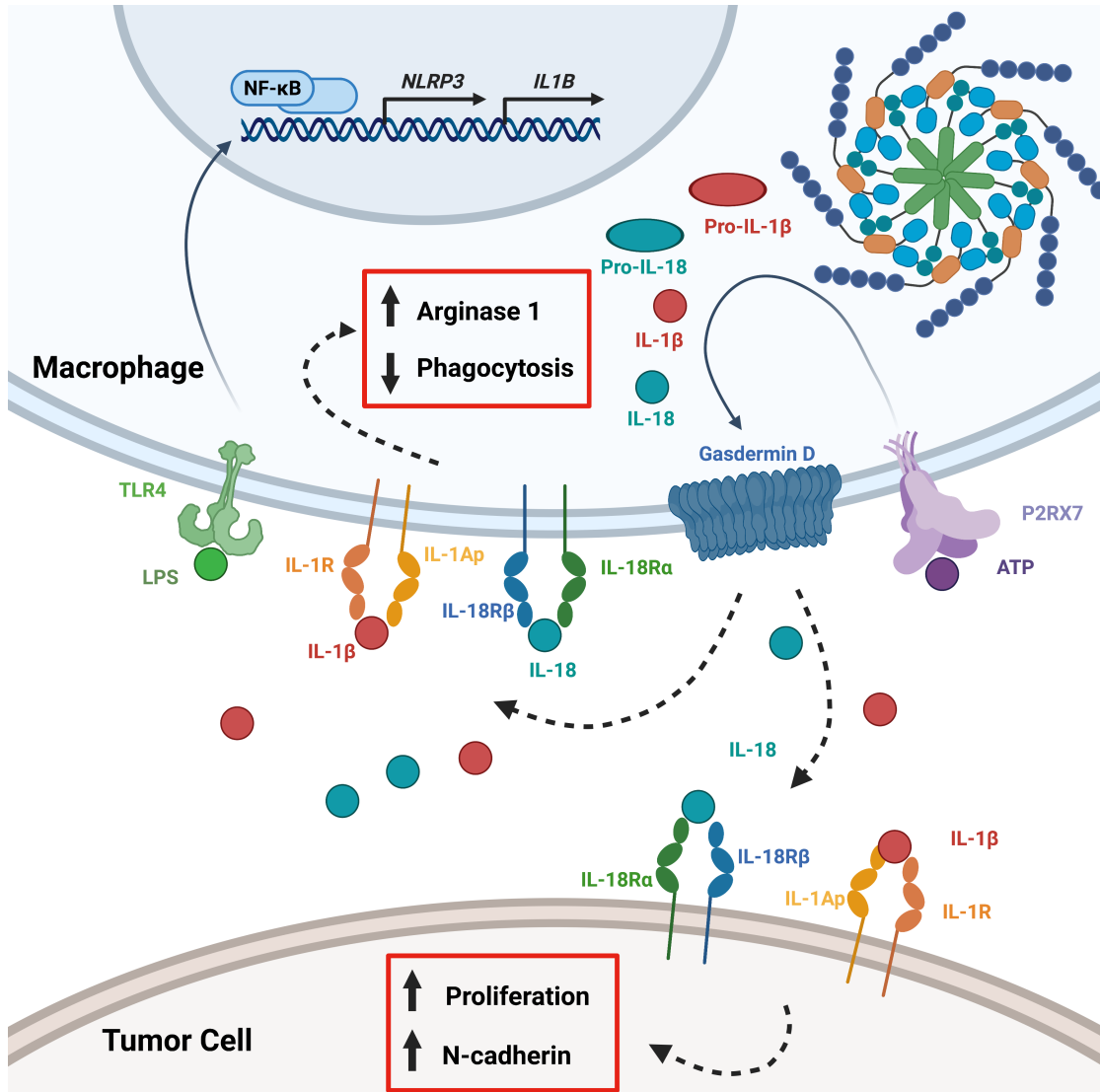


**Figure 5.3. NLRP3 Inflammasome Activation in Macrophages Results in a Pro-Tumorigenic Microenvironment.** In macrophages, NLRP3 inflammasome activation results in a pro-tumorigenic phenotype that promotes tumor proliferation and stemness (Chapter 2). We demonstrated that, *in vivo*, macrophage's NLRP3 inflammasome activation led to a worsening of tumor burden and a combination treatment of NLRP3-inhibiting MCC950 and 5-Fluorouracil abrogated the tumor supporting effects of this inflammation (Chapter 3). Finally, we demonstrated that autocrine, pro-inflammatory cytokine signaling by macrophages induces the shift toward a pro-tumorigenic phenotype (Chapter 4). Generated by KH using BioRender.com

## REFERENCES

1. Hara H, Seregin SS, Yang D, Fukase K, Chamaillard M, Alnemri ES, et al. The NLRP6 inflammasome recognizes lipoteichoic acid and regulates Gram-positive pathogen infection. *Cell*. 2018;175(6):1651-64.e14.
2. Faustin B, Lartigue L, Bruey J-M, Luciano F, Sergienko E, Bailly-Maitre B, et al. Reconstituted NALP1 Inflammasome Reveals Two-Step Mechanism of Caspase-1 Activation. *Molecular Cell*. 2007;25:713-24.
3. Johnson DC, Taabazuing CY, Okondo MC, Chui AJ, Rao SD, Brown FC, et al. DPP8/9 inhibitor-induced pyroptosis for treatment of acute myeloid leukemia. *Nature Medicine*. 2018;24(8):1151-6.
4. Zhong FL, Robinson K, Teo DET, Tan K-Y, Lim C, Harapas CR, et al. Human DPP9 represses NLRP1 inflammasome and protects against autoinflammatory diseases via both peptidase activity and FIIND domain binding. *Journal of Biological Chemistry*. 2018;293(49):18864-78.
5. Chu J-Q, Shi G, Fan Y-M, Choi I-W, Cha G-H, Zhou Y, et al. Production of IL-1 $\beta$  and Inflammasome with Up-Regulated Expressions of NOD-Like Receptor Related Genes in *Toxoplasma gondii*-Infected THP-1 Macrophages. *Korean Journal of Parasitology* 2016;54(6):711-7.
6. Ball DP, Taabazuing CY, Griswold AR, Orth EL, Rao SD, Kotliar IB, et al. Caspase-1 interdomain linker cleavage is required for pyroptosis. *Life Science Alliance*. 2020;3(3):e202000664.
7. Lu WL, Zhang L, Song DZ, Yi XW, Xu WZ, Ye L, et al. NLRP6 suppresses the inflammatory response of human periodontal ligament cells by inhibiting NF- $\kappa$ B and ERK signal pathways. *International Endodontic Journal* 2019;52(7):999-1009.
8. Conti BJ, Davis BK, Zhang J, Jr WOC, Williams KL, Ting JP-Y. CATERPILLER 16.2 (CLR16.2), a novel NBD/LRR family member that negatively regulates T cell function. *The Journal of Biological Chemistry*. 2005;280(18):18375-85.
9. Minkiewicz J, Vaccari JPdR, Keane RW. Human astrocytes express a novel NLRP2 inflammasome. *GLIA*. 2013;61(7):1113-21.
10. Mariathasan S, Weiss DS, McBride KN, O'Rourke K, Roose-Girma M, Lee WP, et al. Cryopyrin activates the inflammasome in response to toxins and ATP. *Nature*. 2006;440:228-32.
11. Grenier JM, Wang L, Manji GA, Huang WJ, Al-Garawi A, Kelly R, et al. Functional screening of five PYPAF family members identifies PYPAF5 as a novel regulator of NF-kappaB and caspase-1. *FEBS Letters*. 2002;530(1-3):73-8.



12. Khare S, Dorfleutner A, Bryan NB, Yun C, Radian AD, Almeida Ld, et al. An NLRP7-Containing Inflammasome Mediates Recognition of Microbial Lipopeptides in Human Macrophages. *Immunity*. 2012;36:464-76.
13. Duncan JA, Gao X, Huang M, O'Connor BP, Thomas CE, Willingham SB, et al. *Neisseria gonorrhoeae* activates the proteinase Cathepsin B to mediate the signaling activities of the NLRP3 and ASC - containing inflammasome. *Journal of Immunology*. 2009;182(10):6460-9.
14. Schiwitza A, Schildhaus H-U, Zwerger B, Rüschhoff J, Reinhardt C, Leha A, et al. Monitoring efficacy of checkpoint inhibitor therapy in patients with non-small-cell lung cancer. *Immunotherapy*. 2019;11(9):769-82.
15. Kanneganti T-D, Lamkanfi M, Kim Y-G, Chen G, Park J-H, Franchi L, et al. Pannexin-1-Mediated Recognition of Bacterial Molecules Activates the Cryopyrin Inflammasome Independent of Toll-like Receptor Signaling. *Immunity*. 2007;26:433-43.
16. Gross O, Poeck H, Bscheider M, Dostert C, Hanneschläger N, Endres S, et al. Syk kinase signalling couples to the Nlrp3 inflammasome for anti-fungal host defence. *Nature*. 2009;459(7245):433-6.
17. Muruve DA, Pétrilli V, Zaiss AK, White LR, Clark SA, Ross PJ, et al. The inflammasome recognizes cytosolic microbial and host DNA and triggers an innate immune response. *Nature*. 2008;452:103-7.
18. Kanneganti T-D, Body-Malapel M, Amer A, Park J-H, Whitfield J, Franchi L, et al. Critical role for Cryopyrin/Nalp3 in activation of caspase-1 in response to viral infection and double-stranded RNA. *Journal of Biological Chemistry*. 2006;281(48):36560-8.
19. Smart M, Goyal S, Zilman A. Roles of phenotypic heterogeneity and microenvironment feedback in early tumor development. *Phys Rev E*. 2021;103.
20. Polyak K, Haviv I, Campbell IG. Co-evolution of tumor cells and their microenvironment. *Trends Genet*. 2009;25(1):30-8.
21. Marleaux M, Anand K, Latz E, Geyer M. Crystal structure of the human NLRP9 pyrin domain suggests a distinct mode of inflammasome assembly. *FEBS Letters*. 2020;594(15):2383-95.
22. Schmid P, Cortes J, Pusztai L, McArthur H, Kümmel S, Bergh J, et al. Pembrolizumab for Early Triple-Negative Breast Cancer. *N Engl J Med*. 2020;382(9):810-21.
23. Zhu S, Ding S, Wang P, Wei Z, Pan W, Palm NW, et al. Nlrp9b inflammasome restricts rotavirus infection in intestinal epithelial cells. *Nature*. 2017;546(7660):667-70.
24. Ito M, Yanagi Y, Ichinohe T. Encephalomyocarditis Virus Viroporin 2B Activates NLRP3 Inflammasome. *PLOS Pathogens*. 2012;8(8):e1002857.

25. Imamura R, Wang Y, Kinoshita T, Suzuki M, Noda T, Sagara J, et al. Anti-Inflammatory Activity of PYNOD and Its Mechanism in Humans and Mice. *Journal of Immunology*. 2010;184(10):5874-84.
26. Dostert C, Guarda G, Romero JF, Menu P, Gross O, Tardivel A, et al. Malarial hemozoin is a Nalp3 inflammasome activating danger signal. *PLoS One*. 2009;4(8):e6510.
27. Teichgraber DC, Guirguis MS, Whitman GJ. Breast Cancer Staging: Updates in the AJCC Cancer Staging Manual, 8th Edition, and Current Challenges for Radiologists, From the AJR Special Series on Cancer Staging. *AJR Am J Roentgenol*. 2021;217(2):278-90.
28. Wang Y, Hasegawa M, Imamura R, Kinoshita T, Kondo C, Konaka K, et al. PYNOD, a novel Apaf-1/CED4-like protein is an inhibitor of ASC and caspase-1. *International Immunology* 2004;16(6):777-86.
29. Zucca-Matthes G, Urban C, Vallejo A. Anatomy of the nipple and breast ducts. *Gland Surgery* 2016;5(1):32-6.
30. Lautz K, Damm A, Menning M, Wenger J, Adam AC, Zigrino P, et al. NLRP10 enhances Shigella-induced pro-inflammatory responses. *Cellular Microbiology*. 2012;14(10):1568-83.
31. Lee S-J, Choi B-K. Involvement of NLRP10 in IL-1 $\alpha$  induction of oral epithelial cells by periodontal pathogens. *Innate Immunity* 2017;23(7):569-77.
32. Eisenbarth SC, Colegio OR, O'Connor W, Sutterwala FS, Flavell RA. Crucial role for the Nalp3 inflammasome in the immunostimulatory properties of aluminium adjuvants. *Nature*. 2008;453(1122-1126).
33. Dostert C, Pétrilli V, Bruggen RV, Steele C, Mossman BT, Tschopp J. Innate Immune Activation Through Nalp3 Inflammasome Sensing of Asbestos and Silica. *Science*. 2008;320(58776):674-7.
34. Javed A, Lteif A. Development of the Human Breast. *Seminars in Plastic Surgery* 2013;27(1):5-12.
35. Loi S, Giobbie-Hurder A, Gombos A, Bachelot T, Hui R, Curigliano G, et al. Pembrolizumab plus trastuzumab in trastuzumab-resistant, advanced, HER2-positive breast cancer (PANACEA): a single-arm, multicentre, phase 1b-2 trial. *Lancet Oncol*. 2019;20(3):371-82.
36. Dostert C, Pétrilli V, Bruggen RV, Steele C, Mossman BT, Tschopp J. Innate Immune Activation Through Nalp3 Inflammasome Sensing of Asbestos and Silica. *Science*. 2008;320(5876):674-7.

37. Cassel SL, Eisenbarth SC, Iyer SS, Sadler JJ, Colegio OR, Tephly LA, et al. The Nalp3 inflammasome is essential for the development of silicosis. *PNAS*. 2008;105(26):9035-40.
38. Hansen RK, Bissell MJ. Tissue architecture and breast cancer: the role of extracellular matrix and steroid hormones. *Endocrine-Related Cancer*. 2000;7(2):95-113.
39. Qin Y, Su Z, Wu Y, Wu C, Jin S, Xie W, et al. NLRP11 disrupts MAVS signalosome to inhibit type I interferon signaling and virus-induced apoptosis. *EMBO Reports*. 2017;18:2160-71.
40. Brady NJ, Chuntova P, Schwertfeger KL. Macrophages: Regulators of the Inflammatory Microenvironment during Mammary Gland Development and Breast Cancer. *Mediators of Inflammation*. 2016;2016.
41. Watanabe H, Gaide O, Pétrilli V, Martinon F, Contassot E, Roques S, et al. Activation of the IL-1 $\beta$ -Processing Inflammasome Is Involved in Contact Hypersensitivity. *Journal of Investigative Dermatology* 2007;127(8):1956-63.
42. Feldmeyer L, Keller M, Niklaus G, Hohl D, Werner S, Beer H-D. The inflammasome mediates UVB-induced activation and secretion of interleukin-1 $\beta$  by keratinocytes. *Current Biology*. 2007;17(13):1140-5.
43. Ellwanger K, Becker E, Kienes I, Sowa A, Postma Y, Gloria YC, et al. The NLR family pyrin domain containing 11 protein contributes to the regulation of inflammatory signalling. *Journal of Biological Chemistry*. 2018;293:2701-10.
44. Martinon F, Pétrilli V, Mayor A, Tardivel A, Tschopp J. Gout-associated uric acid crystals activate the NALP3 inflammasome. *Nature*. 2006;440:237-41.
45. Masters SL, Dunne A, Subramanian SL, Hull RL, Tannahill GM, Sharp FA, et al. Activation of the NLRP3 inflammasome by islet amyloid polypeptide provides a mechanism for enhanced IL-1 $\beta$  in type 2 diabetes. *Nature Immunology*. 2010;11(10):897-904.
46. Halle A, Hornung V, Petzold GC, Stewart CR, Monks BG, Reinheckel T, et al. The NALP3 inflammasome is involved in the innate immune response to amyloid-beta. *Nature Immunology*. 2008;9(8):857-65.
47. Tuncer S, Fiorillo MT, Sorrentino R. The multifaceted nature of NLRP12. *Journal of Leukocyte Biology*. 2014;96:991-1000.
48. Jin C, Frayssinet P, Pelker R, Cwirka D, Hu B, Vignery A, et al. NLRP3 inflammasome plays a critical role in the pathogenesis of hydroxyapatite-associated arthropathy. *PNAS*. 2011;108(36):14867-72.
49. Vladimer GI, Weng D, Paquette SWM, Vanaja SK, Rathinam VAK, Aune MH, et al. The NLRP12 inflammasome recognizes *Yersinia pestis*. *Immunity*. 2012;37(1):96-107.

50. Yamasaki K, Muto J, Taylor KR, Cogen AL, Audish D, Bertin J, et al. NLRP3/cryopyrin is necessary for interleukin-1beta (IL-1beta) release in response to hyaluronan, an endogenous trigger of inflammation in response to injury. *Journal of Biological Chemistry*. 2009;284(19):12762-71.
51. Zhou R, Tardivel A, Thorens B, Choi I, Tschopp J. Thioredoxin-interacting protein links oxidative stress to inflammasome activation. *Nature Immunology*. 2010;11:136-40.
52. Witz IP. The Tumor Microenvironment: The Making of a Paradigm. *Cancer Microenviron*. 2009;2:9-17.
53. Wen H, Gris D, Lei Y, Jha S, Zhang L, Huang MT-H, et al. Fatty acid-induced NLRP3-ASC inflammasome activation interferes with insulin signaling. *Nature Immunology*. 2011;12(408-415).
54. Sirishma Kalli M, Alan Semine M, Sara Cohen M, Stephen P. Naber M, PhD , Shital S. Makim M, Manisha Bahl M, MPH. American Joint Committee on Cancer's Staging System for Breast Cancer, Eighth Edition: What the Radiologist Needs to Know. *RadioGraphics*. 2018;38:1921-33.
55. Breast Cancer Facts & Figures 2019-2020. American Cancer Society 2019.
56. Subramanian N, Natarajan K, Clatworthy MR, Wang Z, Germain RN. The Adaptor MAVS Promotes NLRP3 Mitochondrial Localization and Inflammasome Activation. *Cell*. 2013;153:348-61.
57. Cui J, Li Y, Zhu L, Liu D, Songyang Z, Wang HY, et al. NLRP4 negatively regulates type I interferon signaling by targeting the kinase TBK1 for degradation via the ubiquitin ligase DTX4. *Nature Immunology*. 2012;13:387-95.
58. Eibl C, Grigoriu S, Hessenberger M, Wenger J, Puehringer S, Pinheiro AS, et al. Structural and Functional Analysis of the NLRP4 Pyrin Domain. *Biochemistry* 2012;51(37):7330-41.
59. Wolfe J. Breast patterns as an index of risk for developing breast cancer. *American Journal of Roentgenology* 1976;126:1130-7.
60. Inflammatory Breast Cancer: The American Cancer Society 2021 [Available from: <https://www.cancer.org/cancer/breast-cancer/about/types-of-breast-cancer/inflammatory-breast-cancer.html>].
61. Treatment of Ductal Carcinoma in Situ (DCIS): The American Cancer Society; 2019 [Available from: <https://www.cancer.org/cancer/breast-cancer/treatment/treatment-of-breast-cancer-by-stage/treatment-of-ductal-carcinoma-in-situ-dcis.html>].
62. Treatment of Breast Cancer Stages I-III: The American Cancer Society; 2019 [Available from: <https://www.cancer.org/cancer/breast-cancer/treatment/treatment-of-breast-cancer-by-stage/treatment-of-breast-cancer-stages-i-iii.html>].

63. Treatment of Stage IV (Metastatic) Breast Cancer: The American Cancer Society 2020 [Available from: <https://www.cancer.org/cancer/breast-cancer/treatment/treatment-of-breast-cancer-by-stage/treatment-of-stage-iv-advanced-breast-cancer.html>].
64. Chemotherapy for Breast Cancer: The American Cancer Society 2019 [Available from: <https://www.cancer.org/cancer/breast-cancer/treatment/chemotherapy-for-breast-cancer.html>].
65. Mehanna J, Haddad FG, Eid R, Lambertini M, Kourie HR. Triple-negative breast cancer: current perspective on the evolving therapeutic landscape. *International Journal of Women's Health* 2019;11:431-7.
66. Larissa A. Korde M, Mark R. Somerfield P, Lisa A. Carey M, Jennie R. Crews M, Neelima Denduluri M, E. Shelley Hwang M, et al. Neoadjuvant Chemotherapy, Endocrine Therapy, and Targeted Therapy for Breast Cancer: ASCO Guideline. *Journal of Clinical Chemistry*. 2021;39(13):1485-505.
67. Sagiv-Barfi I, Czerwinski DK, Levy S, Alam IS, Mayer AT, Gambhir SS, et al. Eradication of spontaneous malignancy by local immunotherapy. *Science Translational Medicine*. 2018;10.
68. Gandhi L, Rodríguez-Abreu D, Gadgeel S, Esteban E, Felip E, Angelis FD, et al. Pembrolizumab plus Chemotherapy in Metastatic Non-Small-Cell Lung Cancer. *N Engl J Med*. 2018;378(22):2078-92.
69. Gandini S, Massi D, Mandalà M. PD-L1 expression in cancer patients receiving anti PD-1/PD-L1 antibodies: A systematic review and meta-analysis. *Crit Rev Oncol Hematol*. 2016;100:88-98.
70. André T, Shiu K-K, Kim TW, Jensen BV, Jensen LH, Punt C, et al. Pembrolizumab in Microsatellite-Instability-High Advanced Colorectal Cancer. *N Engl J Med*. 2020;383(23):2207-18.
71. Colombo N, Dubot C, Lorusso D, Caceres MV, Hasegawa K, Shapira-Frommer R, et al. Pembrolizumab for Persistent, Recurrent, or Metastatic Cervical Cancer. *N Engl J Med*. 2021;Online ahead of Print.
72. Natrajan R, Sailem H, Mardakheh FK, Garcia MA, Tape CJ, Dowsett M, et al. Microenvironmental Heterogeneity Parallels Breast Cancer Progression: A Histology–Genomic Integration Analysis. *PLoS Med*. 2016;13(2).
73. Nassar A, Radhakrishnan A, Cabrero IA, Cotsonis GA, Cohen C. Intratumoral Heterogeneity of Immunohistochemical Marker Expression in Breast Carcinoma. *Appl Immunohistochem Mol Morphol* 2010;18(5):433-41.
74. Meacham CE, Morrison SJ. Tumor heterogeneity and cancer cell plasticity. *Nature*. 2013;501(7467):328-37.

75. Hölzel M, Bovier A, Tüting T. Plasticity of tumour and immune cells: a source of heterogeneity and a cause for therapy resistance? *Nature Reviews Cancer*. 2013;13:365-76.
76. Brooks MD, Burness ML, Wicha MS. Therapeutic Implications of Cellular Heterogeneity and Plasticity in Breast Cancer. *Cell Stem Cell*. 2015;17:260-71.
77. Bianchini G, Balko JM, Mayer IA, Sanders ME, Gianni L. Triple-negative breast cancer: challenges and opportunities of a heterogeneous disease. *Nat Rev Clin Oncol*. 2016;13(11):674-0.
78. Baliu-Piqué M, Pandiella A, Ocana A. Breast Cancer Heterogeneity and Response to Novel Therapeutics. *Cancers*. 2020;12(11).
79. Angelis MLD, Francescangeli F, Zeuner A. Breast Cancer Stem Cells as Drivers of Tumor Chemoresistance, Dormancy and Relapse: New Challenges and Therapeutic Opportunities. *Cancers* 2019;11(1569).
80. Lee K-L, Kuo Y-C, Ho Y-S, Huang Y-H. Triple-Negative Breast Cancer: Current Understanding and Future Therapeutic Breakthrough Targeting Cancer Stemness. *Cancers*. 2019;11(1334).
81. Kim S-Y, Kang JW, Song X, Kim BK, Yoo YD, Kwon YT, et al. Role of the IL-6-JAK1-STAT3-Oct-4 pathway in the conversion of non-stem cancer cells into cancer stem-like cells. *Cell Signal* 2013;25(4):961-9.
82. Morel A-P, Lièvre M, Thomas C, Hinkal G, Ansieau S, Puisieux A. Generation of Breast Cancer Stem Cells through Epithelial-Mesenchymal Transition. *PLoS ONE*. 2008;3(8).
83. Chen Y, Song J, Jiang Y, Yu C, Ma Z. Predictive value of CD44 and CD24 for prognosis and chemotherapy response in invasive breast ductal carcinoma *International Journal of Clinical Experimental Pathology*. 2015;8(9):11287-95.
84. Ricardo S, Vieira AF, Gerhard R, Leitão D, Pinto R, Cameselle-Teijeiro JF, et al. Breast cancer stem cell markers CD44, CD24 and ALDH1: expression distribution within intrinsic molecular subtype. *Journal of Clinical Pathology* 2011;64:937-46.
85. Wang X, Wang G, Zhao Y, Liu X, Ding Q, Shi J, et al. STAT3 mediates resistance of CD44(+)CD24(-/low) breast cancer stem cells to tamoxifen in vitro. *Journal of Biomedical Research* 2012;26(5):325-35.
86. Sansone P, Ceccarelli C, Berishaj M, Chang Q, Rajasekhar VK, Perna F, et al. Self-renewal of CD133hi cells by IL6/Notch3 signalling regulates endocrine resistance in metastatic breast cancer. *Nature Communications*. 2016;7.

87. Creighton CJ, Li X, Landis M, Dixon JM, Neumeister VM, Sjolund A, et al. Residual breast cancers after conventional therapy display mesenchymal as well as tumor-initiating features. PNAS. 2009;106(33):13820-5.
88. Al-Hajj M, Wicha MS, Benito-Hernandez A, Morrison SJ, Clarke MF. Prospective identification of tumorigenic breast cancer cells. PNAS. 2003;100(7):3983-8.
89. Multhoff G, Molls M, Radons J. Chronic inflammation in cancer development. Frontiers in Immunology. 2012;2(98).
90. Perez-Yepe EA, Ayala-Sumuan J-T, Lexama R, Meza I. A novel  $\beta$ -catenin signaling pathway activation by IL-1 $\beta$  leads to the onset of epithelial-mesenchymal transition in breast cancer cells. Cancer Letters 2014;354:164-71.
91. Truong D, Puleo J, Llave A, Mouneimne G, Kamm RD, Nikkhah M. Breast Cancer Cell Invasion into a Three Dimensional Tumor-Stroma Microenvironment. Scientific Reports. 2016;6.
92. Zhai Q, Fan J, Lin Q, Liu X, Li J, Hong R, et al. Tumor stromal type is associated with stromal PD-L1 expression and predicts outcomes in breast cancer. PLoS ONE. 2019;14(10).
93. Casey T, Bond J, Tighe S, Hunter T, Lintault L, Patel O, et al. Molecular signatures suggest a major role for stromal cells in development of invasive breast cancer. Breast Cancer Research and Treatment 2009;114:47-62.
94. Chen J-Y, Li C-F, Kuo C-C, Tsai KK, Hou M-F, Hung W-C. Cancer/stroma interplay via cyclooxygenase-2 and indoleamine 2,3-dioxygenase promotes breast cancer progression. Breast Cancer Research. 2014;16.
95. Oskarsson T. Extracellular matrix components in breast cancer progression and metastasis. The Breast. 2013;22:S66-S72.
96. Li Y, Li L, Brown TJ, Heldin P. Silencing of hyaluronan synthase 2 suppresses the malignant phenotype of invasive breast cancer cells. International Journal of Cancer. 2007;120(12):2557-67.
97. Bernert B, Porsch H, Heldin P. Hyaluronan Synthase 2 (HAS2) Promotes Breast Cancer Cell Invasion by Suppression of Tissue Metalloproteinase Inhibitor 1 (TIMP-1). Glycobiology and Extracellular Matrices. 2011;286(49):42349-59.
98. Badaoui M, Mimsy-Julienne C, Saby C, Gulick LV, Peretti M, Jeannesson P, et al. Collagen type 1 promotes survival of human breast cancer cells by overexpressing Kv10.1 potassium and Orail calcium channels through DDR1-dependent pathway. Oncotarget. 2017;9(37):24653-71.
99. Barcus CE, O'Leary KA, Brockman JL, Rugowski DE, Liu Y, Garcia N, et al. Elevated collagen-I augments tumor progressive signals, intravasation and metastasis of

prolactin-induced estrogen receptor alpha positive mammary tumor cells. *Breast Cancer Research*. 2017;19.

100. Liu J, Shen J-X, Wu H-T, Li X-L, Wen X-F, Du C-W, et al. Collagen 1A1 (COL1A1) Promotes Metastasis of Breast Cancer and Is a Potential Therapeutic Target. *Discovery Medicine* 2018;139:211-23.

101. Ignatz RA, Massagué J. Transforming growth factor-beta stimulates the expression of fibronectin and collagen and their incorporation into the extracellular matrix. *Journal of Biological Chemistry*. 1986;261(9):4337-45.

102. Czaja MJ, Weiner FR, Eghbali M, Giambrone MA, Eghbali M, Zern MA. Differential effects of gamma-interferon on collagen and fibronectin gene expression. *Journal of Biological Chemistry*. 1987;262(27):13348-51.

103. Yao ES, Zhang H, Chen Y-Y, Lee B, Chew K, Moore D, et al. Increased beta1 integrin is associated with decreased survival in invasive breast cancer. *Cancer Research*. 2007;67(2):659-64.

104. Li C-L, Yang D, Cao X, Wang F, Hong D-Y, Wang J, et al. Fibronectin induces epithelial-mesenchymal transition in human breast cancer MCF-7 cells via activation of calpain. *Oncology Letters*. 2017;13(5):3889-95.

105. Balanis N, Wendt MK, Schiemann BJ, Wang Z, Schiemann WP, Carlin CR. Epithelial to mesenchymal transition promotes breast cancer progression via a fibronectin-dependent STAT3 signaling pathway. *Journal of Biological Chemistry*. 2013;288(25):17954-67.

106. Weber CE, Kothari AN, Wai PY, Li NY, Driver J, Zapf MAC, et al. Osteopontin mediates an MZF1-TGF- $\beta$ 1-dependent transformation of mesenchymal stem cells into cancer-associated fibroblasts in breast cancer. *Oncogene*. 2015;34(37):4821-33.

107. Kojima Y, Acar A, Eaton EN, Mellody KT, Scheel C, Ben-Porath I, et al. Autocrine TGF-beta and stromal cell-derived factor-1 (SDF-1) signaling drives the evolution of tumor-promoting mammary stromal myofibroblasts. *PNAS*. 2010;107(46):20009-20014.

108. Houthuijzen JM, Jonkers J. Cancer-associated fibroblasts as key regulators of the breast cancer tumor microenvironment. *Cancer and Metastasis Reviews*. 2018;37:577-97.

109. Bates AL, Pickup MW, Hallett MA, Dozier EA, Thomas S, Fingleton B. Stromal matrix metalloproteinase 2 regulates collagen expression and promotes the outgrowth of experimental metastases. *The Journal of Pathology* 2015;235(5):773-83.

110. Korkaya H, Liu S, Wicha MS. Breast cancer stem cells, cytokine networks, and the tumor microenvironment. *THE Journal of Clinical Investigation* 2011;121(10):3804-9.

111. Davies G, Cunnick GH, Mansel RE, Mason MD, Jiang WG. Levels of expression of endothelial markers specific to tumour-associated endothelial cells and their correlation



with prognosis in patients with breast cancer. *Clinical & Experimental Metastasis*. 2004;21:31-7.

112. Valković T, Dobrila F, Melato M, Sasso F, Rizzardi C, Jonjić N. Correlation between vascular endothelial growth factor, angiogenesis, and tumor-associated macrophages in invasive ductal breast carcinoma. *Virchows Archiv*. 2001;440:583-8.

113. Gatti-Mays ME, Balko JM, Gameiro SR, Bear HD, Prabhakaran S, Fukui J, et al. If we build it they will come: targeting the immune response to breast cancer. *npj Breast Cancer*. 2019;5.

114. DeNardo DG, Coussens LM. Balancing immune response: crosstalk between adaptive and innate immune cells during breast cancer progression. *Breast Cancer Research*. 2007;9(4).

115. Yuan Z-Y, Luo R-Z, Peng R-J, Wang S-S, Xue C. High infiltration of tumor-associated macrophages in triple-negative breast cancer is associated with a higher risk of distant metastasis. *OncoTargets and Therapy*. 2014;7:1475-80.

116. Ali HR, Chlon L, Pharoah PDP, Markowitz F, Caldas C. Patterns of Immune Infiltration in Breast Cancer and Their Clinical Implications: A Gene-Expression-Based Retrospective Study. *PLoS Med*. 2016;13(12).

117. Huang Y, Ma C, Zhang Q, Ye J, Wang F, Zhang Y, et al. CD4<sup>+</sup> and CD8<sup>+</sup> T cells have opposing roles in breast cancer progression and outcome. *Oncotarget*. 2015;6(19):17462-78.

118. Azab B, Bhatt VR, Phookan J, Murukutla S, Kohn N, Terjanian T, et al. Usefulness of the Neutrophil-to-Lymphocyte Ratio in Predicting Short- and Long-Term Mortality in Breast Cancer Patients. *Annals of Surgical Oncology* 2011;19:217-24.

119. Plitas G, Konopacki C, Wu K, Bos P, Morrow M, Putintseva EV, et al. Regulatory T cells exhibit distinct features in human breast cancer. *Immunity*. 2016;45(5):1122-34.

120. Martinez LM, Robila V, Clark NM, Du W, Idowu MO, Rutkowski MR, et al. Regulatory T Cells Control the Switch From in situ to Invasive Breast Cancer. *Front Immunol*. 2019;10.

121. Ma L, Gonzalez-Junca A, Zheng Y, Ouyang H, Illa-Bochaca I, Horst KC, et al. Inflammation Mediates the Development of Aggressive Breast Cancer Following Radiotherapy. *Clinical Cancer Research* 2021;27:1778-91.

122. Allen MD, Jones LJ. The role of inflammation in progression of breast cancer: Friend or Foe? . *International Journal of Oncology* 2015;47:797-805.

123. Qiu S-Q, Waaijer SJH, Zwager MC, Vries EGED, Vegt Bvd, Schröder CP. Tumor-associated macrophages in breast cancer: Innocent bystander or important player? . *Cancer Treatment Reviews*. 2018;70:178-89.

124. DeNardo DG, Ruffell B. Macrophages as regulators of tumour immunity and immunotherapy. *Nature Reviews Immunology*. 2019;19:369-82.
125. Hanahan D, Weinberg RA. Hallmarks of Cancer: The Next Generation *Cell*. 2011;144:646-74.
126. Richardsen E, Uglehus RD, Johnsen SH, Busund L-T. Macrophage-Colony Stimulating Factor (CSF1) Predicts Breast Cancer Progression and Mortality *Anticancer Research* 2015;35(2):865-74.
127. Lin EY, Li J-F, Gnatovskiy L, Deng Y, Zhu L, Grzesik DA, et al. Macrophages Regulate the Angiogenic Switch in a Mouse Model of Breast Cancer. *Cancer Research*. 2006;66(23):11238-46.
128. DeNardo DG, Brennan DJ, Rexhepaj E, Ruffell B, Shiao SL, Madden SF, et al. Leukocyte Complexity Predicts Breast Cancer Survival and Functionally Regulates Response to Chemotherapy. *Cancer Discovery*. 2011;1(1):54-67.
129. Zhang L, Wang C-C. Inflammatory response of macrophages in infection. *Hepatobiliary Pancreat Dis Int*. 2014;13(2):138-52.
130. Solinas G, Germano G, Mantovani A, Allavena P. Tumor-associated macrophages (TAM) as major players of the cancer-related inflammation. *Journal of Leukocyte Biology*. 2009;86:1065-73.
131. Zhang X, Mosser D. Macrophage activation by endogenous danger signals. *J Pathol* 2009;214(2):161-78.
132. Gong T, Liu L, Jiang W, Zhou R. DAMP-sensing receptors in sterile inflammation and inflammatory diseases. *Nature Reviews Immunology*. 2019;20:95-112.
133. Hirayama D, Iida T, Nakase H. The Phagocytic Function of Macrophage-Enforcing Innate Immunity and Tissue Homeostasis. *International Journal of Molecular Sciences*. 2017;19.
134. Williams CB, Yeh ES, Soloff AC. Tumor-associated macrophages: unwitting accomplices in breast cancer malignancy. *npj Breast Cancer*. 2016.
135. Tarique AA, Logan J, Thomas E, Holt PG, Sly PD, Fantino E. Phenotypic, Functional, and Plasticity Features of Classical and Alternatively Activated Human Macrophages. *American Journal of Respiratory Cell and Molecular Biology* 2015;53(5):676-88.
136. Yazdi AS, Drexler SK, Tschopp J. The Role of the Inflammasome in Nonmyeloid Cells. *Journal of Clinical Immunology* 2010;30:623-7.

137. Watanabe A, Sohail MA, Gomes DA, Hashmi A, Nagata J, Sutterwala FS, et al. Inflammasome-mediated regulation of hepatic stellate cells. *American Journal of Physiology Gastrointestinal and Liver Physiology*. 2009;296(6):1248-57.
138. Csak T, Ganz M, Pespisa J, Kodys K, Dolganiuc A, Szabo G. Fatty acid and endotoxin activate inflammasomes in mouse hepatocytes that release danger signals to stimulate immune cells. *Hepatology* 2011;54(1):133-44.
139. Gómez DM, Urcuqui-Inchima S, Hernandez JC. Silica nanoparticles induce NLRP3 inflammasome activation in human primary immune cells. *Innate Immunity*. 2017;23(8):697-708.
140. Linder A, Bauernfried S, Cheng Y, Albanese M, Jung C, Keppler OT, et al. CARD8 inflammasome activation triggers pyroptosis in human T cells. *The EMBO Journal*. 2020;39.
141. Ghiringhelli F, Apetoh L, Tesniere A, Aymeric L, Ma Y, Ortiz C, et al. Activation of the NLRP3 inflammasome in dendritic cells induces IL-1 $\beta$ -dependent adaptive immunity against tumors. *Nature Medicine*. 2009;15:1170-8.
142. Erlich Z, Shlomovitz I, Edry-Botzer L, Cohen H, Frank D, Wang H, et al. Macrophages, rather than DCs, are responsible for inflammasome activity in the GM-CSF BMDC model. *Nature Immunology*. 2019;20:397-406.
143. Lim K-H, Chen L-C, Hsu K, Chang C-C, Chang C-Y, Kao C-W, et al. BAFF-driven NLRP3 inflammasome activation in B cells. *Cell Death and Disease*. 2020;11.
144. Zhang W, Ba G, Tang R, Li M, Lin H. Ameliorative effect of selective NLRP3 inflammasome inhibitor MCC950 in an ovalbumin-induced allergic rhinitis murine model. *International Immunopharmacology* 2020;83.
145. Tian X, Pascal G, Monget P. Evolution and functional divergence of NLRP genes in mammalian reproductive systems. *BMC Evolutionary Biology* 2009;9.
146. Zhang P, Dixon M, Zucchelli M, Hambiliki F, Levkov L, Hovatta O, et al. Expression Analysis of the NLRP Gene Family Suggests a Role in Human Preimplantation Development. *PLoS ONE*. 2008;3(7).
147. Ponsuksili S, Brunner RM, Goldammer T, Kühn C, Walz C, Chomdej S, et al. Bovine NALP5, NALP8, and NALP9 Genes: Assignment to a QTL Region and the Expression in Adult Tissues, Oocytes, and Preimplantation Embryos. *Biology of Reproduction* 2006;74(3):577-84.
148. Tong Z-B, Gold L, Pol AD, Vanevski K, Dorward H, Sena P, et al. Developmental expression and subcellular localization of mouse MATER, an oocyte-specific protein essential for early development. *Endocrinology*. 2004;145(3):1427-34.

149. Wu X. Maternal depletion of NLRP5 blocks early embryogenesis in rhesus macaque monkeys (*Macaca mulatta*). *Human Reproduction* 2008;24(2):415-24.
150. Xu Y, Qian Y, Liu Y, Wang Q, Wang R, Zhou Y, et al. A novel homozygous variant in NLRP5 is associate with human early embryonic arrest in a consanguineous Chinese family *Clinical Genetics* 2020;98:69-73.
151. Grenier JM, Wang L, Manji GA, Huang W-J, Al-Garawi A, Kelly R, et al. Functional screening of five PYPAF family members identifies PYPAF5 as a novel regulator of NF- $\kappa$ B and caspase-1. *FEBS Letters*. 2002;530:73-8.
152. Chen I-F, Ou-Yang F, Hung J-Y, Liu J-C, Wang H, Wang S-C, et al. AIM2 suppresses human breast cancer cell proliferation in vitro and mammary tumor growth in a mouse model. *Mol Cancer Ther* 2006;5(1):1-7.
153. Wang D, Zou J, Dai J, Cheng Z. Absent in melanoma 2 suppresses gastric cancer cell proliferation and migration via inactivation of AKT signaling pathway. *Scientific Reports*. 2021;11.
154. JJ C, ZJ W, SS Y. AIM2 regulates viability and apoptosis in human colorectal cancer cells via the PI3K/Akt pathway. *OncoTargets and Therapy*. 2016;10:811-7.
155. Sagulenko V, Thygesen SJ, Sester DP, Idris A, Cridland JA, Vajjhala PR, et al. AIM2 and NLRP3 inflammasomes activate both apoptotic and pyroptotic death pathways via ASC. *Cell Death Differ*. 2013;20(9):1149-60.
156. Sharma M, Alba Ed. Structure, Activation and Regulation of NLRP3 and AIM2 Inflammasomes. *Int J Mol Sci*. 2021;22.
157. Denes A, Coutts G, Lénárt N, Cruickshank SM, Pelegrin P, Skinner J, et al. AIM2 and NLRC4 inflammasomes contribute with ASC to acute brain injury independently of NLRP3. *PNAS*. 2015;112(13):4050-5.
158. Corrales L, Woo S-R, Williams JB, McWhirter SM, Jr. TWD, Gajewski TF. Antagonism of the STING Pathway via Activation of the AIM2 Inflammasome by Intracellular DNA. *The Journal of Immunology*. 2016;196(7):3191-8.
159. Wang Y, Zhang H, Xu Y, Peng T, Meng X, Zou F. NLRP3 induces the autocrine secretion of IL-1 $\beta$  to promote epithelial-mesenchymal transition and metastasis in breast cancer. *Biochemical and Biophysical Research Communications*. 2021;560:72-9.
160. Zhang L, Li H, Zang Y, Wang F. NLRP3 inflammasome inactivation driven by mrR-223-3p reduces tumor growth and increase anticancer immunity in breast cancer. *Molecular Medicine Reports* 2019;19(2180-2188).
161. Karki R, Kanneganti T-D. Diverging inflammasome signals in tumorigenesis and potential targeting *Nature Reviews*. 2019;19(197-214).

162. Guo B, Fu S, Zhang J, Liu B, Li Z. Targeting inflammasome/IL-1 pathways for cancer immunotherapy Scientific Reports. 2016;6(36107).
163. Ershaid N, Sharon Y, Doron H, Raz Y, Shani O, Cohen N, et al. NLRP3 inflammasome in fibroblasts links tissue damage with inflammation in breast cancer progression and metastasis. Nature Communications. 2019;10.
164. Ershaid N, Sharon Y, Doron H, Raz Y, Shani O, Cohen N, et al. NLRP3 inflammasome in fibroblasts links tissue damage with inflammation in breast cancer progression and metastasis. Nature Communications. 2019;10(4375).
165. Karki R, Man SM, Kanneganti T-D. Inflammasomes and Cancer. Cancer Immunology Research 2017;5(2):94-9.
166. Chow MT, Sceneay J, Paget C, Wong CSF, Duret H, Tschopp J, et al. NLRP3 Suppresses NK Cell-Mediated Responses to Carcinogen-Induced Tumors and Metastases. Cancer Research. 2012;72(22):5721-32.
167. Lu A, Magupalli VG, Ruan J, Fitzgerald KA, Wu H, Egelman EH. Unified Polymerization Mechanism for the Assembly of ASC-Dependent Inflammasomes. Cell. 2014;156(6):1193-206.
168. Duan Y, Zhang L, Angosto-Bazarra D, Pelegrín P, Núñez G, He Y. RACK1 Mediates NLRP3 Inflammasome Activation by Promoting NLRP3 Active Conformation and Inflammasome Assembly. Cell Rep 2020;33(7).
169. Zhu Q, Zheng M, Balakrishnan A, Karki R, Kanneganti T-D. Gasdermin D Promotes AIM2 Inflammasome Activation and Is Required for Host Protection against *Francisella novicida*. The Journal of Immunology. 2018;201(12):3662-8.
170. Song Y, Na HS, Park E, Park MH, Lee HA, Chung J. *Streptococcus mutans* activates the AIM2, NLRP3 and NLRC4 inflammasomes in human THP-1 macrophages. International Journal of Oral Science. 2018;10(23).
171. Hu G-Q, Song P-X, Li N, Chen W, Lei Q-Q, Yu S-X, et al. AIM2 contributes to the maintenance of intestinal integrity via Akt and protects against *Salmonella* mucosal infection. Mucosal Immunology 2016;9:1330-9.
172. Sharif H, Wang L, Wang WL, Magupalli VG, Andreeva L, Qiao Q, et al. Structural mechanism for NEK7-licensed activation of NLRP3 inflammasome Nature. 2019;570:338-43.
173. He Y, Zeng MY, Yang D, Motro B, Núñez G. Nek7 is an essential mediator of NLRP3 activation downstream of potassium efflux. Nature. 2016;530(7590):354-7.
174. Tang T, Lang X, Xu C, Wang X, Gong T, Yang Y, et al. CLICs-dependent chloride efflux is an essential and proximal upstream event for NLRP3 inflammasome activation. Nature Communications. 2017;8.

175. Domingo-Fernández R, Coll RC, Kearney J, Breit S, O'Neill LAJ. The intracellular chloride channel proteins CLIC1 and CLIC4 induce IL-1 $\beta$  transcription and activate the NLRP3 inflammasome. *Journal of Biological Chemistry*. 2017;292(29):12077-87.
176. Green JP, Yu S, Martín-Sánchez F, Pelegrin P, Lopez-Castejon G, Lawrence CB, et al. Chloride regulates dynamic NLRP3-dependent ASC oligomerization and inflammasome priming. *PNAS*. 2018;115(40):E9371-E80.
177. Shi H, Wang Y, Li X, Zhan X, Tan M, Fina M, et al. NLRP3 activation and mitosis are mutually exclusive events coordinated by NEK7, a new inflammasome component. *Nature Immunology*. 2016;17(3):250-8.
178. Alba E. Structure, interactions and self-assembly of ASC-dependent inflammasomes. *Archive of Biochemistry and Biophysics*. 2019;670:15-31.
179. Saponaro C, Scarpi E, Sonnessa M, Cioffi A, Buccino F, Giotta F, et al. Prognostic Value of NLRP3 Inflammasome and TLR4 Expression in Breast Cancer Patients. *Frontiers in Oncology* 2021;11.
180. Cai X, Chen J, Xu H, Liu S, Jiang Q-X, Halfmann R, et al. Prion-like Polymerization Underlies Signal Transduction in Antiviral Immune Defense and Inflammasome Activation. *Cell*. 2014;156:1207-22.
181. Zheng D, Liwinski T, Elinav E. Inflammasome activation and regulation: toward a better understanding of complex mechanisms. *Cell Discovery* 2020;6.
182. Lu A, Li Y, Schmidt FI, Yin Q, Chen S, Fu T-M, et al. Molecular basis of caspase-1 polymerization and its inhibition by a new capping mechanism. *Nature Structural & Molecular Biology* 2016;23(5):416-25.
183. Karan D. Inflammasomes: Emerging Central Players in Cancer Immunology and Immunotherapy. *Frontiers in Immunology*. 2018;9(3028).
184. Moossavi M, Parsamanesh N, Bahrami A, Atkin SL, Sahebkar A. Role of the NLRP3 inflammasome in cancer. *Molecular Cancer*. 2018;17(158).
185. Yang Y, Wang H, Kouadir M, Song H, Shi F. Recent advances in mechanisms of NLRP3 inflammasome activation and its inhibitors. *Cell Death and Disease* 2019;10(128).
186. Bauernfeind FG, Horvath G, Stutz A, Alnemri ES, MacDonald K, Speert D, et al. Cutting Edge: NF- $\kappa$ B Activating Pattern Recognition and Cytokine Receptors License NLRP3 Inflammasome Activation by Regulating NLRP3 Expression. *The Journal of Immunology*. 2009;183:787-91.
187. Muñoz-Planillo R, Kuffa P, Martínez-Colón G, Smith BL, Rajendiran TM, Núñez G. K<sup>+</sup> efflux is the Common Trigger of NLRP3 inflammasome Activation by Bacterial Toxins and Particulate Matter. 2013;38(6):1142-53.

188. Juliana C, Fernandes-Alnemri T, Kang S, Farias A, Qin F, Alnemri ES. Non-transcriptional Priming and Deubiquitination Regulate NLRP3 Inflammasome Activation. *Journal of Biological Chemistry*. 2012;287(43):36617-22.
189. Han S, Lear TB, Jerome JA, Rajbhandari S, Snaveley CA, Gulick DL, et al. Lipopolysaccharide Primes the NALP3 Inflammasome by Inhibiting Its Ubiquitination and Degradation Mediated by the SCFFBXL2 E3 Ligase. *Journal of Biological Chemistry*. 2015;290(29):18124-33.
190. Liang Z, Damianou A, Daniel ED, Kessler BM. Inflammasome activation controlled by the interplay between post-translational modifications: emerging drug target opportunities. *Cell Communication and Signaling* 2021;19.
191. Williams KL, Taxman DJ, Linhoff MW, Reed W, Ting JP-Y. Cutting Edge: Monarch-1: A Pyrin/Nucleotide-Binding Domain/Leucine-Rich Repeat Protein That Controls Classical and Nonclassical MHC Class I Genes. *Journal of Immunology*. 2003;170(11):5354-8.
192. Song N, Liu Z-S, Xue W, Bai Z-F, Wang Q-Y, Dai J, et al. NLRP3 Phosphorylation Is an Essential Priming Event for Inflammasome Activation. *Molecular Cell*. 2017;68:185-97.
193. Yang D, He Y, Muñoz-Planillo R, Liu Q, Núñez G. Caspase-11 Requires the Pannexin-1 Channel and the Purinergic P2X7 Pore to Mediate Pyroptosis and Endotoxic Shock. *Immunity*. 2015;43(5):923-32.
194. Murakamia T, Ockinger J, Yua J, Bylesa V, McColla A, Hoferb AM, et al. Critical role for calcium mobilization in activation of the NLRP3 inflammasome. *PNAS*. 2012;109(28):11282-7.
195. Zhou R, Yazdi AS, Menu P, Tschopp J. A role for mitochondria in NLRP3 inflammasome activation. *Nature*. 2010;469:221-5.
196. Iyer SS, He Q, Janczy JR, Elliott EI, Zhong Z, Olivier AK, et al. Mitochondrial Cardiolipin Is Required for Nlrp3 Inflammasome Activation. *Immunity*. 2013;39(2):311-23.
197. Elliott EI, Miller AN, Banoth B, Iyer SS, Stotland A, Weiss JP, et al. Cutting Edge: Mitochondrial Assembly of the NLRP3 Inflammasome Complex Is Initiated at Priming. *The Journal of Immunology*. 2018;200:3047-52.
198. Park S, Juliana C, Hong S, Datta P, Hwang I, Fernandes-Alnemri T, et al. The Mitochondrial Antiviral Protein MAVS Associates with NLRP3 and Regulates Its Inflammasome Activity. *The Journal of Immunology*. 2013;191:4358-66.
199. Guan K, Wei C, Zheng Z, Song T, Wu F, Zhang Y, et al. MAVS Promotes Inflammasome Activation by Targeting ASC for K63-Linked Ubiquitination via the E3 Ligase TRAF3. *The Journal of Immunology*. 2015;194:4880-90.

200. Zhang Z, Meszaros G, He W-t, Xu Y, Magliarelli HdF, Mailly L, et al. Protein kinase D at the Golgi controls NLRP3 inflammasome activation. *Journal of Experimental Medicine*. 2017;214(9):2671-93.
201. Chen J, Chen ZJ. PtdIns4P on dispersed trans-Golgi network mediates NLRP3 inflammasome activation. *Nature*. 2018;564:71-6.
202. Nakahira K, Haspel JA, Rathinam VAK, Lee S-J, Dolinay T, Lam HC, et al. Autophagy proteins regulate innate immune responses by inhibiting the release of mitochondrial DNA mediated by the NALP3 inflammasome. *Nature Immunology*. 2010;12:222-30.
203. Shimada K, Crother TR, Karlin J, Dagvadorj J, Chiba N, Chen S, et al. Oxidized Mitochondrial DNA Activates the NLRP3 Inflammasome during Apoptosis. *Immunity*. 2012;36(3):401-14.
204. Zhong Z, Liang S, Sanchez-Lopez E, He F, Shalapour S, Lin X-j, et al. New mitochondrial DNA synthesis enables NLRP3 inflammasome activation. *Nature*. 2018;560:198-203.
205. Hornung V, Bauernfeind F, Halle A, Samstad EO, Kono H, Rock KL, et al. Silica crystals and aluminum salts activate the NALP3 inflammasome through phagosomal destabilization. *Nature Immunology*. 2008;9:847-56.
206. Schorn C, Frey B, Lauber K, Janko C, Stryio M, Keppeler H, et al. Sodium Overload and Water Influx Activate the NALP3 Inflammasome. *Journal of Biological Chemistry*. 2011;286(1):35-41.
207. Duewell P, Kono H, Rayner KJ, Sirois CM, Vladimer G, Bauernfeind FG, et al. NLRP3 inflammasomes are required for atherogenesis and activated by cholesterol crystals. *Nature*. 2010;464(7293):1357-61.
208. Chevriaux A, Pilot T, Derangère V, Simonin H, Martine P, Chalmin F, et al. Cathepsin B Is Required for NLRP3 Inflammasome Activation in Macrophages, Through NLRP3 Interaction. *Frontiers in Cell and Developmental Biology* 2020;8.
209. Weber K, Schilling JD. Lysosomes Integrate Metabolic-Inflammatory Cross-talk in Primary Macrophage Inflammasome Activation. *The Journal of Biological Chemistry*. 2014;289(12):9158-71.
210. Orlowski GM, Colbert JD, Sharma S, Bogoy M, Robertson SA, Rock KL. Multiple Cathepsins Promote Pro-IL-1 $\beta$  Synthesis and NLRP3-Mediated IL-1 $\beta$  Activation. *Journal of Immunology*. 2015;195(4):1685-97.
211. Puren AJ, Fantuzzi G, Dinarello CA. Gene expression, synthesis, and secretion of interleukin 18 and interleukin 1 $\beta$  are differentially regulated in human blood mononuclear cells and mouse spleen cells. *PNAS*. 1999;96(5):2256-61.



212. Liang MD, Zhang Y, McDevit D, Marecki S, Nikolajczyk BS. The Interleukin-1 $\beta$  Gene Is Transcribed from a Poised Promoter Architecture in Monocytes. *Journal of Biological Chemistry*. 2006;281(14):9227-37.
213. Cornut M, Bourdonnay E, Henry T. Transcriptional Regulation of Inflammasomes. *International Journal of Molecular Sciences*. 2020;21.
214. Toda Y, Tsukada J, Misago M, Kominato Y, Auron PE, Tanaka Y. Autocrine Induction of the Human Pro-IL-1 $\beta$  Gene Promoter by IL-1  $\beta$  in Monocytes. *The Journal of Immunology*. 2002;168:1984-91.
215. He W-t, Wan H, Hu L, Chen P, Wang X, Huang Z, et al. Gasdermin D is an executor of pyroptosis and required for interleukin-1 $\beta$  secretion. *Cell Research* 2015;25:1285-98.
216. Liu X, Zhang Z, Ruan J, Pan Y, Magupalli VG, Wu H, et al. Inflammasome-activated gasdermin D causes pyroptosis by forming membrane pores. *Nature* 2016;535:153-8.
217. Shi J, Zhao Y, Wang K, Shi X, Wang Y, Huang H, et al. Cleavage of GSDMD by inflammatory caspases determines pyroptotic cell death. *Nature*. 2015;526:660-5.
218. Xia S, Zhang Z, Magupalli VG, Pablo JL, Dong Y, Vora SM, et al. Gasdermin D pore structure reveals preferential release of mature interleukin-1. *Nature*. 2021.
219. Zhou B, Abbot DW. Gasdermin E permits interleukin-1 beta release in distinct sublytic and pyroptotic phases. *Cell Reports*. 2021;35.
220. Wang Y, Gao W, Shi X, Ding J, Liu W, He H, et al. Chemotherapy drugs induce pyroptosis through caspase-3 cleavage of a gasdermin. *Nature*. 2017;547:99-103.
221. Rühl S, Shkarina K, Demarco B, Heilig R, Santos JC, Broz P. ESCRT-dependent membrane repair negatively regulates pyroptosis downstream of GSDMD activation. *Science*. 2018;362(6417):956-60.
222. Liu J, Kang R, Tang D. ESCRT-III-mediated membrane repair in cell death and tumor resistance. *Cancer Gene Therapy*. 2020;28:1-4.
223. Martin MU, Wesche H. Summary and comparison of the signaling mechanisms of the Toll/interleukin-1 receptor family. *Biochimica et Biophysica Acta* 1592. 2002:265-80.
224. Garlanda C, Dinarello CA, Mantovani A. The Interleukin-1 Family: Back to the Future. *Immunity*. 2014;39(6):1003-18.
225. Lee J-K, Kim S-H, Lewis EC, Azam T, Reznikov LL, Dinarello CA. Differences in signaling pathways by IL-1 $\beta$  and IL-18. *PNAS*. 2004;101(23):8815-20.

226. La E, Rundhaug JE, Pavone A, Fischer SM. Regulation of transcription of the intracellular interleukin-1 receptor antagonist gene by AP-1 in mouse carcinoma cells. *Mol Carcinog*. 2002;33(4):237-43.
227. Darragh J, Ananieva O, Courtney A, Elcombe S, Arthur JSC. MSK1 regulates the transcription of IL-1ra in response to TLR activation in macrophages *Biochem J*. 2010;425(3):595-602.
228. Kim S-H, Eisenstein M, Reznikov L, Fantuzzi G, Novick D, Rubinstein M, et al. Structural requirements of six naturally occurring isoforms of the IL-18 binding protein to inhibit IL-18. *PNAS*. 2000;97(3):1190-5.
229. Nakanishi K. Unique Action of interleukin-18 on T Cells and Other immune Cells. *Frontiers in Immunology*. 2018;9.
230. Voronov E, Shouval DS, Krelin Y, Cagnano E, Benharroch D, Iwakura Y, et al. IL-1 is required for tumor invasiveness and angiogenesis. *PNAS*. 2003;100(5):2645-50.
231. Tulotta C, Ottewell P. The role of IL-1B in breast cancer bone metastasis. *Endocrine-Related Cancer*. 2018;25(7):R421-R34.
232. Tulotta C, Lefley DV, Moore CK, Amariutei AE, Spicer-Hadlington AR, Quayle LA, et al. IL-1B drives opposing responses in primary tumours and bone metastases; harnessing combination therapies to improve outcome in breast cancer. *npj Breast Cancer*. 2021;7.
233. Holen I, Lefley DV, Francis SE, Rennicks S, Bradbury S, Coleman RE, et al. IL-1 drives breast cancer growth and bone metastasis in vivo *Oncotarget*. 2016;7(46):75571-84.
234. Wu T-C, Xu K, Martinek J, Young RR, Banchereau R, George J, et al. IL1Receptor Antagonist Controls Transcriptional Signature of Inflammation in Patients with Metastatic Breast Cancer. *Cancer Research*. 2018;78(18):5243-58.
235. Ma L, Lan F, Zheng Z, Xie F, Wang L, Liu W, et al. Epidermal growth factor (EGF) and interleukin (IL)-1 $\beta$  synergistically promote ERK1/2-mediated invasive breast ductal cancer cell migration and invasion. *Molecular Cancer*. 2012;11.
236. Storr SJ, Safuan S, Ahmad N, El-Refaei M, Jackson AM, Martin SG. Macrophage-derived interleukin-1 $\beta$  promotes human breast cancer cell migration and lymphatic adhesion in vitro. *Cancer Immunology, Immunotherapy* 2017;66:1287-94.
237. Tulotta C, Lefley DV, Freeman K, Gregory WM, Hanby AM, Heath PR, et al. Endogenous Production of IL1B by Breast Cancer Cells Drives Metastasis and Colonization of the Bone Microenvironment. *Clin Cancer Res*. 2019;25(9):2769-82.
238. Yang Y, Cheon S, Jung MK, Song SB, Kim D, Kim HJ, et al. Interleukin-18 enhances breast cancer cell migration via down-regulation of claudin-12 and induction of

the p38 MAPK pathway. *Biochemical and Biophysical Research Communications*. 2015;459(3):379-86.

239. Soria G, Ofri-Shahak M, Haas I, Yaal-Hahoshen N, Leider-Trejo L, Leibovich-Rivkin T, et al. Inflammatory mediators in breast cancer: Coordinated expression of TNF $\alpha$  & IL-1 $\beta$  with CCL2 & CCL5 and effects on epithelial-to-mesenchymal transition. *BMC Cancer*. 2011;11.

240. EISSA SAL, ZAKI SA, EL-MAGHRABY SM, KADRY DY. Importance of Serum IL-18 and RANTES as Markers for Breast Carcinoma Progression. *Journal of the Egyptian Nat Cancer Inst* 2005;17(1):51-5.

241. INOUE N, LI W, FUJIMOTO Y, MATSUSHITA Y, KATAGIRI T, OKAMURA H, et al. High Serum Levels of Interleukin-18 Are Associated With Worse Outcomes in Patients With Breast Cancer. *Anticancer Research*. 2019;39(9):5009-18.

242. Lim HX, Hong H-J, Cho D, Kim TS. IL-18 Enhances Immunosuppressive Responses by Promoting Differentiation into Monocytic Myeloid-Derived Suppressor Cells. *Journal of Immunology*. 2014;193(11):5453-60.

243. Park IH, Yang HN, Lee KJ, Kim T-S, Lee ES, Jung S-Y, et al. Tumor-derived IL-18 induces PD-1 expression on immunosuppressive NK cells in triple-negative breast cancer. *Oncotarget*. 2017;8(20):32722-30.

244. Macciò A, Clelia Madeddu. Blocking inflammation to improve immunotherapy of advanced cancer. *Immunology* 2019;159 (4):357-64.

245. Vajaitu C, Draghici CC, Solomon I, Lisievici CV, Popa AV, Lupu M, et al. The Central Role of Inflammation Associated with Checkpoint Inhibitor Treatments. *Journal of Immunology Research* 2018;2018.

246. Gomillion CT, Yang C-C, Dréau D, Burg KJL. Engineered Composites for 3D Mammary Tissue Systems. In: Burg KJL, Dréau D, Burg T, editors. *Engineering 3D Tissue Test Systems*: CRC Press Taylor & Francis Group; 2018.

247. Gao J, Aksoy BA, Dogrusoz U, Dresdner G, Gross B, Sumer SO, et al. Integrative Analysis of Complex Cancer Genomics and Clinical Profiles Using the cBioPortal Science Signaling 2013;6(269):11.

248. Taylor AM, Shih J, Ha G, Gao GF, Zhang X, Berger AC, et al. Genomic and Functional Approaches to Understanding Cancer Aneuploidy. *Cancer Cell*. 2018;33(4):676-89.

249. Sanchez-Vega F, Mina M, Armenia J, Chatila WK, Luna A, La KC, et al. Oncogenic Signaling Pathways in The Cancer Genome Atlas. *Cell*. 2018;173(2):321-37.

250. Gao Q, Liang W-W, Foltz SM, Mutharasu G, Jayasinghe RG, Cao S, et al. Driver Fusions and Their Implications in the Development and Treatment of Human Cancers. *Cell Rep* 2018;23(1):227-38.
251. Cerami E, Gao J, Dogrusoz U, Gross BE, Sumer SO, Aksoy BA, et al. The cBio Cancer Genomics Portal: An Open Platform for Exploring Multidimensional Cancer Genomics Data. *Cancer Discovery*. 2012;2(5):401-4.
252. Razavi P, Dickler MN, Shah PD, Toy W, Brown DN, Won HH, et al. Alterations in PTEN and ESR1 promote clinical resistance to alpelisib plus aromatase inhibitors. *Nat Cancer*. 2020;1(4):382-93.
253. Razavi P, Chang MT, Xu G, Bandlamudi C, Ross DS, Vasan N, et al. The Genomic Landscape of Endocrine-Resistant Advanced Breast Cancers. *Cancer Cell*. 2018;34(3):427-38.
254. Rueda OM, Sammut S-J, Seoane JA, Chin S-F, Caswell-Jin JL, Callari M, et al. Dynamics of breast-cancer relapse reveal late-recurring ER-positive genomic subgroups. *Nature*. 2019;567(7748):399-404.
255. Pereira B, Chin S-F, Rueda OM, Vollan H-KM, Provenzano E, Bardwell HA, et al. The somatic mutation profiles of 2,433 breast cancers refines their genomic and transcriptomic landscapes. *Nat Commun*. 2016;10(7).
256. Curtis C, Shah SP, Chin S-F, Turashvili G, Rueda OM, Dunning MJ, et al. The genomic and transcriptomic architecture of 2,000 breast tumours reveals novel subgroups. *Nature*. 2012;486(346-352).
257. Pareja F, Brown DN, Lee JY, Paula ADC, Selenica P, Bi R, et al. Whole-Exome Sequencing Analysis of the Progression from Non-Low-Grade Ductal Carcinoma In Situ to Invasive Ductal Carcinoma. *Clin Cancer Res*. 2020;26(14):3682-93.
258. D'Alfonso TM, Pareja F, Paula ADC, Vahdatinia M, Gazzo A, Ferrando L, et al. Whole-exome sequencing analysis of juvenile papillomatosis and coexisting breast carcinoma. *J Pathol Clin Res*. 2021;7(2):113-20.
259. Shah SP, Roth A, Goya R, Oloumi A, Ha G, Zhao Y, et al. The clonal and mutational evolution spectrum of primary triple-negative breast cancers. *Nature*. 2012;486(7403):395-9.
260. Eirew P, Steif A, Khattra J, Ha G, Yap D, Farahani H, et al. Dynamics of genomic clones in breast cancer patient xenografts at single-cell resolution. *Nature*. 2015;518(7539):422-6.
261. Nixon MJ, Formisano L, Mayer IA, Estrada MV, González-Ericsson PI, Isakoff SJ, et al. PIK3CA and MAP3K1 alterations imply luminal A status and are associated with clinical benefit from pan-PI3K inhibitor buparlisib and letrozole in ER+ metastatic breast cancer. *npj Breast Cancer*. 2019;5(31).

262. Kan Z, Ding Y, Kim J, Jung HH, Chung W, Lal S, et al. Multi-omics profiling of younger Asian breast cancers reveals distinctive molecular signatures. *Nat Commun.* 2018;9(1).
263. Banerji S, Cibulskis K, Rangel-Escareno C, Brown KK, Carter SL, Frederick AM, et al. Sequence analysis of mutations and translocations across breast cancer subtypes. *Nature.* 2012;486(7403):405-9.
264. Stephens PJ, Tarpey PS, Davies H, Loo PV, Greenman C, Wedge DC, et al. The landscape of cancer genes and mutational processes in breast cancer. *Nature.* 2012;486(7403):400-4.
265. Koboldt DC, Fulton RS, McLellan MD, Schmidt H, Kalicki-Veizer J, McMichael JF, et al. Comprehensive molecular portraits of human breast tumors. *Nature.* 2012;490(7418):61-70.
266. Ciriello G, Gatza ML, Beck AH, Wilkerson MD, Rhie SK, Pastore A, et al. Comprehensive Molecular Portraits of Invasive Lobular Breast Cancer. *Cell* 2015;163(2):506-19.
267. Liu J, Lichtenberg T, Hoadley KA, Poisson LM, Lazar AJ, Cherniack AD, et al. An Integrated TCGA Pan-Cancer Clinical Data Resource to Drive High-Quality Survival Outcome Analytics. *Cell.* 2018;173(2):400-16.
268. Hoadley KA, Yau C, Hinoue T, Wolf DM, Lazar AJ, Drill E, et al. Cell-of-Origin Patterns Dominate the Molecular Classification of 10,000 Tumors from 33 Types of Cancer. *Cell* 2018;173(2):291-304.
269. Ding L, Bailey MH, Porta-Pardo E, Thorsson V, Colaprico A, Bertrand D, et al. Perspective on Oncogenic Processes at the End of the Beginning of Cancer Genomics. *Cell.* 2018;173(2):305-20.
270. Lefebvre C, Bachelot T, Filleron T, Pedrero M, Campone M, Soria J-C, et al. Mutational Profile of Metastatic Breast Cancers: A Retrospective Analysis. *PLoS Med.* 2016;13(12).
271. Ellrott K, Bailey MH, Saksena G, Covington KR, Kandath C, Stewart C, et al. Scalable Open Science Approach for Mutation Calling of Tumor Exomes Using Multiple Genomic Pipelines. *Cell Syst* 2018;6(3):271-81.
272. Bonneville R, Krook MA, Kautto EA, Miya J, Wing MR, Chen H-Z, et al. Landscape of Microsatellite Instability Across 39 Cancer Types. *JCO Precis Oncol.* 2017;2017.
273. Bhandari V, Hoey C, Liu LY, Lalonde E, Ray J, Livingstone J, et al. Molecular landmarks of tumor hypoxia across cancer types. *Nat Genet.* 2019;51(2):308-18.

274. Poore GD, Kopylova E, Zhu Q, Carpenter C, Fraraccio S, Wandro S, et al. Microbiome analyses of blood and tissues suggest cancer diagnostic approach. *Nature*. 2020;579(7800):567-74.
275. Ghonime MG, Shamaa OR, Das S, Eldomany RA, Fernandes-Alnemri T, Alnemri ES, et al. Inflammasome Priming by Lipopolysaccharide Is Dependent upon ERK Signaling and Proteasome Function. *Journal of Immunology*. 2014;192(8):3881-8.
276. Wang W, Hu D, Feng Y, Wu C, Song Y, Liu W, et al. Paxillin mediates ATP-induced activation of P2X7 receptor and NLRP3 inflammasome. *BMC Biology*. 2020;18.
277. Amores-Iniesta J, Barberà-Cremades M, Martínez CM, Pons JA, Revilla-Nuin B, Martínez-Alarcón L, et al. Extracellular ATP Activates the NLRP3 Inflammasome and Is an Early Danger Signal of Skin Allograft Rejection. *Cell Reports*. 2017;21:3414-26.
278. Dinarello CA, Novick D, Kim S, Kaplanski G. Interleukin-18 and IL-18 binding protein. *Frontiers in Immunology*. 2013;4.
279. Hormone Therapy for Breast Cancer: The American Cancer Society 2019 [Available from: <https://www.cancer.org/cancer/breast-cancer/treatment/hormone-therapy-for-breast-cancer.html>].
280. Targeted Drug Therapy for Breast Cancer: The American Cancer Society 2021 [Available from: <https://www.cancer.org/cancer/breast-cancer/treatment/targeted-therapy-for-breast-cancer.html>].
281. Immunotherapy for Breast Cancer: The American Cancer Society 2021 [Available from: <https://www.cancer.org/cancer/breast-cancer/treatment/immunotherapy.html>].
282. Siegel RL, Miller KD, Fuchs HE, Jemal A. Cancer Statistics, 2021. *CA: A Cancer Journal for Clinicians*. 2021;71:7-33.
283. Choi J, Gyamfi J, Jang H, Koo JS. The role of tumor-associated macrophage in breast cancer biology. *Histol Histopathol* 2017;33(2):133-45.
284. Jeong H, Hwang I, Kang SH, Shin HC, Kwon SY. Tumor-Associated Macrophages as Potential Prognostic Biomarkers of Invasive Breast Cancer. *J Breast Cancer* 2019;22(1):38-51.
285. Sousa S, Brion R, Lintunen M, Kronqvist P, Sandholm J, Mönkkönen J, et al. Human breast cancer cells educate macrophages toward the M2 activation status. *Breast Cancer Research*. 2015;17.
286. Orecchioni M, Ghosheh Y, Pramod AB, Ley K. Macrophage Polarization: Different Gene Signatures in M1(LPS+) vs. Classically and M2(LPS-) vs. Alternatively Activated Macrophages. *Front Immunol*. 2019;10.

287. Jayasingam SD, Citartan M, Thang TH, Zin AAM, Ang KC, Ch'ng ES. Evaluating the Polarization of Tumor-Associated Macrophages Into M1 and M2 Phenotypes in Human Cancer Tissue: Technicalities and Challenges in Routine Clinical Practice. *Front Oncol*. 2020;9.
288. Jablonski KA, Amici SA, Webb LM, Ruiz-Rosado JdD, Popovich PG, Partida-Sanchez S, et al. Novel Markers to Delineate Murine M1 and M2 Macrophages PLoS ONE. 2015;10(12).
289. Arlauckas SP, Garren SB, Garriss CS, Kohler RH, Oh J, Pittet MJ, et al. Arg1 expression defines immunosuppressive subsets of tumor-associated macrophages. *Theranostics*. 2018;8(21):5842-54.
290. Modolell M, Corraliza IM, Link F, Soler G, Klaus Eichmann. Reciprocal regulation of the nitric oxide synthase/arginase balance in mouse bone marrow-derived macrophages by TH 1 and TH 2 cytokines. *European Journal of Immunology* 1995;25(4):1101-4.
291. Hao N-B, Lü M-H, Fan Y-H, Cao Y-L, Zhang Z-R, Yang S-M. Macrophages in Tumor Microenvironments and the Progression of Tumors. *Journal of Immunology Research*. 2012;2012.
292. Lee C-H, Choi EY. Macrophages and Inflammation. *J Rheum Dis* 2018;25(1):11-8.
293. Mosser DM, Hamidzadeh K, Goncalves R. Macrophages and the maintenance of homeostasis. *Cellular & Molecular Immunology*. 2021;18:579-87.
294. Thapa A, Adamiak M, Bujko K, Ratajczak J, Abdel-Latif AK, Kucia M, et al. Danger-associated molecular pattern molecules take unexpectedly a central stage in Nlrp3 inflammasome–caspase-1-mediated trafficking of hematopoietic stem/progenitor cells. *Leukemia*. 2021;35:2658-71.
295. Kong H, Wang Y, Zeng X, Wang Z, Wang H, Xie W. Differential expression of inflammasomes in lung cancer cell lines and tissues. *Tumor Biology* 2015;36:7501-13.
296. Weichland B, Popp R, Dziumbila S, Mora J, Strack E, Elwakeel E, et al. The Journal of Experimental Medicine. 214. 2017;9(2695-2713).
297. Depke M, Breitbach K, Dang KDH, Brinkmann L, Salazar MG, Dhople VM, et al. Bone marrow-derived macrophages from BALB/c and C57BL/6 mice fundamentally differ in their respiratory chain complex proteins, lysosomal enzymes and components of antioxidant stress systems. *Journal of Proteomics*. 2014;103:72-86.
298. Anisiewicz A, Łabędź N, Krauze I, Wietrzyk J. Calcitriol in the Presence of Conditioned Media from Metastatic Breast Cancer Cells Enhances Ex Vivo Polarization of M2 Alternative Murine Bone Marrow-Derived Macrophages. *Cancers*. 2020;12(11).

299. P.Wong A, RaquelPerez-Castillejos, Love JC, M.Whitesides G. Partitioning microfluidic channels with hydrogel to construct tunable 3-D cellular microenvironments. *Biomaterial*. 2008;29(12):1853-61.
300. Aslakson CJ, Miller FR. Selective Events in the Metastatic Process Defines by Analysis of the Sequential Dissemination of Subpopulations of a Mammary Tumor. *Cancer Research*. 1992;52:1399-405.
301. Case JR, Young MA, Dréau D, Trammell SR. Noninvasive enhanced mid-IR imaging of breast cancer development in vivo. *J of Biomedical Optics* 2015;20(11).
302. Cruz CM, Rinna A, Forman HJ, Ventura ALM, Persechini PM, Ojcius DM. ATP Activates a Reactive Oxygen Species-dependent Oxidative Stress Response and Secretion of Proinflammatory Cytokines in Macrophages. *Journal of Biological Chemistry*. 2007;282(5):2871-9.
303. Roy S, Bag AK, Dutta S, Polavaram NS, Islam R, Schellenburg S, et al. Macrophage-Derived Neuropilin-2 Exhibits Novel Tumor-Promoting Functions. *Cancer Research*. 2018;78(19):5600-17.
304. Bonaventura P, Shekarian T, Alcazer V, Valladeau-Guilemond J, Valsesia-Wittmann S, Amigorena S, et al. Cold Tumors: A Therapeutic Challenge for Immunotherapy. *Front Immunol*. 2019;10.
305. Cho HJ, Jung JI, Lim DY, Kwon GT, Her S, Park JH, et al. Bone marrow-derived, alternatively activated macrophages enhance solid tumor growth and lung metastasis of mammary carcinoma cells in a Balb/C mouse orthotopic model. *Breast Cancer Research* 2012;14(R81).
306. Linde N, Casanova-Acebes M, Sosa MS, Mortha A, Rahman A, Farias E, et al. Macrophages orchestrate breast cancer early dissemination and metastasis. *Nature Communications*. 2018;9(21).
307. Glass CK, Natoli G. Molecular control of activation and priming in macrophages. *Nature Immunology*. 2015;17:26-33.
308. Kowal J, Kornete M, Joyce JA. Re-education of macrophages as a therapeutic strategy in cancer. *Immunotherapy* 2019;11(8):677-89.
309. Liu Y, Gao X, Miao Y, Wang Y, Wang H, Cheng Z, et al. NLRP3 regulates macrophage M2 polarization through up-regulation of IL-4 in asthma. *Biochem J*. 2018;475(12):1995-2008.
310. Wilcz-Villega E, Carter E, Ironside A, Xu R, Mataloni I, Holdsworth J, et al. Macrophages induce malignant traits in mammary epithelium via IKK $\epsilon$ /TBK1 kinases and the serine biosynthesis pathway. *EMBO Mol Med*. 2020;12.



311. Weichand B, Popp R, Dziumbila S, Mora J, Strack E, Elwakeel E, et al. S1PR1 on tumor-associated macrophages promotes lymphangiogenesis and metastasis via NLRP3/IL-1 $\beta$ . *The Journal of Experimental Medicine*. 2017;214(9):2695-713.
312. Yaw ACK, Chan EWL, Yap JKY, Mai CW. The effects of NLRP3 inflammasome inhibition by MCC950 on LPS-induced pancreatic adenocarcinoma inflammation. *Journal of Cancer Research and Clinical Oncology* 2020;146:2219-29.
313. Hirano S, Zhou Q, Furuyama A, Kanno S. Differential Regulation of IL-1 $\beta$  and IL-6 Release in Murine Macrophages. *Inflammation*. 2017;40(6):1933-43.
314. Martin BN, Wang C, Willette-Brown J, Herjan T, Gulen MF, Zhou H, et al. IKK $\alpha$  negatively regulates ASC-dependent inflammasome activation. *Nature Communications*. 2014;5.
315. Aki T, Funakoshi T, Noritake K, Unuma K, Uemura K. Extracellular glucose is crucially involved in the fate decision of LPS-stimulated RAW264.7 murine macrophage cells. *Scientific Reports*. 2020;10.
316. Czystowska-Kuzmich M, Sosnowska A, Nowis D, Ramji K, Szajnik M, Chlebowska-Tuz J, et al. Small extracellular vesicles containing arginase-1 suppress T-cell responses and promote tumor growth in ovarian carcinoma. *Nature Communications*. 2019;10.
317. Zhang J, Liu X, Wan C, Liu Y, Wang Y, Meng C, et al. NLRP3 inflammasome mediates M1 macrophage polarization and IL-1 $\beta$  production in inflammatory root resorption. *J Clin Periodontol* 2020;47(4):451-60.
318. Awad F, Assrawi E, Jumeau C, Georgin-Lavialle S, Cobret L, Duquesnoy P, et al. Impact of human monocyte and macrophage polarization on NLR expression and NLRP3 inflammasome activation. *PLoS ONE*. 2017;12(4).
319. Hudson CA, Christophi GP, Gruber RC, Wilmore JR, Lawrence DA, Massa PT. Induction of IL-33 expression and activity in central nervous system glia. *J Leukoc Biol*. 2008;84(3):631-43.
320. Sarmiento-Castro A, Caamaño-Gutiérrez E, Sims AH, Hull NJ, James MI, Santiago-Gómez A, et al. Increased Expression of Interleukin-1 Receptor Characterizes Anti-estrogen-Resistant ALDH + Breast Cancer Stem Cells. *Stem Cell Reports*. 2020;15(2):307-16.
321. Biswas SK, Sica A, Lewis CE. Plasticity of Macrophage Function during Tumor Progression: Regulation by Distinct Molecular Mechanisms. *Journal of Immunology*. 2008;180:2011-7.
322. Chen X, Gao Y, Zhang G, Li B, Ma T, Ma Y, et al. Bevacizumab Plays a double-edged role in Neoadjuvant Therapy for Non-metastatic Breast Cancer: A Systemic Review and Meta-Analysis. *J Cancer*. 2021;12(9):2643-53.

323. Theivanthiran B, Evans KS, DeVito NC, Plebanek M, Sturdivant M, Wachsmuth LP, et al. A tumor-intrinsic PD-L1/NLRP3 inflammasome signaling pathway drives resistance to anti-PD-1 immunotherapy. *J Clin Invest*. 2020;130(5):2570-86.
324. Tarantino P, Gandini S, Trapani D, Criscitiello C, Curigliano G. Immunotherapy addition to neoadjuvant chemotherapy for early triple negative breast cancer: A systematic review and meta-analysis of randomized clinical trials. *Crit Rev Oncol Hematol*. 2021;159.
325. Gradishar WJ, Anderson BO, Abraham J, Aft R, Agnese D, Allison KH, et al. Breast Cancer, Version 3.2020, NCCN Clinical Practice Guidelines in Oncology. *JNCCN*. 2020;18(4):452-78.
326. Longley DB, Harkin DP, Johnston PG. 5-Fluorouracil: mechanisms of action and clinical strategies. *Nature Reviews Cancer*. 2003;3:330-8.
327. Cameron DA, Gabra H, Leonard RC. Continuous 5-fluorouracil in the treatment of breast cancer. *Br J Cancer*. 1994;70(1):120-4.
328. Yi J, Chen S, Yi P, Luo J, Fang M, Du Y, et al. Pyrotinib Sensitizes 5-Fluorouracil-Resistant HER2 + Breast Cancer Cells to 5-Fluorouracil. *Oncol Res*. 2020;28(5):519-31.
329. Christensen S, Roest BVd, Besselink N, Janssen R, Boymans S, Martens JWM, et al. 5-Fluorouracil treatment induces characteristic T>G mutations in human cancer. *Nature Communications*. 2019;10.
330. Paulus P, Stanley ER, Schäfer R, Abraham D, Aharinejad S. Colony-Stimulating Factor-1 Antibody Reverses Chemoresistance in Human MCF-7 Breast Cancer Xenografts. *Cancer Research*. 2006;66(8):4349-56.
331. Wei C, Yang C, Wang S, Shi D, Zhang C, Lin X, et al. M2 macrophages confer resistance to 5-fluorouracil in colorectal cancer through the activation of CCL22/PI3K/AKT signaling. *Onco Targets Ther*. 2019;12:3051-63.
332. Grugan KD, McCabe FL, Kinder M, Greenplate AR, Harman BC, Ekert JE, et al. Tumor-Associated Macrophages Promote Invasion while Retaining Fc-Dependent Anti-Tumor Function. *The Journal of Immunology*. 2012;189:5457-66.
333. Pupa SM, Bufalino R, Invernizzi AM, Andreola S, Rilke F, Lombardi L, et al. Macrophage infiltrate and prognosis in c-erbB-2-overexpressing breast carcinomas. *J Clin Oncol*. 1996;14(1):85-94.
334. Ma R-Y, Zhang H, Li X-F, Zhang C-B, Selli C, Tagliavini G, et al. Monocyte-derived macrophages promote breast cancer bone metastasis outgrowth. *Journal of Experimental Medicine*. 2020;217(11).
335. Bednarczyk RB, Tuli NY, Hanly EK, Rahoma GB, Maniyar R, Mittelman A, et al. Macrophage inflammatory factors promote epithelial-mesenchymal transition in breast cancer. *Oncotarget*. 2018;9:24272-82.

336. O'Brien J, Lyons T, Monks J, Lucia MS, Wilson RS, Hines L, et al. Alternatively Activated Macrophages and Collagen Remodeling Characterize the Postpartum Involuting Mammary Gland across Species. *Am J Pathol* 2010;176(3):1241-55.
337. Kim H, Chung H, Kim J, Choi D-H, Shin Y, Kang YG, et al. Macrophages-Triggered Sequential Remodeling of Endothelium-Interstitial Matrix to Form Pre-Metastatic Niche in Microfluidic Tumor Microenvironment. *Advanced Science*. 2019;6(11).
338. Lu F, Zhao Y, Pang Y, Ji M, Sun Y, Wang H, et al. NLRP3 inflammasome upregulates PD-L1 expression and contributes to immune suppression in lymphoma. *Cancer Letters*. 2021;497:178-89.
339. Deng Q, Geng Y, Zhao L, Li R, Zhang Z, Li K, et al. NLRP3 inflammasomes in macrophages drive colorectal cancer metastasis to the liver. *Cancer Letters*. 2019;442:21-30.
340. Daley D, Mani VR, Mohan N, Akkad N, Pandian GSDB, Savadkar S, et al. NLRP3 signaling drives macrophage-induced adaptive immune suppression in pancreatic carcinoma. *Journal of Experimental Medicine*. 2017;214(6):1711-24.
341. Martínez-García JJ, Martínez-Banaclocha H, Angosto-Bazarra D, Torre-Minguela Cd, Baroja-Mazo A, Alarcón-Vila C, et al. P2X7 receptor induces mitochondrial failure in monocytes and compromises NLRP3 inflammasome activation during sepsis. *Nature Communications*. 2019;10.
342. Kinoshita T, Wang Y, Hasegawa M, Imamura R, Suda T. PYPAF3, a PYRIN-containing APAF-1-like Protein, Is a Feedback Regulator of Caspase-1-dependent Interleukin-1 $\beta$  Secretion. *The Journal of Biological Chemistry*. 2005;280(21720-21725).
343. Chen L, Huang C-F, Li Y-C, Deng W-W, Mao L, Wu L, et al. Blockage of the NLRP3 Inflammasome by MCC950 improves anti-tumor immune responses in head and neck squamous cell carcinoma. *Cellular and Molecular Life Sciences*. 2018;75:2045-58.
344. Chen S-P, Zhou Y-Q, Wang X-M, Sun J, Cao F, HaiSam S, et al. Pharmacological inhibition of the NLRP3 inflammasome as a potential target for cancer-induced bone pain. *Pharmacol Res* 2019;147.
345. Huang C-F, Chen L, Li Y-C, Wu L, Yu G-T, Zhang W-F, et al. NLRP3 inflammasome activation promotes inflammation-induced carcinogenesis in head and neck squamous cell carcinoma. *Journal of Experimental & Clinical Cancar Research* 2017;36(116).
346. Coll RC, Robertson AAB, Chae JJ, Higgins SC, Muñoz-Planillo R, Inserra MC, et al. A small molecule inhibitor of the NLRP3 inflammasome is a potential therapeutic for inflammatory diseases. *Nature Medicine*. 2015;21(3):248-55.

347. Tapia-Abellán A, Angosto-Bazarra D, Martínez-Banaclocha H, Torre-Minguela Cd, Cerón-Carrasco JP, Pérez-Sánchez H, et al. MCC950 closes the active conformation of NLRP3 to an inactive state. *Nat Chem Biol.* 2019;15(6):560-4.
348. Coll RC, Hill JR, Day CJ, Zamoshnikova A, Boucher D, Massey NL, et al. MCC950 directly targets the NLRP3 ATP-hydrolysis motif for inflammasome inhibition. *Nat Chem Biol.* 2019;15:556-9.
349. Son S, Shim D-W, Hwang I, Park J-H, Yu J-W. Chemotherapeutic Agent Paclitaxel Mediates Priming of NLRP3 Inflammasome Activation. *Frontiers in Immunology.* 2019;10(1108).
350. Bruchard M, Mignot G, Derangère V, Chalmin F, Chevriaux A, Végran F, et al. Chemotherapy-triggered cathepsin B release in myeloid-derived suppressor cells activates the Nlrp3 inflammasome and promotes tumor growth. *Nat Med.* 2013;19(1):57-64.
351. Pilot T, Fratti A, Thinselin C, Perrichet A, Demontoux L, Limagne E, et al. Heat shock and HSP70 regulate 5-FU- mediated caspase-1 activation in myeloid-derived suppressor cells and tumor growth in mice. *Journal for ImmunoTherapy of Cancer.* 2020;8.
352. El-Ghannam A, Ricci K, Malkawi A, Jahed K, Vedantham K, Wyan H, et al. A ceramic-based anticancer drug delivery system to treat breast cancer. *J Mater Sci Mater Med.* 2010;21(9):2701-10.
353. Orecchioni S, Talarico G, Labanca V, Calleri A, Mancuso P, Bertolini F. Vinorelbine, cyclophosphamide and 5-FU effects on the circulating and intratumoural landscape of immune cells improve anti-PD-L1 efficacy in preclinical models of breast cancer and lymphoma. *British Journal of Cancer.* 2018;118:1329-36.
354. Dréau D, Wang S, Clemens M, Elliott GD. Structure and Function of Porcine Arteries Are Preserved for up to 6 Days Using the HypoRP Cold-storage Solution. *Transplantation.* 2020;104(5):e125-e34.
355. Dréau D, Moore LJ, Wu M, Roy LD, Dillion L, Porter T, et al. Combining the Specific Anti-MUC1 Antibody TAB004 and Lip-MSA-IL-2 Limits Pancreatic Cancer Progression in Immune Competent Murine Models of Pancreatic Ductal Adenocarcinoma. *Front Oncol* 2019;9.
356. Maghdouri-White Y, Bowlin GL, Lemmon CA, Dréau D. Bioengineered silk scaffolds in 3D tissue modeling with focus on mammary tissues. *Mater Sci Eng C Mater Biol Appl.* 2016;59:1168-80.
357. Jewell AN, Swamydas M, Castillo CI, Wyan H, Allen LD, McDermott KA, et al. The Endothelin Axis Stimulates the Expression of Pro-Inflammatory Cytokines and Pro-Migratory Molecules in Breast Cancer. *Cancer Investigation.* 2010;28(9):932-43.

358. Geng Y, Chandrasekaran S, Hsu J-W, Gidwani M, Hughes AD, King MR. Phenotypic Switch in Blood: Effects of Pro-Inflammatory Cytokines on Breast Cancer Cell Aggregation and Adhesion. *PLOS ONE*. 2013;8(1).
359. Pierce BL, Ballard-Barbash R, Bernstein L, Baumgartner RN, Neuhouser ML, Wener MH, et al. Elevated Biomarkers of Inflammation Are Associated With Reduced Survival Among Breast Cancer Patients. *Journal of Clinical Oncology* 2009;27(21):3437-44.
360. Li Y, Wang L, Pappan L, Galliher-Beckley A, Shi J. IL-1 $\beta$  promotes stemness and invasiveness of colon cancer cells through Zeb1 activation. *Molecular Cancer*. 2012;11(87).
361. Iannitti RG, Napolioni V, Oikonomou V, Luca AD, Galosi C, Pariano M, et al. IL-1 receptor antagonist ameliorates inflammasome-dependent inflammation in murine and human cystic fibrosis. *Nature Communications*. 2016;7.
362. Roy LD, Ghosh S, Pathangey LB, Tinder TL, Gruber HE, Mukherjee P. Collagen induced arthritis increases secondary metastasis in MMTV-PyV MT mouse model of mammary cancer. *BMC Cancer*. 2011;11.
363. Xu L, Cai P, Li X, Wu X, Gao J, Liu W, et al. Inhibition of NLRP3 inflammasome activation in myeloid-derived suppressor cells by andrographolide sulfonate contributes to 5-FU sensitization in mice. *Toxicology and Applied Pharmacology*. 2021;428.
364. Dumont A, Rosny Cd, Kieu T-L-V, Perrey S, Berger H, Fluckiger A, et al. Docosahexaenoic acid inhibits both NLRP3 inflammasome assembly and JNK-mediated mature IL-1 $\beta$  secretion in 5-fluorouracil-treated MDSC: implication in cancer treatment. *Cell Death & Disease* 2019;10.
365. Feng X, Luo Q, Zhang H, Wang H, Chen W, Meng G, et al. The role of NLRP3 inflammasome in 5-fluorouracil resistance of oral squamous cell carcinoma. *J Exp Clin Cancer Res*. 2017;36(1).
366. Fusco R, Gugliandolo E, Biundo F, Campolo M, Paola RD, Cuzzocrea S. Inhibition of inflammasome activation improves lung acute injury induced by carrageenan in a mouse model of pleurisy. *FASEB J*. 2017;31(8):3497-511.
367. Xu X, Yin D, Ren H, Gao W, Li F, Sun D, et al. Selective NLRP3 inflammasome inhibitor reduces neuroinflammation and improves long-term neurological outcomes in a murine model of traumatic brain injury. *Neurobiol Dis* 2018;117:15-27.
368. Zhang M, Fan Y, Che X, Hou K, Zhang C, Li C, et al. 5-FU-Induced Upregulation of Exosomal PD-L1 Causes Immunosuppression in Advanced Gastric Cancer Patients. *Frontiers in Oncology*. 2020;10.
369. Zhang W-j, Hu C-g, Zhu Z-m, Luo H-l. Effect of P2X7 receptor on tumorigenesis and its pharmacological properties. *Biomedicine & Pharmacotherapy*. 2020;125.

370. Skinner MD, Lahmek P, Pham H, Aubin H-J. Disulfiram Efficacy in the Treatment of Alcohol Dependence: A Meta-Analysis. *PLoS One*. 2014;9(2).
371. Skrott Z, Mistrik M, Andersen KK, Friis S, Majera D, Gursky J, et al. Alcohol-abuse drug disulfiram targets cancer via p97 segregase adaptor NPL4. *Nature* 2017;552:194-9.
372. Kaiser J. An old drug for alcoholism finds new life as cancer treatment. *Science*. 2017.
373. Brar SS, Grigg C, Wilson KS, Jr WDH, Dreau D, Austin C, et al. Disulfiram inhibits activating transcription factor/cyclic AMP-responsive element binding protein and human melanoma growth in a metal-dependent manner in vitro, in mice and in a patient with metastatic disease. *Mol Cancer Ther*. 2004;3(9):1049-60.
374. Hu JJ, Liu X, Xia S, Zhang Z, Zhang Y, Zhao J, et al. FDA-approved disulfiram inhibits pyroptosis by blocking gasdermin D pore formation. *Nature Immunology* 2020;21:736-45.
375. Foster JG, Carter E, Kilty I, MacKenzie AB, Ward SG. Mitochondrial Superoxide Generation Enhances P2X7R-Mediated Loss of Cell Surface CD62L on Naive Human CD4<sup>+</sup> T Lymphocytes. *Journal of Immunology*. 2013;190(4):1551-9.
376. Tao Y, Wang F, Xu Z, Lu X, Yang Y, Wu J, et al. Gasdermin D in peripheral nerves: the pyroptotic microenvironment inhibits nerve regeneration. *Cell Death and Discovery* 2021;7.
377. Liu T, Wang L, Liang P, Wang X, Liu Y, Cai J, et al. USP19 suppresses inflammation and promotes M2-like macrophage polarization by manipulating NLRP3 function via autophagy. *Cellular & Molecular Immunology*. 2021;18:2431-42.
378. Liang M, Chen X, Wang L, Qin L, Wang H, Sun Z, et al. Cancer-derived exosomal TRIM59 regulates macrophage NLRP3 inflammasome activation to promote lung cancer progression. *Journal of Experimental & Clinical Cancer Research*. 2020;39.
379. Fu S, Liu L, Han L, Yu Y. Leptin promotes IL-18 secretion by activating the NLRP3 inflammasome in RAW 264.7 cells. *Mol Med Rep*. 2017;16(6):9770-6.
380. Chen K, Zhang J, Zhang W, Zhang J, Yang J, Li K, et al. ATP-P2X4 signaling mediates NLRP3 inflammasome activation: a novel pathway of diabetic nephropathy. *Int J Biochem Cell Biol*. 2013;45(5):932-43.
381. Nobel CSI, Kimland M, Nicholson DW, Orrenius S, Slater AFG. Disulfiram Is a Potent Inhibitor of Proteases of the Caspase Family. *Chem Res Toxicol* 1997;10(12):1319-24.

382. Teng X, Zhang H, Snead C, Catravas JD. Molecular mechanisms of iNOS induction by IL-1 beta and IFN-gamma in rat aortic smooth muscle cells. *Am J Physiol Cell Physiol*. 2002;282:C114-52.
383. Adams V, Nehrhoff B, Späte U, Linke A, Schulze PC, Baur A, et al. Induction of iNOS expression in skeletal muscle by IL-1b and NFkB activation: an in vitro and in vivo study. *Cardiovascular Research* 2002;54:95-104.
384. Zhang Y, Yang B, Zhao J, Xiaoli Li, Zhang L, Zhai Z. Proteasome Inhibitor Carbobenzoxymethyl-L-Leucyl-L-Leucyl-L-Leucinal (MG132) Enhances Therapeutic Effect of Paclitaxel on Breast Cancer by Inhibiting Nuclear Factor (NF)-kB Signaling. *Med Sci Monit* 2018;24:294-304.
385. Pérez-Flores G, Hernández-Silva C, Gutiérrez-Escobedo G, Peñas ADL, Castaño I, Arreola J, et al. P2X7 from j774 murine macrophages acts as a scavenger receptor for bacteria but not yeast. *Biochem Biophys Res Commun*. 2016;481(1-2):19-24.
386. Zhao P, Wang Y, Kang X, Wu A, Yin W, Tang Y, et al. Dual-targeting biomimetic delivery for anti-glioma activity via remodeling the tumor microenvironment and directing macrophage-mediated immunotherapy. *Chem Sci* 2018;9:2674-89.
387. Parny M, Bernad J, Prat M, Salon M, Aubouy A, Bonnafé E, et al. Comparative study of the effects of ziram and disulfiram on human monocyte-derived macrophage functions and polarization: involvement of zinc. *Cell Biology and Toxicology*. 2020.
388. Ording AG, Heide-Jørgensen U, Christiansen CF, Nørgaard M, Acquavella J, Sørensen HT. Site of metastasis and breast cancer mortality: a Danish nationwide registry-based cohort study. *Clin Exp Metastasis*. 2017;34(1):93-101.
389. Ren Z, Li Y, Hameed O, Siegal GP, Wei S. Prognostic factors in patients with metastatic breast cancer at the time of diagnosis. *Pathol Res Pract*. 2014;210(5):301-6.
390. Survival Rates for Breast Cancer: The American Cancer Society 2021 [Available from: <https://www.cancer.org/cancer/breast-cancer/understanding-a-breast-cancer-diagnosis/breast-cancer-survival-rates.html>].
391. Zhang Y, Li F, Wang L, Lou Y. A438079 affects colorectal cancer cell proliferation, migration, apoptosis, and pyroptosis by inhibiting the P2X7 receptor. *Biochem Biophys Res Commun*. 2021;558:147-53.
392. Bianchi G, Vuerich M, Pellegatti P, Marimpietri D, Emionite L, Marigo I, et al. ATP/P2X7 axis modulates myeloid-derived suppressor cell functions in neuroblastoma microenvironment. *Cell Death Dis*. 2014;5(3).
393. Terashima Y, Toda E, Itakura M, Otsuji M, Yoshinaga S, Okumura K, et al. Targeting FROUNT with disulfiram suppresses macrophage accumulation and its tumor-promoting properties. *Nature Communications*. 2020;11.

394. Fang Y, Wang L, Wan C, Sun Y, Jeught KVd, Zhou Z, et al. MAL2 drives immune evasion in breast cancer by suppressing tumor antigen presentation. *J Clin Invest.* 2021;131(1).
395. Bates JP, Derakhshandeh R, Jones L, Webb TJ. Mechanisms of immune evasion in breast cancer. *BMC Cancer.* 2018;18.
396. Thelen M, Wennhold K, Lehmann J, Garcia-Marquez M, Klein S, Kochen E, et al. Cancer-specific immune evasion and substantial heterogeneity within cancer types provide evidence for personalized immunotherapy. *npj Precision Oncology.* 2021;5.
397. Vinay DS, Ryan EP, Pawelec G, H.Talib W, Stagg J, Elkord E, et al. Immune evasion in cancer: Mechanistic basis and therapeutic strategies. *Seminars in Cancer Biology.* 2015;35:S185-98.
398. Dhatchinamoorthy K, Colbert JD, Rock KL. Cancer Immune Evasion Through Loss of MHC Class I Antigen Presentation. *Front Immunol.* 2021;12.
399. Sakuishi K, Apetoh L, Sullivan JM, Blazar BR, Kuchroo VK, Anderson AC. Targeting Tim-3 and PD-1 pathways to reverse T cell exhaustion and restore anti-tumor immunity. *J, Exp Med.* 2010;207(20):2187-94.
400. Liu Q, Cheng R, Kong X, Wang Z, Fang Y, Wang J. Molecular and Clinical Characterization of PD-1 in Breast Cancer Using Large-Scale Transcriptome Data. *Front Immunol.* 2020;11.
401. Xia A, Zhang Y, Xu J, Yin T, Lu X-J. T Cell Dysfunction in Cancer Immunity and Immunotherapy. *Front Immunol.* 2019;10.
402. Xu D, Li J, Li R-Y, Lan T, Xiao C, Gong P. PD-L1 Expression Is Regulated By NF- $\kappa$ B During EMT Signaling In Gastric Carcinoma. *Onco Targets Ther.* 2019;12:10099-105.
403. Xu G-L, Ni C-F, Liang H-S, Xu Y-H, Wang W-S, Shen J, et al. Upregulation of PD-L1 expression promotes epithelial-to-mesenchymal transition in sorafenib-resistant hepatocellular carcinoma cells *Gastroenterology Report* 2020;8(5):390-8.
404. Raimondi C, Carpino G, Nicolazzo C, Gradilone A, Gianni W, Gelibter A, et al. PD-L1 and epithelial-mesenchymal transition in circulating tumor cells from non-small cell lung cancer patients: A molecular shield to evade immune system? *OncoImmunology.* 2017;6(12).
405. Noman MZ, Janji B, Abdou A, Hasmim M, Terry S, Tan TZ, et al. The immune checkpoint ligand PD-L1 is upregulated in EMT-activated human breast cancer cells by a mechanism involving ZEB-1 and miR-200. *OncoImmunology.* 2017;6(1).



406. Eger A, Aigner K, Sonderegger S, Dampier B, Oehler S, Schreiber M, et al. DeltaEF1 is a transcriptional repressor of E-cadherin and regulates epithelial plasticity in breast cancer cells. *Oncogene*. 2005;24:2375-85.
407. Gordon SR, Maute RL, Dulken BW, Hutter G, George BM, McCracken MN, et al. PD-1 expression by tumour-associated macrophages inhibits phagocytosis and tumour immunity. *Nature* 2017;545:495-9.

## APPENDIX A: LAY ABSTRACT

KATHERINE HOLTZMAN, 2021. *Inflammation, NLRP3 Inflammasome, macrophages and Breast Cancer Progression*. (Under the direction of DR. DIDIER DRÉAU) PhD Dissertation, UNC Charlotte)

One in 8 women will be diagnosed with breast cancer in their lifetime. While breast cancer mortality has declined since the 1980's, it remains the 2<sup>nd</sup> leading cause of cancer-related deaths among women. Breast cancer treatments vary from person to person, based on cancer stage and characteristics of the breast tumor cells. However, many treatments that target tumor growth and the development of therapeutic resistance is common. Immune cells residing within tumors and their resulting inflammation are, in part, responsible for therapeutic resistance.

Here, we investigated the effect of local inflammation originating from immune cells on promoting tumor-supporting characteristics in immune cells and whether drugs reducing local inflammation could reduce breast cancer growth and spread – especially when combined with existing treatments. We found that reducing local inflammation initiated by immune cells reduces tumor-supporting characteristics of immune cells and, in turn, led to reduced growth and reduced potential to spread of breast cancer. Additionally, combining treatments that reduce local inflammation by immune cells along with currently used anti-tumor growth treatments limit tumor growth and spread. However, such combination treatments had a substantial effect only on tumors laced with immune cells that generated a local inflammation.